ANALYSIS OF AMMONIUM CONCENTRATION USING TiO_2-BASED SENSOR SYSTEM AND FUZZY LOGIC APPROACH

BY

MUHAMMAD HAFIZUDDIN BIN HAMID

A dissertation submitted in fulfillment of the requirement for the degree of Master of Science in Engineering

Kulliyyah of Engineering
International Islamic University Malaysia

MARCH 2025

ABSTRACT

Ammonia is poisonous and harmful to environment. Ammonia is the most common pollutant in water streams and most of them come from agricultural, industrial, and domestic wastewater. The biggest problem for current method in ammonia monitoring detection is too much time taken to examine the water quality and the process is complicated. This is because the machine is not portable and the examination cannot be done at the measurement site. In addition, the effect of different concentration of ammonia and the distance of UV needs to be analyse to improve the measurement of output voltage to its optimum. The objectives of this study are to develop a portable PEC-based UV-assisted ammonia monitoring system using the TiO_2-based sensor and analyse the data using fuzzy logic approach. This can help to shorten the time of examination of the water quality, portable to everywhere and can give more precise estimation of ammonia concentration. The basic item of this experimental setup are ammonium samples, ultraviolet (UV) light, TiO_2-based sensor in photoelectrochemical cell (PEC) structure, microcontroller interfacing system and fuzzy logic system. We executed an experiment that measure the voltage generated with digital multimeter and our ammonia detection system using Arduino and make sure the error of voltage differences between them is low to make sure the output is accurate. Then, we varied the ammonia concentration and the distance of UV light from TiO_2-based sensor to measure the output voltage. The measured data was analysed using fuzzy logic approach to estimate the output voltage. Lastly, the fuzzy logic method is also used in reverse the calculation to predict the ammonia concentration based on the output voltage and UV distance. UV assisted TiO_2-based ammonia sensor in PEC structure was successfully fabricated and developed into a portable device for measuring the voltage at different ammonia concentrations. The fuzzy logic approach for estimating the output voltage was successfully designed. The result between Arduino and digital multimeter output has a very low percentage of error with the lowest is 0 % and the highest is 3.02 %. In the fuzzy logic calculation, we get the best result at 6.12 % error of difference between the prediction and experiment in the range of 1-13 cm distance between UV ray and the sensor. As for the conclusion, analysis of ammonium concentration using TiO_2-based sensor system and fuzzy logic approach can be used to advance the ammonia monitoring and estimate the output in shorter time.

ملخص البحث

تُعدّ الأمونيا مادة سامة وضارة بالبيئة. تُعتبر الأمونيا من أكثر الملوثات شيوعًا في مصادر المياه، وينبع معظمها من مياه الصرف الزراعية والصناعية والمنزلية. تتمثل أكبر المشكلات في الأساليب الحالية لمراقبة تركيز الأمونيا في طول مدة الفحص وتعقيد العملية. ويرجع ذلك إلى أن الأجهزة المستخدمة ليست محمولة، مما يجعل من غير الممكن إجراء الفحص في موقع القياس مباشرة. بالإضافة إلى ذلك، فإن تأثير اختلاف تركيزات الأمونيا والمسافة بين الأشعة فوق البنفسجية والمستشعر بحاجة إلى تحليل دقيق لتحسين قياس الجهد الناتج إلى مستواه الأمثل. تهدف هذه الدراسة إلى تطوير نظام محمول PEC لمراقبة تركيز الأمونيا بمساعدة الأشعة فوق البنفسجية باستخدام مستشعر يعتمد على تحليل TiO_2 باستخدام نهج المنطق الضبابي. يمكن لهذا النظام أن يسهم في تقليل زمن فحص جودة المياه، وجعله قابلاً للحمل والاستخدام في أي مكان، وتحقيق تقدير أكثر دقة لتركيز الأمونيا .يتكون الأعداد التجريبي من عينات الأمونيوم ، ومصدر للأشعة فوق البنفسجية ومستشعر TiO_2 في هيكل الخلية الكهروضوئية PEC بالإضافة إلى نظام تفاعل مع متحكم دقيق، ونظام معالجة بيانات يعتمد على المنطق الضبابي. تم تنفيذ تجربة لقياس الجهد الناتج باستخدام مقياس متعدد رقمي Digital Multimeter ونظام كشف الأمونيا القائم على Arduino مع ضمان أن يكون الخطأ في فرق الجهد بين الطريقتين ضئيلاً لضمان

دقة الإخراج. بعد ذلك، تم تعيير تركيز الأمونيا ومسافة الأشعة فوق البنفسجية عن مستشعر TiO_2 لقياس تأثيرهما على الجهد الناتج. خضعت البيانات المقاسة للتحليل باستخدام نهج المنطق الضبابي بهدف تقدير الجهد الناتج .أخيرًا، تم استخدام نهج المنطق الضبابي لعكس العملية الحسابية بهدف التنبؤ بتركيز الأمونيا بناءً على الجهد الناتج والمسافة بين الأشعة فوق البنفسجية والمستشعر. تم بنجاح تصنيع وتطوير المستشعر ليصبح جهازًا محمولًا قادرًا على قياس الجهد عند تركيزات مختلفة من الأمونيا. تم تصميم نهج المنطق الضبابي بدقة لتقدير الجهد الناتج بنجاح. ختامًا، يمكن لاستخدام مستشعر تركيز الأمونيوم TiO_2ونظام المنطق الضبابي في أن يسهم في تحسين مراقبة الأمونيا وتقديم تقديرات أسرع وأكثر دقة لتركيزها في المياه.

APPROVAL PAGE

I certify that I have supervised and read this study and that in my opinion, it conforms to acceptable standards of scholarly presentation and is fully adequate, in scope and quality, as a dissertation for the degree of Master of Science in Engineering.

…….
Marmeezee Bin Mohd. Yusoff
Supervisor

…….
Nurul Sakinah Binti Engliman
Co-Supervisor

…….
Mohd Asyraf Bin Mohd Razib
Co-Supervisor

I certify that I have read this study and that in my opinion it conforms to acceptable standards of scholarly presentation and is fully adequate, in scope and quality, as a dissertation for the degree of Master of Science in Engineering.

…….
Abd Halim Bin Embong
Examiner

…….
Amir Syahir Bin Amir Hamzah
External Examiner

This dissertation was submitted to the Department of Mechatronics and is accepted as a fulfilment of the requirement for the degree of Master of Science in Engineering.

…….
Ali Sophian
Head, Department of Mechatronics

This dissertation was submitted to the Kulliyyah of Mechatronics and is accepted as a fulfillment of the requirement for the degree of Master of Science in Engineering.

…….
Khairul Azami Sidek
Dean, Kulliyyah of Engineering

DECLARATION

I hereby declare that this dissertation is the result of my own investigations, except where otherwise stated. I also declare that it has not been previously or concurrently submitted as a whole for any other degrees at IIUM or other institutions.

Muhammad Hafizuddin bin Hamid

Signature…… 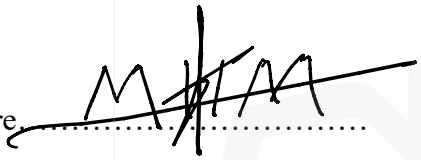 …… Date…21/2/2024……

INTERNATIONAL ISLAMIC UNIVERSITY MALAYSIA

DECLARATION OF COPYRIGHT AND AFFIRMATION OF FAIR USE OF UNPUBLISHED RESEARCH

ANALYSIS OF AMMONIUM CONCENTRATION USING TiO2-BASED SENSOR SYSTEM AND FUZZY LOGIC APPROACH

I declare that the copyright holder of this dissertation is jointly owned by the student and IIUM.

By signing this form, I acknowledged that I have read and understand the IIUM Intellectual Property Right and Commercialization policy.

Affirmed by Student Name

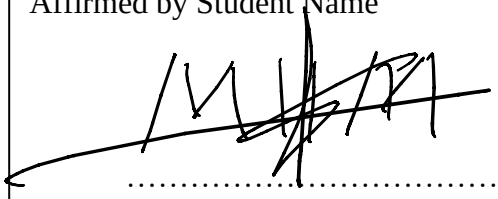

…… Signature

21/2/2024
…….. Date

ACKNOWLEDGEMENTS

Alhamdulillah, all praise to Allah for giving me a clear path to finish my dissertation. I read journals. Alhamdulillah, I praise Allah for guiding me through the completion of my dissertation. The process involved extensive reading of journals and numerous experiments conducted day and night. I am grateful to Allah for enabling me to finish on time.

I would like to express my gratitude to Dr. Marmeezee Bin Mohd. Yusoff, my supervisor, for his constant assistance and support throughout this research. His friendly behaviour made me feel at ease during our consultations. He provided invaluable help and guidance during my experiments.

I also want to thank my family and friends for their unwavering support. They have been there for me through all the stress and challenges, helping me stay motivated during this demanding final year.

Lastly, I appreciate everyone who shared their opinions and moments with me during this journey. May Allah S.W.T bless all of them.

TABLE OF CONTENTS

LIST OF TABLES

LIST OF FIGURES

LIST OF SYMBOLS AND ACRONYMS

TiO_2	Titanium Dioxide
UV	Ultraviolet
DMM	Digital Multimeter
WAM	Wight Average Method
MOC	Mean of Center Method
MWAM	Modified Weight Average Method
COM	Center of Maximum Method
CoS	Center of Sums Method

CHAPTER ONE

INTRODUCTION

1.1 INTRODUCTION

Ammonia, a chemical compound composed of hydrogen and nitrogen, stands as the second-largest chemical produced around the globe. Regardless of its widespread industrial use, it poses an extreme threat to both animals and humans due to its toxicity. Consequently, the monitoring of ammonia toxicity levels has become paramount, especially in applications focused on evaluating water quality. In addressing this important need, extensive research has been undertaken to develop effective and efficient ammonia monitoring systems. A notable development in this field involves the utilization of UV photosensors and Titanium Dioxide (TiO_2) materials, TiO_2 exhibits a remarkable sensitivity to ultraviolet (UV) irradiation, distinguishing it from visible light due to its wide band gap energy of approximately 3.0 eV. This unique property renders TiO_2 highly competent for applications involving UV photosensors.

The focus on TiO_2's inherent responsiveness to UV irradiation forms the basis for the innovation of a novel portable ammonia monitoring system. This development not only addresses the recent need for ammonia monitoring but also paves the way for future research exploring high-performance portable ammonia monitoring systems. The implications of this research extend beyond technical advancements, aligning with the Sustainable Development Goal 3 (SDG3) of ensuring good health and well-being. By contributing to the research and development of cutting-edge water quality monitoring technologies, this study directly supports wider initiatives aimed at safeguarding public health and encouraging sustainable implementation in water management.

As we delve into this realm of innovation, the capability applications of high-performance portable water quality systems are vast. The interrelationship to SDG3 underscores the societal influence of such advancements, emphasizing the significant of ensuring access to clean water, a fundamental aspect of nurture well-being and preventing waterborne diseases. The envisioned future research in this domain hold promises for facilitating our understanding of water quality dynamics, offering solutions that can be pivotal in achieving resilient and sustainable communities.

In summary, the amalgamation of UV photosensors and TiO_2 materials in ammonia monitoring systems represents an important stride towards developing a portable water quality monitoring system. This study not only addresses immediate environmental concerns but also aligns with global sustainability goal objective, demonstrating the potential for transformative impacts on human health and well-being.

1.2 PROBLEM STATEMENT

Ammonia monitoring in water faces significant challenges, including time-consuming and complex detection methods. Conventional processes, often requiring intricate laboratory techniques, are prone to errors and delay accurate results. The lack of portability in current devices adds to these difficulties, as water samples must be sent to centralized labs for analysis, impeding real-time monitoring and response in critical situations. Additionally, the transportation of samples raises concerns about maintaining their integrity, potentially compromising the reliability of results.

Furthermore, there is limited research exploring the relationship between ammonia concentration, UV irradiation distance, and output voltage in experimental setups. A better

understanding of this relationship is essential to enhancing detection sensitivity and improving overall system performance

These challenges highlight the need for innovative, portable, and efficient ammonia monitoring systems. To address this, advancements in sensor technologies and data analysis techniques are necessary, alongside further research into the factors that influence output voltage in ammonia detection

A more reliable and streamlined monitoring system could significantly improve real-time water quality assessment, reduce risks associated with ammonia toxicity, and ensure quicker responses. This progress would also align with broader sustainability goals, contributing to more effective resource management and environmental protection.

By overcoming these obstacles, researchers can contribute to the development of next-generation monitoring systems that improve both the accuracy and efficiency of ammonia detection, benefiting both ecosystems and communities globally.

1.3 OBJECTIVES

1. To design the PEC-based UV-assisted ammonia monitoring sensor using the TiO_2.
2. Develop portable ammonia monitoring system for ammonia detection using the designed sensor.

3. Evaluate the performance of the developed portable ammonia monitoring system using fuzzy logic.

1.4 RESEARCH SCOPE AND LIMITATION

The scope that will be focused on this research is the concentration of ammonia. Ammonia is chosen because it is the most common substance that pollute water stream. The voltage reading between chemical reaction of UV and TiO_2 will be taken. Higher concentration will give more electricity. This research uses fuzzy logic as a medium of calculation to predict the concentration of ammonia. The voltage and the distance of UV ray from TiO_2 will become the input of the fuzzy logic and the output is the concentration of ammonia.

The detection range of UV light and the TiO_2 sensor is limited to a maximum of 19 cm. Beyond this distance, the intensity of the UV light diminishes, leading to a reduction in the TiO_2 sensor's ability to detect it accurately. The sensor operates within a detection area of 1 cm x 1 cm, thereby restricting the spatial extent of measurements. This limitation ensures that the sensor can maintain consistent and reliable performance within its operational range. For distances within this range, fuzzy logic is applied to model the relationship between UV light intensity, the distance between the UV light source and the TiO_2 sensor, and the ammonia concentration. Fuzzy logic allows for a more flexible approach to handling uncertainties and variations in the system, facilitating a more accurate estimation of ammonia concentrations under diverse conditions.

1.5 SIGNIFICANT OF THE RESEARCH

The research is predicted to contribute to huge knowledge in several areas. The novel analysis of ammonium concentration using TiO_2-based sensor system and fuzzy logic approach is a new approach to predict the concentration of ammonia. Hence, it will open a new window of study of ammonia monitoring research.

Furthermore, advancement based on the performance of the fuzzy logic prediction can also be discovered through the studies by executing ample series of experiment to maximize the investigated variable. The combination of TiO_2 and fuzzy logic through this practice could contribute to enhance the effectiveness and accuracy of ammonia detection.

1.6 HYPOTHESIS

Higher concentrations of ammonia result in an increased voltage output from the TiO_2 sensor, as the sensor's response to ammonia leads to a proportional rise in electrical output due to the interaction between ammonia molecules and the sensor surface, altering its electrical properties. This relationship demonstrates how the sensor’s voltage is directly influenced by ammonia concentration, providing valuable data for ammonia detection and measurement.

Similarly, the distance between the UV light source and the TiO_2 sensor significantly affects the voltage output, with a shorter distance leading to a higher voltage. This is because the intensity of UV light decreases as the distance between the source and the sensor increases, and closer proximity results in higher UV intensity, enhancing the sensor's detection capability. Both

ammonia concentration and UV light distance are critical factors influencing the voltage output, and understanding their relationship is essential for optimizing sensor performance. To address these complexities, fuzzy logic calculations are utilized to model and analyze the impact of these variables, offering a more accurate estimation of ammonia concentration based on the sensor's voltage response under varying conditions.

CHAPTER TWO

LITERATURE REVIEW OF AMMONIA, UV LIGHT AND FUZZY LOGIC

2.1 OVERVIEW

Titanium dioxide (TiO_2) is widely studied for its potential in UV-assisted sensing applications due to its large band gap energy of approximately 3.0 eV, which makes it responsive to UV radiation while being unaffected by visible light. Incorporating nanostructured TiO_2, such as one-dimensional (1D) TiO_2 nanorod arrays, enhances UV sensitivity by increasing photocurrent generation, improving responsivity, and enabling rapid response and recovery times. Additionally, these nanostructures help in miniaturizing the device, reducing power consumption, and boosting overall performance due to their high surface-to-volume ratio and efficient light scattering properties.

Despite these advantages, TiO_2 nanorod arrays (TNAs) face a significant challenge in the form of recombination losses of photogenerated charge on their surface. This issue reduces the photocurrent gain and limits the practical application of TNAs in low-power mobile systems, which require enhanced sensing mechanisms. To address this, TNAs can be heterostructured with functionalized materials, such as magnetic Fe_3O_4 nanoparticles, to improve their performance. Fe_3O_4 enhances the oxidation-reduction reaction on the surface of TNAs, helping to reduce the recombination of electron-hole pairs and increase the sensitivity of the sensor, particularly in water-based applications.

The coupling of TiO_2 with Fe_3O_4 has shown promising results in various applications, although much of the research has focused on areas other than UV-assisted sensing. The integration of these two materials could provide superior performance compared to standalone materials, making it an attractive area for further research. As the demand for self-powered, efficient UV-assisted sensing systems grows, there is a need for continued exploration of Fe_3O_4/TiO_2 heterostructures to improve their reliability and efficiency.

One of the key challenges in UV-assisted sensing is the need for an external power source, which limits the mobility and independence of the sensing systems. While some studies have explored TiO_2 photoelectrodes in photoelectrochemical cells (PECs) that operate at 0V bias, the efficiency of these systems is still low due to recombination losses and limited material use. This makes the development of highly sensitive, self-powered UV-assisted sensing methods a critical area for future research. Innovations in nanostructure design and the use of metal oxide heterostructures like Fe_3O_4 could offer significant improvements in the photocurrent gain, reducing the need for external bias and allowing for more efficient and mobile sensing systems.

Sensor array technology also presents a promising avenue for enhancing UV-assisted detection systems. Sensor arrays, capable of simultaneously evaluating multiple chemical signals, have proven effective in various applications due to their ability to recognize patterns and cross-detect different compounds. This method can significantly improve the efficiency of chemical detection by enabling real-time, multi-parameter analysis. Custom-designed sensor arrays tailored to specific applications, such as ammonia detection, offer the potential for enhanced accuracy and reliability, addressing the current limitations in existing commercial sensor technologies.

2.2 TITANIUM DIOXIDE (TiO_2)

Titanium dioxide (TiO_2) is widely regarded as an excellent material for photosensor applications due to its unique optical, electrical, and photochemical properties. These characteristics make TiO_2 a promising alternative for electronic devices and photocatalytic applications (Yusoff et al., 2016). Photocatalysis involves the combined action of light and a catalyst to trigger a chemical reaction, a process that TiO_2 is highly effective in (Haider et al., 2019). TiO_2 is used extensively across various industries and sectors, including the production of paints, coatings, plastics, electronics, pharmaceuticals, and water treatments, owing to its versatility and wide range of applications (Canu et al., 2020).

When TiO_2 is exposed to UV radiation, it absorbs electromagnetic energy, causing electrons to transition from the valence band to the conduction band, creating electron-hole pairs. These electron-hole pairs play a crucial role in oxidation-reduction reactions with substances on the surface of TiO_2, such as water, organic compounds, hydroxide ions, or oxygen (Haider et al., 2019). The electron in the conduction band possesses strong reducing properties, while the hole in the valence band exhibits high oxidizing potential, facilitating the chemical reactions needed for photocatalytic processes. This ability to generate reactive species upon UV irradiation is what makes TiO_2 a highly effective material for a variety of sensing and catalytic applications.

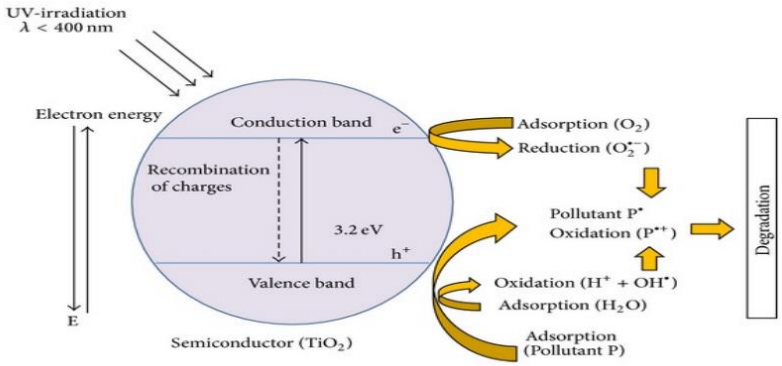

Figure 2.1: The Primary Photocatalytic Mechanism Occurring in TiO_2 Particles (Haider Et Al., 2019).

Titanium dioxide (TiO_2) is an ideal material for electronic devices such as transistors, diodes, solar cells, and sensors due to its excellent electrical properties and versatility (Yusoff et al., 2017). The study of heterojunctions formed by composite nanostructures has become a prominent area in UV irradiation sensing research, as these structures enable better control over the mobility of photogenerated electron-hole pairs, ultimately enhancing the generation of photocurrent, a key factor in sensing applications (Yusoff et al., 2018). TiO_2, as a semiconductor, is widely used across various fields due to its ability to easily form nanostructures and its remarkable electrical properties, including a large bandgap and high excitation binding energy (Yusoff et al., 2018). Ongoing research into photocatalysis has opened up numerous applications in emerging fields, such as environmental conservation, energy generation, water purification, and microbial deactivation (Magalhães et al., 2017).

Self-cleaning	Material for residential and office buildings	Exterior tiles, kitchen and bathroom components, interior furnishings, plastic surfaces, building stones
	Indoor and outdoor lamps and related systems	Translucent paper for indoor lamp covers, coatings on fluorescent lamps and highway tunnel lamp cover glass
	Materials for roads	Tunnel wall, soundproofed wall, traffic signs and reflectors
	Others	Tent material, clothes for hospital garments and uniforms and spray coating for cars
Air-cleaning	Indoor air cleaners	Room air cleaner, photocatalyst-equipped air conditioners and interior air cleaner for factories
	Outdoor air purifiers	Concrete for highways, roadways and footpaths, tunnel walls, soundproofed walls and building
Water disinfection	Drinking water	purification river water, groundwater, lakes and water storage tanks
	Others	Fish feeding tanks, drainage water and industrial wastewater
Antitumor activity	Cancer therapy	Endoscopic-like instruments
Self-sterilizing	Hospital Tiles	to cover the floor and walls of operating rooms, silicone rubber for medical catheters and hospital garments and uniforms

Figure 2.2: An Overview of Various Applications of Photocatalysis (Haider Et Al., 2019).

Titanium dioxide (TiO_2) is a highly stable material in both acidic and alkaline aqueous solutions, with a large bandgap energy of around 3.02 eV, making it ideal for various applications, including electronic devices and photocatalysis (Yusoff et al., 2018). TiO_2's advantages include low cost, high surface area, easy fabrication, low charge carrier recombination, and fast response times. It can operate in "self-powered" mode by converting UV light into electrical signals, eliminating the need for external power sources (Yusoff et al., 2017). As an ultraviolet photodetector, TiO_2 absorbs photons with energy greater than its bandgap, generating photocurrent. This self-powered capability enhances the efficiency and design simplicity of devices, expanding their range of applications (Li et al., 2017).

TiO_2 is also beneficial in antimicrobial applications, particularly when combined with silver nanoparticles (NPs) to induce surface plasmon resonance. This process generates hot electrons that migrate into TiO_2, producing reactive oxygen species (ROS) for bacterial

eradication (Subhapriya & Gomathipriya, 2018). The high surface area of TiO_2 nanoparticles facilitates increased interaction with bacterial cells, improving their ability to disrupt bacterial functions. Its natural abundance, low cost, and excellent chemical stability further enhance TiO_2's potential as an effective antimicrobial agent (Liao et al., 2020).

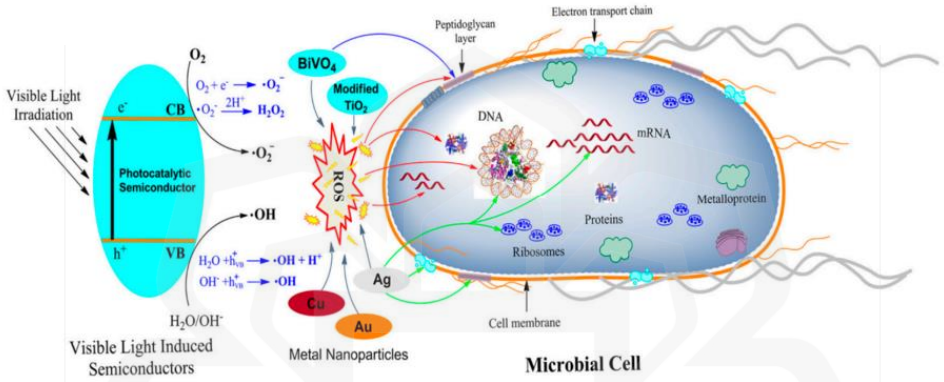

Figure 2.3: Metal NPs and Photocatalytic Semiconductors Produce ROS Under Light, Damaging Bacteria (Liao Et Al., 2020).

Photodetectors are essential devices that convert light from ultraviolet, visible, and infrared spectra into electrical signals, playing a crucial role in various fields such as optical communications, remote sensing, and environmental monitoring. These devices operate based on different principles, including the photoconductive effect of semiconductors, p-n junctions, Schottky barriers, pyroelectric effect, and photovoltaic effect (Huangfu et al., 2020). When exposed to UV light, the active region of a photodetector absorbs the energy from incoming photons, generating electron-hole pairs, which leads to the formation of plasmons as the light interacts with free electrons, exciting the electron cloud (Aggarwal et al., 2017; Kasani et al., 2019).

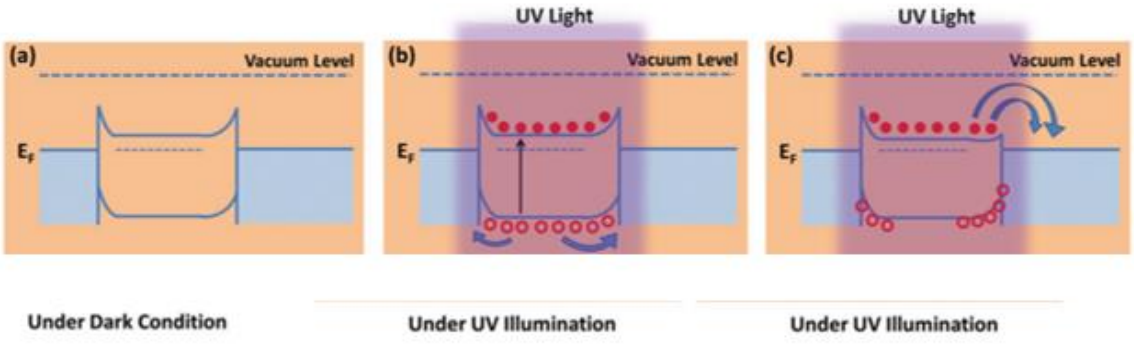

Figure 2.4: How UV Sensor Works Under Present of UV Light and in Dark Condition (Aggarwal Et Al., 2017).

The UV photo response of TiO_2 is limited by the rapid recombination of photogenerated electron-hole pairs, which hinders its performance in various applications. Additionally, surface defects further constrain their effectiveness. Despite these limitations, TiO_2 is highly regarded for its superior electron mobility, scattering abilities, large surface area, and its non-toxic, chemically robust, and physically stable nature. These attributes make TiO_2 a key material in optoelectronic applications such as photocatalysis, sensing devices, and solar cells, where its ability to interact with light plays a crucial role in performance.

When exposed to UV light, TiO_2 experiences a reduction in photocurrent and resistance, which quickly returns to its original dark current level once the light source is removed. In this process, excited electrons migrate towards the FTO substrate, while photogenerated holes move towards the electrolytes due to the built-in field potential. This mechanism is vital for the functionality of TiO_2 in various applications, allowing it to be an effective material for sensing and photocatalysis (Yusoff et al., 2018).

TiO_2 nanorod arrays exhibit high absorbance in the ultraviolet (UV) region, particularly around 400 nm, which makes them highly effective for UV photo sensing applications. The performance of UV photosensors is greatly influenced by techniques such as light and hole trapping, which impact the generation of charge carriers. In the absence of UV light, the TiO_2 interface forms a high-resistance carrier-depletion region due to free electrons in the n-type TiO_2. As radiation intensity increases, more charge carriers are generated, leading to a higher photocurrent. However, with higher radiation intensity, the likelihood of carrier recombination and scattering increases, which can affect device performance. At lower intensities, fewer charge carriers are produced, reducing the potential for scattering and carrier recombination, which impacts the overall photocurrent output.

The efficiency of UV photosensors is also influenced by factors like surface-to-volume ratio, porosity, light trapping, surface defects, and UV light intensity. In this context, manipulating the morphology and architecture of TiO_2 is crucial for improving performance. These structural changes enhance the material's ability to extend light response, facilitate the separation of photogenerated electron-hole pairs, and increase photocatalytic activity. These improvements are essential for optimizing TiO_2-based devices across various applications in fields like photocatalysis and materials chemistry.

The efficiency of TiO_2 can be improved by increasing its surface-to-volume ratio, which can be achieved through various deposition methods such as sputtering, pulsed-laser deposition, solution-based, and chemical vapor deposition. Additionally, metal doping, such as doping TiO_2 with aluminum (Al), enhances the interfacial charge transfer mechanism and aids in the formation of the rutile phase of TiO_2, which further improves its overall performance. These strategies optimize TiO_2 for various applications by enhancing its electronic properties and increasing its effectiveness in photocatalytic processes.

Another effective approach to enhance TiO_2 involves using the aqueous sol-gel method, which provides benefits like ease of operation at low temperatures, rapid deposition, and compatibility with large-scale uniform deposition. This method is particularly useful for producing nanostructured TiO_2 with a high surface-to-volume ratio. The enhanced properties of these nanostructures, including improved thermal stability, are attributed to the lower surface energy compared to bulk TiO_2, especially in electrolyte solutions. This contributes to better performance in photocatalysis and other applications where surface interaction is critical.

TiO_2 has potential applications in the medical sector, particularly for monitoring UV radiation in patients with conditions such as eczema, rickets, jaundice, and psoriasis. TiO_2 exists in three different phases: rutile, anatase, and brookite, with rutile and anatase being the most widely studied and used in industrial applications due to their superior properties for various technological and medical uses.

2.3 ULTRAVIOLET (UV)

UV radiation, with wavelengths ranging from 100 nm to 400 nm, is categorized into three types: UVA (400–315 nm), UVB (315–200 nm), and UVC (less than 200 nm). UV radiation is a known carcinogen, capable of damaging genomic DNA and increasing the risk of cancer. The majority of UV radiation originates from sunlight, making it a significant environmental carcinogen for humans.

In the medical field, UV blood irradiation was widely used between the 1940s and 1950s to treat various health conditions. More recently, UV-based advanced oxidation processes have emerged as effective technologies for water and wastewater treatment, particularly in addressing

pollutants such as bisphenol A (BPA). The water industry is urgently seeking reliable methods to mitigate the effects of particles on online water quality, highlighting the growing need for advanced solutions in this area.

Optical techniques such as fluorescence and UV absorption spectroscopies are effective tools for monitoring water quality, providing valuable insights into water contamination levels. UV disinfection, a key method in water treatment, aims to reduce bacterial contamination, ensuring safer water for consumption. However, UV radiation can be blocked by specific UV blockers, which may limit its effectiveness. Despite this, the strong energy from UV radiation holds potential for various energy conversion applications, offering new opportunities for sustainable energy solutions.

Table 2.1: Properties of UVR (Khan, A. Q et al., 2018).

TABLE I. Properties of UVR

Properties of UV Radiation (UVR)			
Properties	UVC	UVB	UVA
Wavelength range	100–280 nm	280–320 nm	320–400 nm
% of UVR in terrestrial sunlight	Completely blocked by ozone layer	2–10%	90–98%
Penetration through glass	Blocked	Blocked	Passes
Penetration through skin	Reaches top part of epidermis	Only penetrates epidermis	Epidermis and dermis

UV radiation has significant therapeutic potential, especially in the field of phototherapy, which is widely recognized for being safe, well-tolerated, and effective for treating various skin conditions. The short treatment duration associated with UV phototherapy minimizes the likelihood of unpleasant side effects, making it a preferred choice for many patients. Among the

different UV radiation types, UVA accounts for around 6% of total solar emission and is considered the least harmful, yet it still plays an important role in both medical treatments and environmental effects. UVA is particularly effective in promoting biomass production and enhancing leaf size, but it is also implicated in accelerating skin aging, making its regulation crucial in medical practices (Surjadinata et al., 2017; Chen et al., 2019).

In the medical domain, UVA radiation is used for treating localized scleroderma, also known as morphea, demonstrating its therapeutic benefits (Marrani et al., 2018). On the other hand, Narrowband UVB phototherapy is more commonly used to treat moderate to severe cases of psoriasis, a chronic inflammatory skin condition characterized by vasodilation and immunological imbalance. The efficacy of UVB in treating such conditions highlights its importance in managing a wide array of dermatological diseases, further cementing UV radiation's role in modern medical treatments (Hönigsmann, 2020; Ye et al., 2020).

UVB radiation has been recognized for its potential to reduce the risk of certain types of cancer (Moukayed & Grant, 2017). Additionally, UVB has therapeutic applications, such as treating verruca plana, a type of skin condition (Zhang et al., 2020). UVC light, on the other hand, is primarily used for microbial disinfection due to its powerful germicidal properties, which make it effective in eliminating microorganisms (Dallavecchia et al., 2019). In hospitals, UVC is commonly employed for surface decontamination (Dos Santos & de Castro, 2021), and it is also widely utilized in water, air, and surface sterilization processes due to its cost-effectiveness and high efficiency (Ploydaeng et al., 2021).

In the food industry, UVC is applied to prevent postharvest decay of products, ensuring their quality and longevity (Sabir et al., 2018). However, it is important to note that overexposure to UVC radiation can lead to health issues, including photokeratitis in the eyes and sunburn, highlighting the need for controlled usage in various applications (Ploydaeng et al., 2021).

2.4 AMMONIA

Ammonia is the second most produced chemical globally, largely due to its safe, easily transportable nature, low ignition energy, low burning velocity, and narrow flammability limits (Giddey et al., 2017). However, it is also one of the most common pollutants found in water bodies, raising significant environmental concerns due to its toxic effects on aquatic life and its widespread presence in surface water (Karri et al., 2018; Wang et al., 2020). Ammonia contributes to eutrophication, acidification, and climate change, posing a serious threat to ecosystems (Van Damme et al., 2018). As a critical stressor on water resources, understanding its impact is essential for maintaining ecological balance and preserving aquatic environments (Randhawa et al., 2016).

Ammonia waste primarily originates from industrial, agricultural, and domestic wastewater, with industries such as rubber processing, food processing, and fertilizer plants contributing to high ammonia concentrations in water bodies (Karri et al., 2018). The use of ammonium nitrate fertilizers, which are soluble in water and provide nitrogen for plant growth, also adds to the presence of ammonia in the environment (Kaptan, 2021). This contamination poses serious risks to both human health and aquatic life, making the removal of ammonia from wastewater a critical concern. In 2011, approximately 4.7 million pounds of ammonia were discharged into U.S. surface waters, while annual ammonia emissions in China reached nearly 2.3 million tons, further emphasizing the importance of controlling this pollutant in water bodies like the Liao River, Yellow River, and Songhua River (Wang et al., 2020; Yan et al., 2020).

The discharge of effluents containing high levels of ammonia can have severe consequences on both human health and aquatic ecosystems. Consumption of contaminated water and toxic fish are significant risks for human health, while ammonia in water can intensify diseases like white spot syndrome virus in white shrimp, and increase the mortality rates of fish

under ammonia stress (Karri et al., 2018; Wang et al., 2020). These detrimental effects underscore the importance of managing ammonia levels in water bodies to protect both public health and aquatic life.

The rapid growth in population, industrialization, and agricultural intensification has led to significant chemical and biological changes in water ecosystems, disrupting the delicate balance between species and altering species' composition. Such changes can lead to a decline in biodiversity and affect the overall health of aquatic environments. While water quality monitoring remains essential, recent research emphasizes that it is not sufficient by itself to assess the health of water streams. A comprehensive understanding of ecological interactions and the maintenance of biological integrity are equally important for effective water stream health assessments (Atique & An, 2018).

Assessing the ecological health of rivers and streams is complex, requiring the consideration of various interconnected factors. These factors include physical habitat conditions, such as water chemistry, hydrological elements, structural components, and climatic factors, as well as the diversity of biotic compositions. Together, these elements contribute to the overall ecological functions of these water bodies, making accurate assessment a challenging yet essential task for environmental monitoring (Atique & An, 2018).

Ammonia poses significant risks to both human health and aquatic life due to its ability to cross cellular membranes and cause hyperammonemia, leading to elevated ammonia levels in tissues and organs. The toxic effects of ammonia primarily affect the brain, causing neurological damage, but its impact extends beyond the brain, affecting various cell types throughout the body. Additionally, ammonia toxicity can lead to structural abnormalities in the lungs, inflammatory responses, and disruptions in adrenal gland function, contributing to serious health complications (Dasarathy et al., 2017; Bae et al., 2020). Traditional laboratory-based water

quality assessments, while comprehensive, may not always be practical for continuous monitoring, highlighting the need for more efficient and accessible methods (Randhawa et al., 2016).

Traditional laboratory-based sampling methods for water quality assessment can be time-consuming, often taking several days to produce results, and may not always offer the accuracy needed for real-time monitoring. This limitation has led to growing interest in real-time environmental monitoring sensors, which leverage advancements in sensor technology. These sensors enable continuous data collection, providing real-time monitoring of river ecosystem health, detecting environmental events, and identifying trends. The versatility and control offered by real-time sensor platforms make them invaluable for applications such as pollution monitoring, assessing both short-term and long-term environmental impacts, and supporting operational tasks in various industries.

Several techniques are available for assessing water quality, each with its own advantages and limitations. These include the Spectrophotometric Indophenol Blue (IPB) method, fluorescence detection, colorimetric pH detection using colorimetric films, fiber-optic detection, metal oxide-based sensors, electrochemical detection, surface acoustic wave (SAW) sensors, and field-effect transistor (FET) sensors. Each method has been developed for specific applications, offering various levels of sensitivity, accuracy, and practicality, which will be compared and discussed in the context of this research.

2.4.1 Spectrophotometric IPB (Indophenol Blue) Method

Chemical substances such as phenol, ammonia, and hypochlorite are commonly used in spectrophotometric detection methods for ammonia. When combined, these chemicals undergo a reaction where ammonia is oxidized to chloramine under alkaline conditions. The chloramine then reacts with phenol, leading to a color change that correlates with the ammonia concentration. The intensity of the color change is directly proportional to the concentration of ammonia, making this method an effective approach for detecting varying levels of ammonia in water samples (Li et al., 2020).

2.4.2 Fluorescence Detection

In an alkaline environment, ammonia nitrogen reacts with o-phthalaldehyde (OPA) and sodium sulfite to form a fluorescent compound. This compound emits light at a specific wavelength and intensity when exposed to external energy, with the emitted light intensity being directly proportional to the ammonia concentration. As a result, different ammonia concentrations generate varying light intensities and colors, providing a reliable method for ammonia detection (Li et al., 2020).

2.4.3 Colorimetric pH Detection using Colorimetric Films

This method utilizes colorimetric films designed to detect low concentrations of gaseous ammonia within a waveguide structure. The films, which consist of a pH indicator specific to

ammonia embedded in a polymeric matrix, are applied to an optical waveguide to enhance sensitivity. A plasticizer is added to ensure the flexibility of the film without compromising its integrity. The films are attached to glass waveguides to assess their gas sensing capabilities and optical properties. The study also explores the impact of the pH indicator and matrix composition on the films' gas sensing performance, showing excellent selectivity and cross-selectivity for ammonia detection (Courbat et al., 2009).

2.4.4 Fiber Optic Detection

Light functions as a carrier for sensitive data, with optical fibers acting as the medium to direct and transmit data between locations. The fiber-optic detection mechanism operates by transmitting light rays from a source through an incident optical fiber to the modulation area, where they interact with the measured parameters. The light signal is then sent to a demodulator and photodetector via the outgoing fiber to record the measurements. Variations in ammonia concentrations are detected by observing changes in the physical and chemical interactions between ammonia and the coating materials, which influence the optical properties (Li et al., 2020).

2.4.5 Metal Oxide Based Sensors

Metal oxides are categorized into p-type and n-type semiconducting metal oxides, both exhibiting positive electrical properties within a temperature range of 250°C to 550°C. N-type semiconducting metal oxides are generally favored for gas detection due to their superior sensing response compared to p-type semiconducting metal oxides, as well as their interaction with the

latter. The electronic structure of the metal oxide is crucial in selecting the right material for detecting specific gases and is essential for understanding the gas sensing mechanism (Kwak et al., 2019).

2.4.6 Electrochemical detection

Electrochemical analysis is a technique used to determine the composition of a substance by evaluating its electrochemical properties in a solution. This method offers several benefits for ammonia detection in water, including ease of use and faster detection times (Li et al., 2020).

2.4.7 Surface acoustic wave (SAW) Sensors

A typical surface acoustic wave (SAW) gas sensor setup consists of two interdigitated transducers (IDTs) placed on piezoelectric substrates, such as lithium niobate or quartz, with a delay line situated between the transducers (Kwak et al., 2019). These IDTs, usually made from noble metals like platinum or gold, function as both receiving and transmitting transducers for the SAW. The sensor operates by detecting changes in the surface velocity or amplitude of the wave, which occur due to interactions between the analyte gases and the delay line (Kwak et al., 2019).

2.4.8 Field-effect transistor (FET) Sensors

This type of sensor is based on the metal-insulator-semiconductor (MIS) junction structure and detects gas presence by measuring changes in the current-voltage (I-V) characteristics of the device. The metal-oxide-semiconductor field-effect transistor (MOSFET) model is commonly used in this type of sensor. The gate of the MOSFET, which plays a key role in gas detection, is made from a gas-sensitive film typically composed of catalytic metals such as platinum, palladium, and iridium. The selectivity of these sensors is largely determined by the electrical properties of these metals, with palladium, platinum, and iridium or their combinations being widely used for ammonia sensing. The physical properties, including morphology, film thickness, and structure, of these metals are critical for enhancing the sensor's sensitivity to ammonia (Kwak et al., 2019).

2.4.9 TiO_2 + UV Light + Fuzzy Logic

This research utilizes titanium dioxide, placing it within the category of metal oxide sensors, but with the addition of UV light to enhance detection capabilities. Additionally, a fuzzy logic system is integrated to improve the accuracy of the results. This distinguishes our approach from current methods, which do not incorporate a fuzzy logic system for enhanced performance.

2.4.10 Table of Ammonia Detection Method

Table 2.2: Overview of Various Methods for Ammonia Detection

No	Type	Method
1	Spectrophotometric IPB (Indophenol Blue) Method	This method involves using chemical substances like ammonia, phenol, and hypochlorite, which react to produce color changes that correspond to varying concentrations of ammonia.
2	Fluorescence Detection	In an alkaline medium, ammonia nitrogen reacts with o-phthalaldehyde (OPA) and sodium sulfite to form a fluorescent compound, with varying ammonia concentrations emitting light of different colors.
3	Colorimetric pH Detection using Colorimetric Films	The study evaluates the performance of colorimetric films, adhered to glass waveguides, for detecting low concentrations of gaseous ammonia and assessing their gas-sensing capabilities.
4	Fiber Optic Detection	Ammonia concentrations can be detected by monitoring the changes in the chemical or physical reactions between ammonia and the coating materials, which subsequently affect the optical properties.
5	Metal Oxide Based Sensors	The electronic structure of the metal oxide is a key factor in selecting an appropriate metal oxide for detecting specific gases and is essential for understanding the sensing mechanism.

6	Electrochemical detection	Electrochemical analysis involves determining the composition of a substance by examining its electrochemical properties in a solution, making it a valuable method for detecting ammonia in water.
7	Surface acoustic wave (SAW) Sensors	The working principle of a Surface Acoustic Wave (SAW) gas sensor involves detecting changes in the velocity or amplitude of the wave, which are caused by the interaction between the analyte gases and the delay line.
8	Field-effect transistor (FET) Sensors	This type of sensor utilizes the basic structure of a metal-insulator-semiconductor (MIS) junction and measures changes in the I-V (current-voltage) characteristics of the device caused by the presence of a specific analyte for gas detection.
9	TiO_2 + UV Light + Fuzzy Logic	This research utilizes titanium dioxide, placing it within the category of metal oxide sensors, but enhances detection by incorporating UV light and improves accuracy through the integration of fuzzy logic.

There are various methods for detecting ammonia, each utilizing different principles and technologies. The Spectrophotometric Indophenol Blue (IPB) Method relies on chemical reactions that produce color changes based on ammonia concentration. Similarly, Fluorescence Detection uses a reaction between ammonia and o-phthalaldehyde (OPA) to form fluorescent compounds, where different concentrations emit different colors. Colorimetric pH Detection employs colorimetric films attached to glass waveguides to sense low concentrations of gaseous ammonia. Advanced optical techniques include Fiber Optic Detection, which monitors changes in optical properties due to reactions between ammonia and coating materials. Metal Oxide-Based Sensors utilize changes in electronic structures to detect ammonia, while Electrochemical Detection analyzes electrochemical properties in solutions to determine ammonia presence in

water. Surface Acoustic Wave (SAW) Sensors measure changes in wave velocity or amplitude when ammonia interacts with the sensor's delay line. Other modern approaches include Field-Effect Transistor (FET) Sensors, which detect ammonia by measuring changes in current-voltage characteristics of a metal-insulator-semiconductor (MIS) junction. Finally, a hybrid method using TiO_2 with UV Light and Fuzzy Logic enhances metal oxide sensors with UV light exposure and improves accuracy through fuzzy logic integration. These diverse methods highlight the wide range of techniques available for ammonia detection, each suited to different applications and sensitivity levels.

2.5 FUZZY LOGIC

In 1965, Lotfi A. Zadeh introduced Fuzzy Logic while serving as a computer science professor at the University of California, Berkeley (Hellmann, 2001). This concept has since become a valuable technique in controlling complex systems and industrial processes, enabling the creation of computational models that can perform reasoning and problem-solving tasks similar to human-like intelligence (Yen, 1999). Fuzzy Logic extends classical Boolean logic by incorporating degrees of truth, moving beyond the binary true/false states to allow for more nuanced conditions (Zadeh, 1988). This makes it an important tool for systems that require decision-making capabilities in uncertain or complex environments.

Fuzzy Logic, as defined by Webster's Dictionary, refers to the systematic application of formal reasoning principles, where specific examples are treated as instances of broader principles (Zadeh, 1988). It is rooted in the mathematical theory of fuzzy sets, which generalizes classical set theory. By allowing conditions to exist in varying degrees, Fuzzy Logic enables more flexible and accurate decision-making in a variety of fields, including industrial applications and advanced control systems (Dernoncourt, 2013; Mittal et al., 2020).

Mathematical models are broadly classified into three main types: analytical, semi-analytical, and empirical models. Analytical models describe processes using solutions to nonlinear partial differential equations and often make various assumptions about simultaneous momentum, heat, and mass transfer. Although these models offer theoretical insights, they are complex and challenging to implement in practical systems. On the other hand, empirical models are derived from experimental data without assuming any underlying phenomena, but their applicability is generally limited to specific materials and conditions. Practical application of these models also involves dealing with challenges such as identifying inaccuracies in predictions, performing sensitivity analysis, and understanding model parameters. In cases where complexity and uncertainty are prevalent, fuzzy logic offers a valuable tool for modeling, prediction, optimization, diagnosis, monitoring, and control, particularly in processes like drying (Hosseinpour & Martynenko, 2022).

Fuzzy logic provides a distinct approach to addressing classification and control problems, focusing more on the desired outcomes rather than modeling every internal process. It requires expert knowledge to define rule bases, combine sets, and perform defuzzification (Hellmann, 2001). Unlike traditional systems, fuzzy logic excels in capturing the uncertainty and vagueness that are inherent in human decision-making, particularly in complex environments (Zadeh, 1988). It effectively bridges human reasoning and concept formation through linguistic rules, enabling the control of nonlinear systems and estimation of functions. One of the key advantages of fuzzy logic models is their ability to handle uncertainty and complexity, even when there is limited experimental data or partial expert knowledge. However, a significant limitation is that the complexity of fuzzy logic systems increases as the number of inputs rises, making the selection of relevant variables and managing their interrelations more difficult (Hosseinpour & Martynenko, 2022).

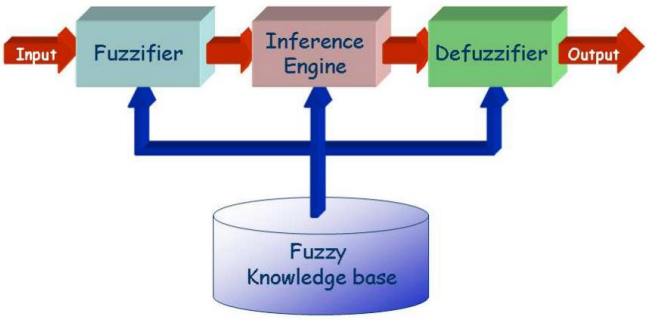

Figure 2.5: A Conceptual Diagram Illustrating The Structure of A Fuzzy System (Dernoncourt, 2013).

Fuzzy logic can be viewed as an attempt to formalize and automate two key human capabilities: the ability to communicate and make decisions in environments characterized by uncertainty, conflicting information, and incomplete data, and the capacity to perform various mental and physical tasks without the need for precise measurements (Zadeh, 2008). Its strength lies in its flexibility, enabling a wide range of mappings and offering limitless possibilities (Mendel, 1995). One of the most effective and widely applied techniques derived from fuzzy sets is the fuzzy if-then rule, which has seen success across diverse industries such as medical imaging, consumer products, automotive control, manufacturing, robotics, process control, financial trading, and medical expertise (Phuong & Kreinovich, 2001). These rules connect conditions based on linguistic variables to infer conclusions (Yen, 1999).

The process of creating a fuzzy logic system involves several key steps: selecting relevant data, fuzzifying input variables using membership functions, applying fuzzy inference through rule-based operations with fuzzy logic operators, and finally, performing defuzzification using the centroid method.

2.5.1 Data Selection

Data selection is the process of gathering relevant data and organizing it into a structured table. A minimum of two input variables is required, as they need to be combined to generate the output. These input variables can represent various parameters, but they must be numerical to ensure accurate processing and analysis.

2.5.2 Fuzzification of input variables using membership function

A membership function of a fuzzy set is a visual representation that illustrates and shows how each point within the input space, usually known as the "universe of discourse" is associated with a membership value ranging from 0 to 1. This graph gives a clear mapping and explanation of how every element relates to the degree of belonging to the fuzzy set.

In this example, the process of mathematically deriving the fuzzy logic procedure is elucidated. The fuzzy set symbolized as "Ã" within the universe of information "U" is described as a collection of ordered pairs. This definition can be mathematically expressed using Equation (1).

$$\tilde{A} = \{(y, \mu_{\tilde{A}}(y)) \mid y \in U\} \quad (1)$$

In Equation (1), the parameters can be described as follows: The parameter " $\mu_{\tilde{A}}$ " represents the membership function of the set Ã. The values of the membership function range

from 0 until 1, symbolized as " $\mu_{\tilde{A}} \in [0,1]$." This membership function " $\mu_{\tilde{A}}$ " maps the elements of the universal set U to the membership space M. The symbol "●" within the membership function denotes elements within the fuzzy set, which can be either continuous or discrete. When it comes to the membership function, there are 3 key factors that need to consider.

In the membership function, it is separated into 3 distinct segments that shape the characteristics of the function that is called the core, the support, and the boundary. For any given fuzzy set " Ã ", the core of the membership function pertains to the portion of the universe of discourse where full membership in the set is evident. The core encompasses all elements "y" for which the universe of information can be explained by Equation (2).

$$\mu_{\tilde{A}}(y) = 1 \tag{2}$$

Next, for any fuzzy set " Ã ", the support of a membership function corresponds to the part of the universe where there is a non-zero membership in the set. In other explanation, the support covers all elements "y" within the universe of information that are explained in Equation (3).

$$\mu_{\tilde{A}}(y) > 0 \tag{3}$$

Then, the third segment is referred to as the "boundary element". In the context of any fuzzy set " Ã ", the boundary of a membership function illustrates the portion of the universe where there is a non-zero but not fully complete membership in the set. In simpler explanation, the boundary encompasses all elements "y" within the universe of information that can be explained using Equation (4).

$1 > \mu_{\tilde{A}}(y) > 0$ (4)

After that, the process of fuzzification was performed for both input and output using membership functions. Fuzzification, in this context, is expressed as the procedure of converting a crisp set into a fuzzy set or transforming a fuzzy set into an even fuzzier set. There are 2 distinct methods of fuzzification: the support fuzzification (s-fuzzification) method and the grade fuzzification (g-fuzzification) method.

In the first type of fuzzification, known as support fuzzification, crisp values are converted into fuzzy sets according to Equation (5).

$$\tilde{A} = \mu_1 Q(x_1) + \mu_2 Q(x_2) + \ldots\ldots\ldots + \mu_n Q(x_n) \quad (5)$$

In Equation (5), the fuzzy set described as " $\tilde{A}$ " stands the core element of the fuzzification process. This mechanism is employed with the presumption that the underlying process of fuzzification with "μ_i" stay remains constant and "x_i" is transformed into a fuzzy set $Q(x_i)$.

The second type of fuzzification, known as g-fuzzification or grade fuzzification, is developed based on Equation (6). It assumes that "x_i" remains constant and "μ_i" is expressed as a fuzzy set.

$$\tilde{A} = x_1 Q(\mu_1) + x_2 Q(\mu_2) + \ldots\ldots\ldots + x_n Q(\mu_n) \quad (6)$$

After collecting the data, it is converted into a membership function for fuzzification, commonly using trapezoidal, triangular, or Gaussian membership functions.

2.5.2.1 *Trapezoidal Membership Function for Fuzzification*

The trapezoidal function is defined by Equation (7).

$$Trapeziodal\ function = \begin{cases} 0, & x < a \\ \frac{x-a}{b-a}, & a \le x \le b \\ 1, & b \le x \le c \\ \frac{d-x}{d-c}, & c \le x \le d \\ 0, & d < x \end{cases} \quad (7)$$

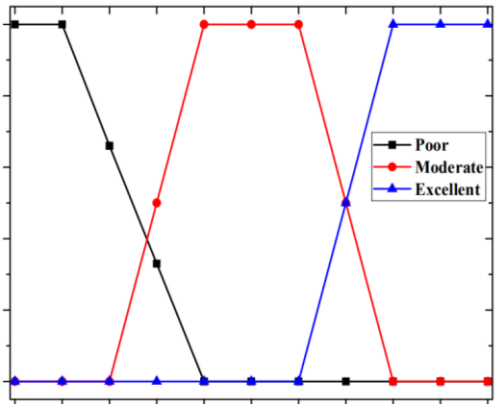

Figure 2.6: The Basic Graph of a Trapezoidal Membership Function Derived From A Trapezoidal Membership Function (Bakar Et Al., 2020).

In Equation (7), the variable x displays a real value, which is a precise or crisp value within the universe of discourse. The parameters "a," "b," "c," and "d" indicate the x-coordinates of the four endpoints that specify the trapezoidal shape. These values must satisfy the following conditions:

$$a<b<c<d \tag{8}$$

In the equation (7), when the real value in the variable "x" is less than the point "a," it contributes to a zero degree of the membership function. Then, when "x" falls between the points "a" and "b," the degree of membership slowly increases as it approaches "b." After that, for real values residing between "b" and "c," the degree of membership reaches its maximum value of 1. Meanwhile, for values falling between "c" and "d," the membership decreases as it approaches "d," eventually converging to zero. When the "x" variable exceeds over the point "d," the membership degree becomes zero.

2.5.2.2 *Triangle Membership Function for Fuzzification*

The triangular function is characterized by Equation (9).

$$Triangle\ function = \begin{cases} 0, & x < a \\ \dfrac{x-a}{b-a}, & a \le x \le b \\ \dfrac{c-x}{c-b}, & b \le x \le c \\ 0, & c < x \end{cases} \quad (9)$$

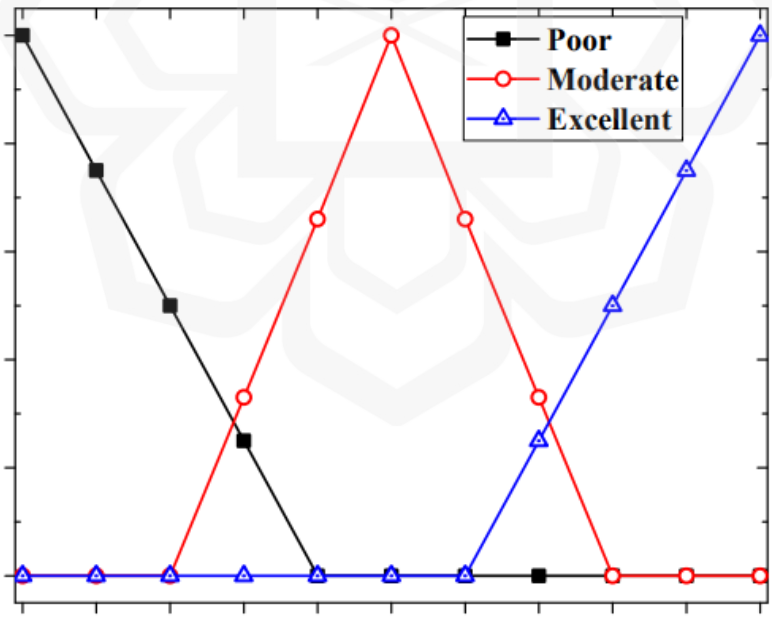

Figure 2.7: The Basic Graph of a Triangular Membership Function Derived From a Triangular Membership Function (Bakar Et Al., 2020).

The parameters "a," "b," and "c" indicate the x-coordinates that interpret a triangular shape. "x" represents the real value from the fuzzy universe of discourse for the private variable. The function's output ranges from 0 to 1, appear for the degree of membership of "x." Particularly, the point "b" corresponds to a membership degree of 1.

As "x" moves from "a" to "b," the membership degree of elements slowly increases, and keep approaching 1. On the other hand, when "x" falls between "b" and "c," the membership degree decreases slowly as it approaches "c." The fulfilment of these conditions is explained by Equation (10).

a<b<c (10)

2.5.2.3 ***Gaussian Membership Function for Fuzzification***

The Gaussian function is defined by Equation (11).

$$Gaussian\ function = \begin{cases} e^{-\frac{(x-c)^2}{2\sigma^2}} \end{cases} \quad (11)$$

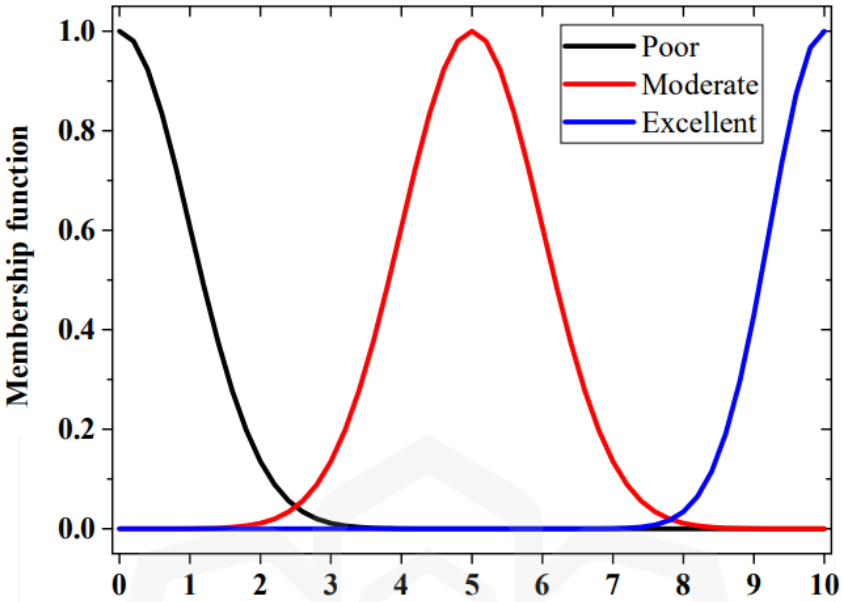

Figure 2.8: The Basic Graph of a Gaussian Membership Function Derived From a Gaussian Membership Function (Bakar Et Al., 2020)

In the Equation (11), the parameter "σ" stand for the standard deviation, and "c" denotes the mean value for the Gaussian membership function. Membership values are calculated for each input value within "x".

The Gaussian function is widely used among various membership functions for various compelling reasons. Ther are:

1. The function is smooth, making it suitable for dealing with continuous values.
2. It is easy and uncomplicated, not requiring multiple options or conditions compared to other functions.

3. All values formulated and derived from the Gaussian function are non-zero, offering consistent and non-null results.

After completing the fuzzy membership, the next step is fuzzy interference. Fuzzy interference is important to define the algorithm to interact and combine the inputs to become the output.

2.5.3 Fuzzy Inference Process using Rule Base Approach

Fuzzy logic operators function similarly to Boolean logic but incorporate membership values to handle uncertainty. The synthesis of fuzzy logic functions introduces minimum and maximum components through a straightforward algorithm. A fuzzy logic function is essentially a combination of these minimum components, where each represents a set of variable combinations within the domain that meet or exceed the function value for that specific domain.

Table 2.3: A Comparative Analysis of Boolean Logic and Fuzzy Logic

Boolean	Fuzzy
AND (x, y)	MIN (x, y)
OR (x, y)	MAX (x, y)
NOT (x)	1 – x

The fuzzy inference system is the core component of a fuzzy logic system, responsible for facilitating reliable decision-making. It operates by applying IF-THEN rules that incorporate logical operators such as AND and OR, making it essential for formulating effective decision rules.

In both fuzzy logic and classical, there are three fundamental operations on fuzzy sets: intersection, union, and complement.

(i) For the union operator: Consider "μ_A" and "μ_B" as membership functions describing the fuzzy sets A and B, respectively, within the universe X. The union of these fuzzy sets A and B is described as by a new fuzzy set, defined by the membership function outlined in Equation (12).

$$\mu_{A \smile B}(x) = \text{Max}\,(\mu_A(x), \mu_B(x)) \quad (12)$$

(i) In reference to the intersection operator: Given the membership functions " μ_A" and "μ_B" that identify the fuzzy sets A and B, respectively, within the universe X, the result of integrate these fuzzy sets A and B using the intersection operation is a new fuzzy set. This new fuzzy set is characterized by the membership function outlined in Equation (13).

$$\mu_{A \frown B}(x) = \text{Min}\,(\mu_A(x), \mu_B(x)) \quad (13)$$

(i) Regarding the complement operator: Suppose " μ_A" is the membership function that describes the fuzzy set A in the universe X. The complement of the set A

results in a new fuzzy set, identify by the membership function provided in Equation (14).

$$\mu_A{}^c(x) = 1 - \mu_A(x) \quad (14)$$

Fuzzy inference systems consist of five key components that work together to generate trusty decisions, starting from crisp inputs and leading to crisp outputs. These components are explained as follows:

(ii) Rule base: This part defines the IF-THEN rules that command the behaviour of the fuzzy system.

(iii) Fuzzy database: It outlines the membership functions related with fuzzy sets used in these rules.

(iv) Decision-making unit: This element is in charge for executing rule computations.

(v) Fuzzification interface unit: This component operates the modification of precise values into fuzzy representations.

(vi) Defuzzification Interface Unit: This element supervises the transformation of fuzzy representations back into precise, crisp values.

The fuzzification unit is essential for implementing various fuzzification techniques, converting crisp inputs into fuzzy inputs. Once the inputs are transformed, a knowledge base—comprising a database and a rule base—is established to guide the decision-making process. Finally, the defuzzification unit converts the fuzzy output back into a precise, crisp value.

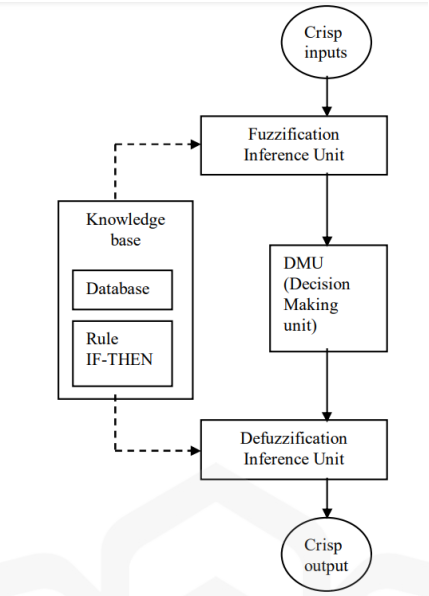

Figure 2.9: A Block Diagram Representing the Structure of a Fuzzy Inference System (Bakar Et Al., 2020)

2.5.4 Defuzzification

Defuzzification is the process of converting fuzzy set outputs into a single numerical value, ensuring that the results of fuzzy inference are translated into clear and precise outputs. The primary objective of defuzzification is to extract a crisp value from a fuzzy membership function, allowing the system to produce interpretable and actionable results. This step is essential in fuzzy logic systems, as it bridges the gap between fuzzy reasoning and real-world applications.

When a crisp output is required, selecting an appropriate defuzzification method becomes crucial. The choice of method depends on the specific application and the nature of the fuzzy system. Different defuzzification techniques exist, each with its advantages in various contexts,

such as control systems, decision-making, and optimization processes (Tóth-Laufer & Takács, 2012).

Several common defuzzification methods are used in fuzzy logic systems to convert fuzzy outputs into precise, crisp values. These techniques are essential for translating fuzzy decision-making processes into actionable results applicable in real-world scenarios. Some of the most widely used defuzzification methods include:

2.5.4.1 *Centroid*

The centroid method evaluates the average position or center of mass of the fuzzy set R. It does so by taking into consideration the weighted average of positions (r) based on their membership degrees $\mu_{\tilde{R}}(r)$. The numerator appears for the weighted sum of positions, and the denominator is the sum of the membership degrees, securing a balance between membership strength and position.

$$\bar{x} = \frac{\int r \cdot \mu_{\tilde{R}}(r)\, dr}{\int \mu_{\tilde{R}}(r)} \quad (1)$$

2.5.4.2 *Weighted-Average Method*

In the weighted average method, every point of (r) is times by a weight function (w(r)) before calculating and evaluating the weighted average. This authorizes for a customized influence of every point on the result. The weights may act as the significance and importance of different positions in the fuzzy set.

$$\bar{x} = \frac{\int w(r) \cdot r \cdot u_R(r)\, dr}{\int w(r) \cdot u_R(r)\, dr} \tag{2}$$

2.5.4.3 *Mean of Centre Method*

The mean of centers method recognizes the maximum membership degree at each position and calculates the average position of these maxima. It captures the central tendency of the most significant parts of the fuzzy set, emphasizing the positions with the highest membership degrees.

$$\bar{x} = \frac{\int r \cdot \max\left(\mu_R(r)\right) dr}{\int \max\left(\mu_R(r)\right) dr} \tag{3}$$

2.5.4.4 *Modified Height Method*

The modified height method is a modification of the weighted average method where the weight h(r) at every position is the height of the membership function. This method gives more crucial to the higher parts of the fuzzy set, allowing for a sharp focus on the regions where membership is stronger.

$$\bar{x} = \frac{\int h(r) \cdot r \cdot u_R(r)\, dr}{\int h(r) u_R(r)\, dr} \tag{4}$$

2.5.4.5 *Centre of Maximum*

The center of maximum method is alike to the centroid method, but it precisely focuses on the point of maximum membership degree. The result is the position and point where the membership function is most intense, appearing for the highest influential part of the fuzzy set.

$$\bar{x} = \frac{\int r \cdot \mu_R(r)\, dr}{\int \mu_R(r)\, dr} \tag{5}$$

2.5.4.6 *Centre of Sum (COS)*

The center of sum method is almost identical to the centroid method, calculating and evaluating the center of mass by taking into account the sum of positions weighted by their membership degrees. This method is comparable to the centroid but without considering the center of gravity, making it a straightforward and easy calculation of the average position.

$$\bar{x} = \frac{\int r \cdot \mu_R(r)\, dr}{\int \mu_R(r)\, dr} \tag{6}$$

2.5.4.7 *Modified Height Method*

The modified height method is a modification of the weighted average method where the weight h(r) at every position is the height of the membership function. This method gives more crucial to the higher parts of the fuzzy set, allowing for a sharp focus on the regions where membership is stronger.

$$\bar{x} = \frac{\int h(r) \cdot r \cdot \mu_R(r)\, dr}{\int h(r) \cdot \mu_R(r)\, dr} \tag{7}$$

2.5.4.8 *Table Defuzzification Method*

Table 2.4: A Comprehensive Collection of Summaries on Various Defuzzification Methods.

No	Type	Method
1	Centroid	The centroid method evaluates the average position or center of mass of the fuzzy set
2	Weighted-Average Method	In the weighted average method, every point of (r) is time by a weight function (w(r)) before calculating and evaluating the weighted average
3	Mean of Centre Method	The mean of centers method recognizes the maximum membership degree at each position and calculates the average position of these maxima.
4	Modified Height Method	The modified height method is a modification of the weighted average method where the weight h(r) at every position is the height of the membership function.
5	Centre of Maximum	The center of maximum method is alike to the centroid method, but it precisely focuses on the point of maximum membership degree.
6	Centre of Sum	The center of sum method is almost identical to the centroid method, calculating and evaluating the center of mass by taking into account the sum of positions weighted by their membership degrees
7	Modified Height Method	The modified height method is a modification of the weighted average method where the weight h(r) at every position is the height of the membership function.

Defuzzification methods are techniques used to convert fuzzy values into precise numerical outputs. The Centroid Method determines the center of mass of a fuzzy set, while the Weighted-Average Method assigns weights to values before calculating the average. The Mean of Centre Method focuses on the positions with the highest membership degrees and averages them. The Modified Height Method, a variation of the weighted-average method, assigns weights based on the height of the membership function. The Centre of Maximum Method is similar to the centroid method but specifically targets the point with the highest membership degree. Lastly, the Centre of Sum Method calculates the center of mass by summing positions weighted by their membership degrees. These methods help refine fuzzy logic outputs for more accurate decision-making.

2.6 CHEMICAL REACTION OVERVIEW

Reaction in Ammonia

Anode Reaction: $NH_3 + 3OH^- \rightarrow 1/2N_2 + 3H_2O + 3e^-$

Cathode Reaction: $3H_2O + 3e^- \rightarrow 3/2H_2 + 3OH^-$

Reaction in Water

Anode Reaction: $4OH^- \rightarrow O_2 + 2H_2O + 4e^-$

Cathode Reaction: $4H_2O + 4e^- \rightarrow 2H_2 + 4OH^-$

The electron donation process in ammonia differs from that in water, leading to variations in the voltage produced when UV rays penetrate the TiO_2 surface. This research anticipates that

the voltage generated from ammonia solution and water will exhibit distinct characteristics due to their differing electron donation capabilities.

Additionally, the concentration of ammonia plays a crucial role in influencing the electron donation process during the reaction. A higher ammonia concentration is expected to enhance electron donation, subsequently increasing the overall voltage output.

2.7 CONCLUSION

There are various methods available for ammonia detection; however, this research introduces a novel approach that uniquely integrates TiO_2, UV rays, and fuzzy logic. Unlike conventional devices that do not incorporate fuzzy logic, this study offers an innovative advantage. TiO_2 functions as a sensor to detect ammonia concentration, while UV rays act as a catalyst to enhance the detection capability of the TiO_2 sensor. Fuzzy logic is utilized to predict voltage output through forward calculation and estimate ammonia concentration via reverse calculation in a short time.

This aligns with the objective of this research, which is to develop a portable, self-sustained sensor for measuring water toxicity. The proposed instrument must be compact, low-cost, user-friendly, and capable of rapid testing (Zhang et al., 2019). Additionally, it should be simple to operate (Zoerner et al., 2018), easily accessible, quick to learn, and highly portable (Alhazmi et al., 2020).

CHAPTER THREE

RESEARCH METHODOLOGY AND EXPERIMENT

3.1 OVERVIEW

This chapter will study the construction consideration of the UV monitoring system and fuzzy logic execution. It includes the clarification in details of the TiO_2 photo sensor in reacting the presence of UV light to generate a small amount of output voltage and the calculation of fuzzy logic system.

This research is divided into two parts. The first part focuses on the preparation of TiO_2. This chapter will detail the experimental procedure, which involves adding varying concentrations of ammonia to TiO_2 and observing the resulting effects. Then radiate UV ray to the TiO_2 and lastly collect the voltage reading. After that, repeat the same method of experiment by using different distances of UV ray from TiO_2. This voltage and the distance will be use as the input at the fuzzy logic calculation later on.

The second part is execution of fuzzy logic. This section will explain the process of performing fuzzy logic calculations, starting with the fuzzy membership function, followed by fuzzy inference, and concluding with defuzzification. The voltage and distance of UV ray from TiO_2 will be use as inputs and the output will be the prediction of ammonia concentration.

3.2 EXPERIMENT OF TiO_2

The considered design of the system will consist of three parts which is the TiO_2 photosensor sensor, the concentration of ammonia and the voltage measurement. The flow of the system and the items and apparatus for the experiment is based on the figure below.

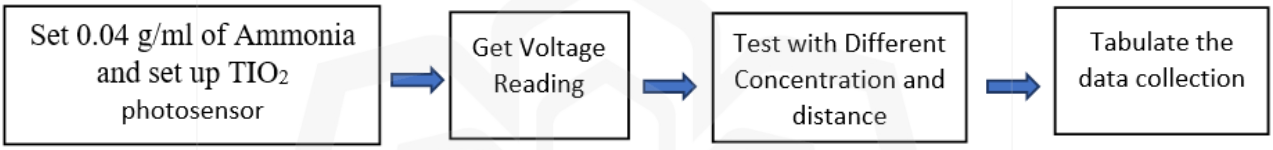

Figure 3.1: A Detailed Block Diagram Illustrating the Process of Ammonia Detection Using TiO_2, Enhanced by Ultraviolet (UV) Rays

3.2.1 The Titanium Dioxide (TiO_2) Photo Sensor

This section elucidates the TiO_2 photosensor utilized for detecting and evaluating ultraviolet (UV) light to generate a small amount of electricity. The TiO_2 photosensor is designed and structured based on a photoelectrochemical (PEC) configuration. It comprises a platinized fluorine tin oxide (FTO) coated glass substrate serving as the counter electrode in the PEC structure. A layer of platinum (Pt) with a thickness of 100 nm is deposited onto the FTO-coated glass substrate using a thermal evaporator. The platinized FTO-coated glass substrate, acting as the counter electrode, is sandwiched with the deposited TiO_2 layer on another FTO-coated glass substrate, which serves as the electrode. A spacer or sealing material is placed between these electrodes. The inner side of the spacer material is filled with a solution of ammonia as a solvent.

Figures below is the displays the device design layout of the TiO_2 electrolyte heterojunction PEC-based UV photosensor.

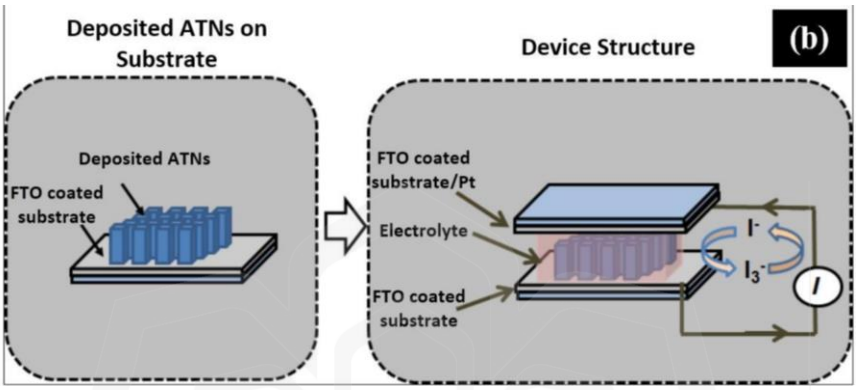

Figure 3.2: A Schematic Diagram Illustrating The Architecture Of The ATNs And The Device Structure Of The PEC-Based Ultraviolet Photosensor (Yusoff Et Al., 2018).

3.2.2 UV Flashlight

For this research, an UV flashlight is employed to radiate the TiO_2 and generate the chemical reaction in ammonia within the sensor. The UV flashlight is akin to a typical white light flashlight but radiate ultraviolet light instead. Operating within a wavelength range of 395-410nm, this standard UV flashlight radiate ultraviolet rays usually found in the market. Powered by three AAA batteries, each with a voltage of 1.5V, the UV flashlight boasts a portable and compact design.

3.2.3 Digital Multimeter

To quantify the output voltage generated by the illuminated TiO_2 photo sensor, a dedicated voltage measurement method has been devised to capture the output voltage fluctuations resulting from the chemical reaction triggered by the ammonia concentration in the sensor. For this project, voltage measurement is measured by employing a digital multimeter (DMM).

3.2.4 Circuit

Circuit is a bridge that connects TiO_2 and the DMM. It is a combination of transistor and capacitor. Capacitors help to charge and discharge TiO_2 while transistor help to stabilize the current flow.

3.2.5 Arduino

Arduino works as a data collector. It will collect voltage value from DMM and direct from circuit. These 2 inputs of data collection to make sure the data collection is accurate and not have huge gap. It can reduce the error.

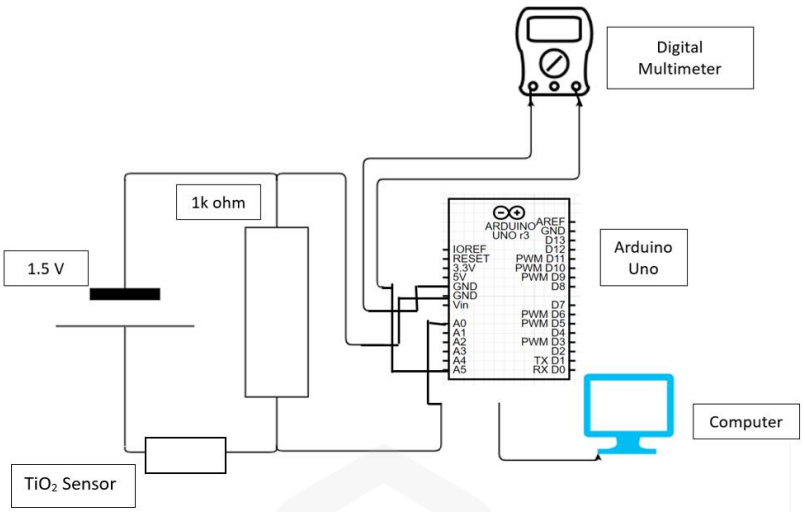

Figure 3.3: Complete Circuit Sketch of Ammonia Detection Using TiO_2 Sensor.

3.3 RESEARCH METHODOLOGY

This research is centered around four essential components: an ultraviolet (UV) light source, titanium dioxide (TiO_2), a water sample, and ammonia. The UV light source provides the necessary energy to activate the TiO_2, which acts as a photocatalyst in the detection or breakdown process. The water sample serves as the medium in which the reactions take place, while ammonia is the primary substance being analyzed. Each of these elements plays a critical role in the study, contributing to a comprehensive understanding of the system's efficiency, behavior, and overall performance in the presence of varying conditions.

3.3.1 Experiment Procedure

The procedure for conducting the experiment begins with preparing the UV light source and the TiO_2 sensor. Ensure that both the UV light source and the TiO_2 sensor are properly set up for the testing process. Next, prepare a series of ammonia concentrations ranging from 0.04 g/ml to 1 g/ml, including specific concentrations such as 0.04, 0.1, 0.14, 0.2, 0.24, 0.3, 0.4, 0.54, 0.64, 0.94, and 1 g/ml. These concentrations will be used to examine the relationship between ammonia concentration and the output voltage generated by the TiO_2 sensor.

For the first trial, place 0.04 g/ml of ammonia concentration on the TiO_2 sensor. Once the ammonia is applied, activate the UV light and direct it towards the TiO_2 sensor. The UV ray should be positioned at a distance between 3 cm and 19 cm from the sensor. The distance can be varied randomly within this range to observe the effects of UV intensity on the voltage output. After turning on the UV light, measure and record the output voltage in the data collection table for this ammonia concentration.

Once the reading for the 0.04 g/ml ammonia concentration is recorded, proceed to the next concentration. Repeat the same procedure for each of the other ammonia concentrations, ranging from 0.1 g/ml to 1 g/ml, ensuring to apply each concentration to the TiO_2 sensor, adjust the UV light distance, and record the corresponding voltage readings. This process allows for a comprehensive collection of data that will be used to analyze the impact of ammonia concentration on the voltage output of the TiO_2 sensor under the influence of UV light.

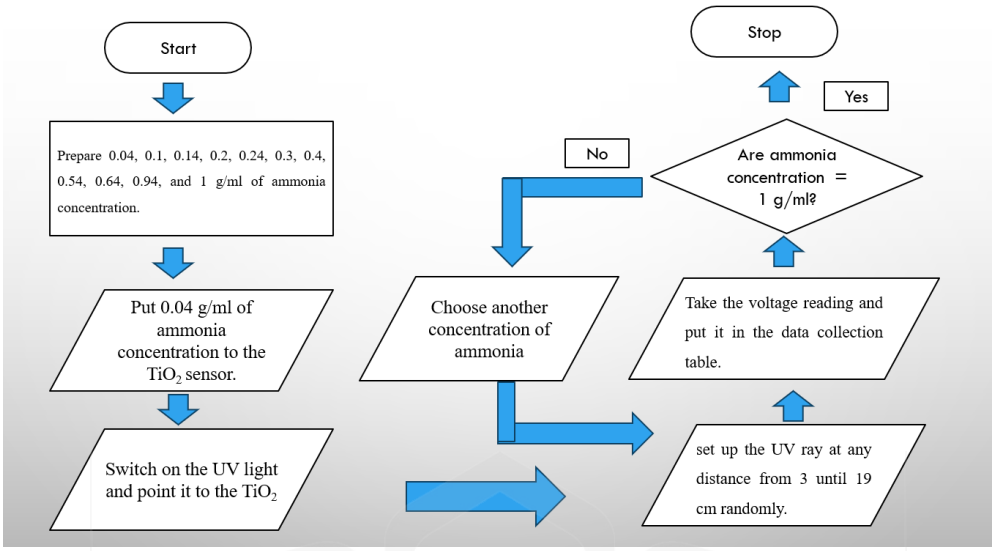

Figure 3.4: Complete Flow Chart of Experiment 1 to Test TiO_2 Sensor by Using Different Ammonia Concentration.

3.4 FUZZY LOGIC EXECUTION

This section explains methodology of classifying for ammonia concentration using fuzzy logic approach with considering 2 inputs from the above experiment that is voltage and distance of UV ray. Figure 3.4 displays the flowchart of research steps in implementing fuzzy logic for ammonia concentration performance in final examination.

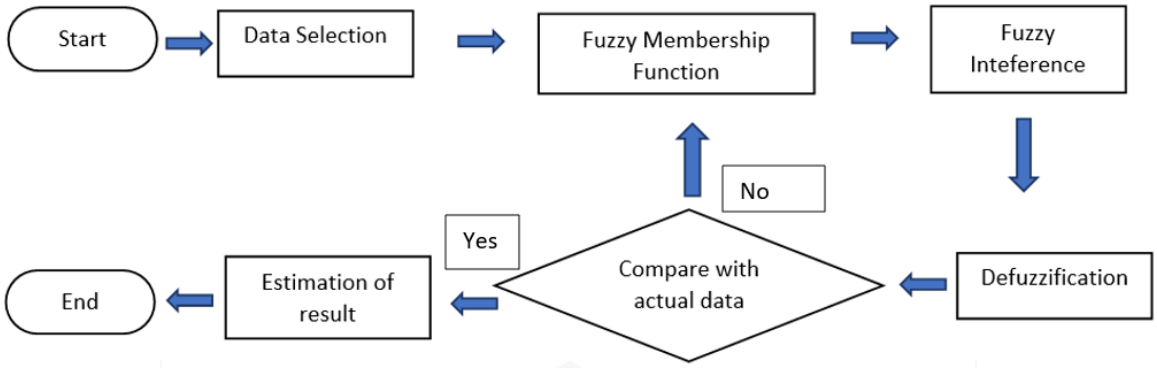

Figure 3.5: A Complete Fuzzy Logic Block Diagram Procedure for Ammonia Detection Using TiO_2 Sensor.

The analysis begins with data selection of input that is voltage and distance of UV ray, defuzzification of the 2 inputs by using fuzzy membership function, fuzzy inference by applying rule base, and defuzzification of output values. Then, the result of output from the fuzzy logic analysis will be compared again with actual data, to decrease the error of estimation.

3.4.1 Data Selection

In this study, data of distance of UV ray from TiO_2, voltage and ammonia concentration are collected from the experiment. The range of distance of UV rays from TiO_2 is set from 1 cm until 19 cm. Meanwhile, the concentration of ammonia in final examination is set from 0.04 until

1 g/ml. All of these 2 variables will be calculated in fuzzy logic in providing a robust estimation of concentration of ammonia.

3.4.2 Fuzzification of Input Variables using Membership Function

This research uses two variables input that is distance of UV rays from TiO_2 and voltage. These 2 inputs need to be transformed into membership function of fuzzy set. Fuzzification is to turn crisp inputs to become fuzzy sets. Membership function of fuzzy set is a graph that explain how each point in the input space is portray to membership value between 0 and 1. Then, this research describes the mechanism of mathematical calculation for fuzzy logic process.

3.4.3 Fuzzification, Fuzzy Interference, Defuzzification

3.4.3.1 *Fuzzification*

$$Trapeziodal\ function\ for\ low\ ammonia\ concentraion = \begin{cases} 1 & , \quad 0 \leq x < 0.25 \\ \dfrac{0.5 - x}{0.5 - 0.25} & , 0.25 \leq x < 0.5 \\ 0 & , \quad x > 0.5 \end{cases} \qquad (1)$$

$$Trapeziodal\ function\ for\ moderate\ ammonia\ concentration = \begin{cases} 0 & , \quad 0 \leq x < 0.25 \\ \dfrac{x - 0.25}{0.5 - 0.25} & , 0.25 \leq x < 0.5 \\ \dfrac{0.75 - x}{0.75 - 0.5} & , 0.5 < x < 0.75 \\ 0 & , x > 0.75 \end{cases} \quad (2)$$

$$Trapeziodal\ function\ for\ high\ ammonia\ concentration = \begin{cases} 0 & , \quad 0 \leq x < 0.5 \\ \dfrac{x - 0.5}{0.75 - 0.5} & , 0.5 \leq x < 0.75 \\ 1 & , x > 0.75 \end{cases} \quad (3)$$

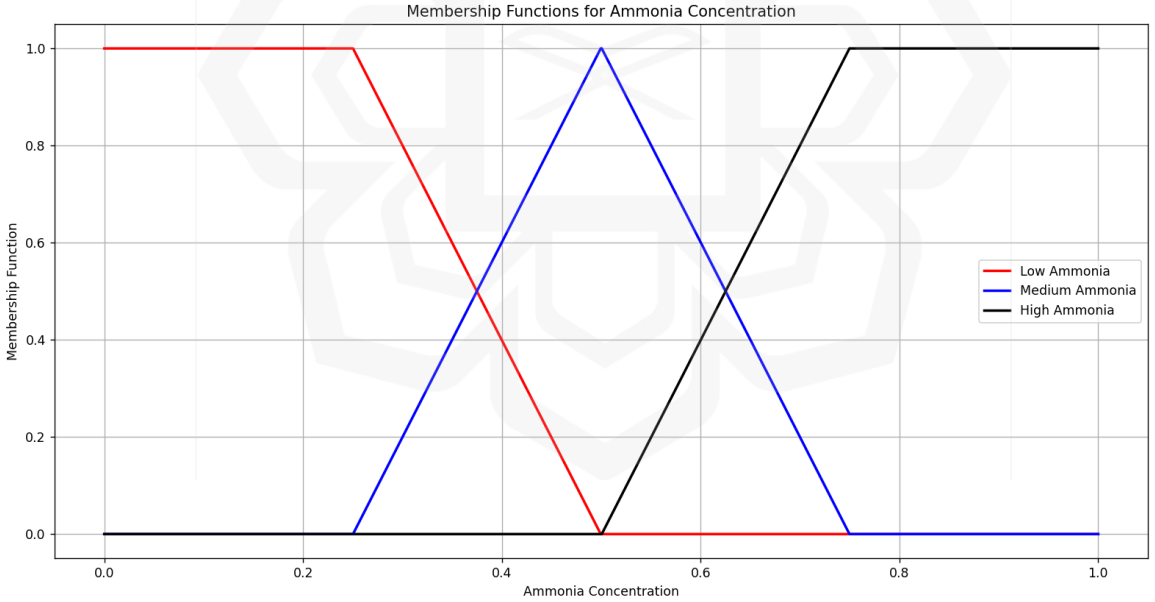

Figure 3.6: The Triangle Membership Function of Ammonia Concentration Derived from A Triangle Membership Function Formula.

Fuzzification is the process of transforming crisp numerical values into fuzzy values, allowing a system to interpret and classify continuous data within different linguistic categories. In the case of ammonia concentration, the input values are categorized into three fuzzy sets: low, moderate, and high. Each category is represented by a trapezoidal membership function, which determines the degree to which a particular ammonia concentration belongs to a specific category.

For low ammonia concentration, the membership function is designed to be fully activated (value = 1) for ammonia levels between 0 and 0.25. This means that any concentration within this range is entirely classified as low. As the ammonia concentration increases beyond 0.25, the membership degree gradually decreases, following a linear function until it reaches zero at 0.5. Beyond this point, the concentration is no longer considered low.

Moderate ammonia concentration is defined by a trapezoidal function with a peak in the middle range. At concentrations below 0.25, the membership value is zero, meaning the concentration does not belong to the moderate category. However, as the concentration increases beyond 0.25, the membership value starts to rise until it reaches its peak at 0.5, where the ammonia concentration is considered fully moderate. After this point, the membership value starts to decrease gradually and becomes zero at 0.75, indicating that the concentration has transitioned out of the moderate range.

For high ammonia concentration, the membership function remains at zero for values below 0.5, meaning ammonia levels in this range are not classified as high. However, as the concentration increases beyond 0.5, the membership value gradually rises until reaching its maximum at 0.75. Beyond this point, any further increase in ammonia concentration is classified as fully high, maintaining a membership value of 1.

Through this fuzzification process, crisp ammonia concentration values are mapped into fuzzy sets, allowing for a more flexible and adaptive interpretation of data. Instead of rigid boundaries, where a concentration is strictly classified into only one category, the fuzzy approach allows for partial membership, meaning a single concentration value can belong to multiple categories with varying degrees. This enables the system to handle uncertainties and gradual transitions more effectively, making it particularly useful in applications such as environmental monitoring, water quality assessment, and industrial ammonia detection systems.

$$Triangle\ function\ for\ low\ milivolt = \begin{cases} \frac{308 - x}{308 - 0}, & 0 \le x < 308 \\ 0, & 308 \le x \end{cases} \quad (1)$$

$$Triangle\ function\ for\ moderate\ milivolt = \begin{cases} \frac{x - 0}{308 - 0}, & 0 \le x < 308 \\ \frac{616 - x}{616 - 308}, & 308 \le x < 616 \\ 0, & 616 \le x \end{cases} \quad (2)$$

$$Triangle\ function\ for\ high\ milivolt = \begin{cases} 0, & 0 \le x < 308 \\ \frac{x - 308}{616 - 308}, & 308 \le x \le 616 \\ 1, & 616 \le x \end{cases} \quad (7)$$

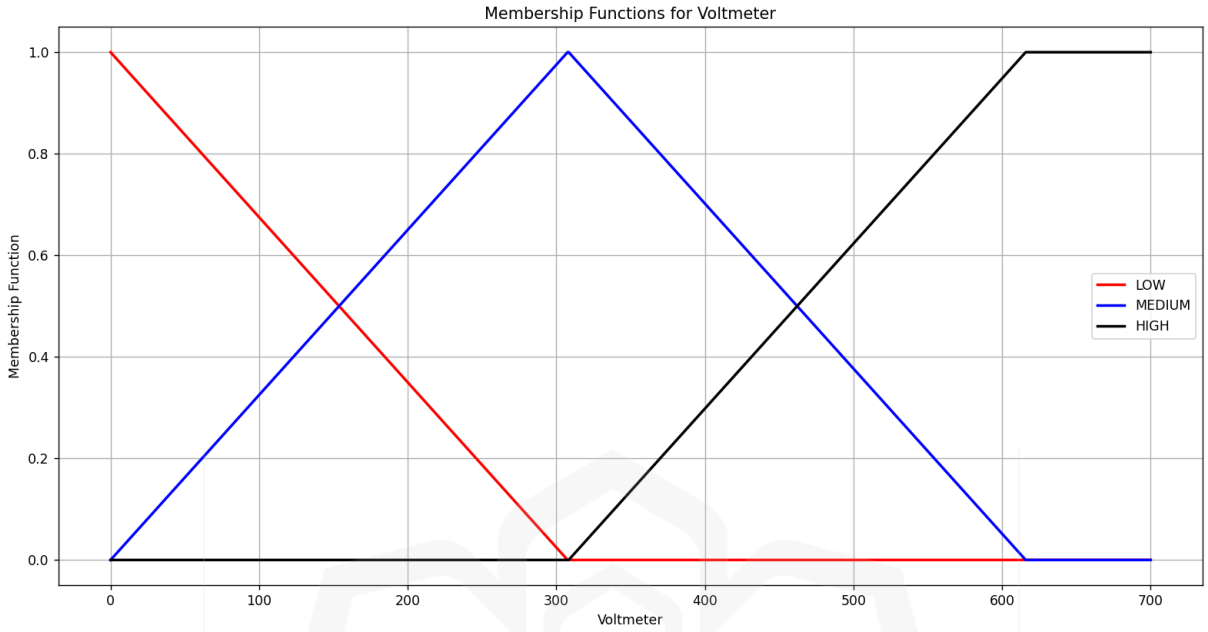

Figure 3.7: The Triangle Membership Function of Voltmeter Derived from A Triangle Membership Function Formula.

Following the same fuzzification approach used for ammonia concentration, the millivolt (mV) values are also classified into three fuzzy sets: low, moderate, and high. Each category is represented by a membership function, which determines the degree to which a specific millivolt value belongs to a given category.

For low millivolt values, the membership function follows a descending linear function from 308 mV to 0 mV. At 0 mV, the membership value is 1, indicating full classification as low. As the voltage increases, the membership degree gradually decreases, reaching 0 at 308 mV. Beyond this point, the millivolt value is no longer considered low.

For moderate millivolt values, the membership function follows a triangular shape. It starts at 0 for values below 0 mV, then increases linearly from 0 to 308 mV, where it reaches its peak membership value of 1. This indicates that at 308 mV, the voltage is fully classified as moderate. Beyond this point, the membership degree starts to decrease, reaching 0 at 616 mV. This means that voltage values above 616 mV are no longer considered moderate.

For high millivolt values, the membership function begins at 308 mV, where the membership value is 0, indicating that voltages below this threshold are not classified as high. However, as the voltage increases beyond 308 mV, the membership degree rises until it reaches 1 at 616 mV. Beyond this point, the voltage is fully classified as high.

By applying fuzzification to millivolt values, the system can handle continuous variations in voltage rather than relying on fixed thresholds. This allows for a smoother transition between categories, making the system more adaptive to gradual changes in sensor readings. Such an approach is beneficial in sensor-based applications, where real-time voltage fluctuations need to be interpreted with flexibility and precision.

$$Triangle\ function\ for\ high\ distance = \begin{cases} \frac{10 - x}{10 - 0}, & 0 \le x < 10 \\ 0, & 10 \le x \le 19 \end{cases}, \quad (1)$$

$$Triangle\ function\ for\ moderate\ distance(2) = \begin{cases} \frac{x - 0}{10 - 0}, & 0 \le x < 10 \\ \frac{19 - x}{19 - 10} & 10 \le x < 19 \end{cases}, \quad (2)$$

$$Triangle\ function\ for\ low\ concentraion = \begin{cases} 0, & 0 \le x < 10 \\ \dfrac{x-10}{19-10}, & 9 \le x \le 19 \end{cases}, \quad (3)$$

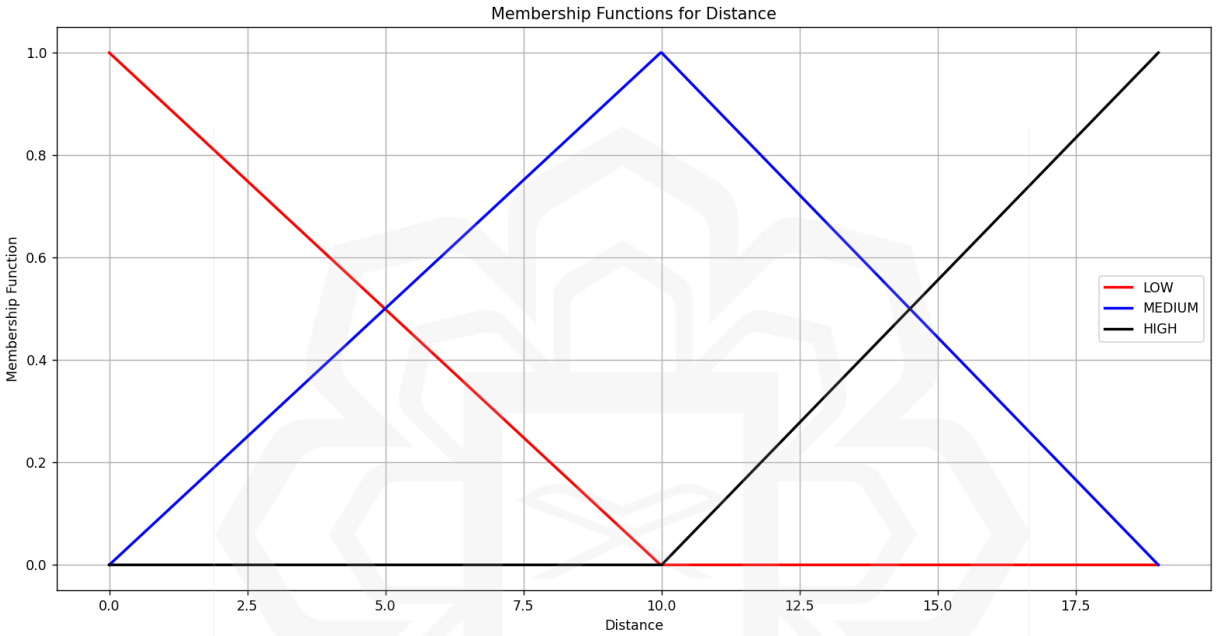

Figure 3.8: The Triangle Membership Function of Distance of UV Light And TiO_2 Sensor Derived from a Triangle Membership Function Formula.

In a similar manner to the fuzzification of millivolt values, distance values are also categorized into three fuzzy sets: low, moderate, and high. These classifications help the system interpret continuous distance measurements in a way that allows for smooth transitions between categories rather than rigid thresholds.

For high distance values, the membership function follows a descending triangular shape. At 0 distance units, the membership value is 1, meaning the distance is fully classified as high. As the distance increases from 0 to 10 units, the membership degree gradually decreases. At 10 units, the membership value reaches 0, indicating that beyond this point, the distance is no longer considered high.

For moderate distance values, the membership function forms a triangular shape, meaning it has a peak at the middle range. Initially, for values below 0 units, the membership degree is 0. As the distance increases, the membership value rises until it reaches 1 at 10 units, indicating that the distance is fully classified as moderate at this point. Beyond 10 units, the membership value starts to decrease linearly until it reaches 0 at 19 units, where the distance is no longer classified as moderate.

For low distance values, the membership function is structured as an increasing triangular function. It starts at 0 for distances below 10 units, meaning that at this stage, the value does not belong to the low category. As the distance increases beyond 10 units, the membership value gradually rises, reaching its maximum at 19 units, where it is fully classified as low.

Applying fuzzification to distance values enables the system to interpret varying measurements in a more flexible manner. Instead of relying on strict boundaries, this approach allows for partial membership, meaning a specific distance value may belong to multiple categories with different degrees of certainty. This method is particularly useful in sensor-based applications, robotics, and environmental monitoring, where precise and adaptive distance classification is essential for decision-making.

3.4.3.2 *Fuzzy Interference*

Table 3.1: The Fuzzy Interference That Has Been Used in The Experiment to Combine 2 Input to Get the Output

Voltage (Input 1)	Distance (Input 2)	Concentration of Ammonia (Output)
Low	Low	Low
Low	Moderate	Moderate
Low	High	Moderate
Moderate	Low	Moderate
Moderate	Moderate	Moderate
Moderate	High	Moderate
High	Low	Moderate
High	Moderate	Moderate
High	High	High

Fuzzy inference is a decision-making process in fuzzy logic systems where input variables are analyzed using predefined rules to produce an output. In this experiment, fuzzy inference is used to determine the concentration of ammonia by combining two input variables: voltage (millivolt) and distance (cm) of the UV light from the TiO_2 sensor. These input variables influence the sensor's photocatalytic response, which in turn affects the ammonia concentration detected. Instead of relying on rigid numerical thresholds, fuzzy logic allows the system to make

smooth and flexible estimations based on linguistic categories such as "Low," "Moderate," and "High."

The first step in fuzzy inference is fuzzification, where the input values are converted into fuzzy sets with membership degrees. In this experiment, voltage and distance are categorized into three levels: Low, Moderate, and High. For example, a voltage value of 200 mV may partially belong to both "Low" and "Moderate" categories, with a certain membership degree in each. Similarly, a distance value of 12 cm may belong to both "Moderate" and "High" distance categories. This allows for a more realistic and gradual transition between categories rather than abrupt cutoffs.

Once the input values are fuzzified, the system applies if-then rules to infer the ammonia concentration. These rules define how voltage and distance interact to determine the output. For instance, a rule might state: "If voltage is Low and distance is Low, then ammonia concentration is Low." Another rule could say: "If voltage is High and distance is High, then ammonia concentration is High." These logical relationships mimic human reasoning, allowing the system to handle complex interactions between variables. The experiment implements nine fuzzy rules, covering all possible combinations of voltage and distance to estimate ammonia concentration.

After applying the rules, the system aggregates the results to determine a fuzzy output. Since some voltage and distance values may partially belong to multiple categories, the resulting ammonia concentration is not a single fixed value but rather a fuzzy range. To convert this into a usable numerical value, the process of defuzzification is applied. This step translates the fuzzy set into a crisp number, usually by using methods like centroid calculation or weighted averaging.

The final output represents the ammonia concentration based on the given voltage and distance conditions.

This fuzzy inference approach allows for a more adaptive and precise estimation of ammonia concentration compared to traditional rigid threshold-based methods. By accounting for gradual changes in sensor readings and environmental factors, the system improves the accuracy and reliability of ammonia detection. This makes it especially useful in real-world applications such as environmental monitoring, industrial chemical sensing, and water quality assessment, where conditions are often variable and uncertain.

3.4.3.3 *Defuzzification*

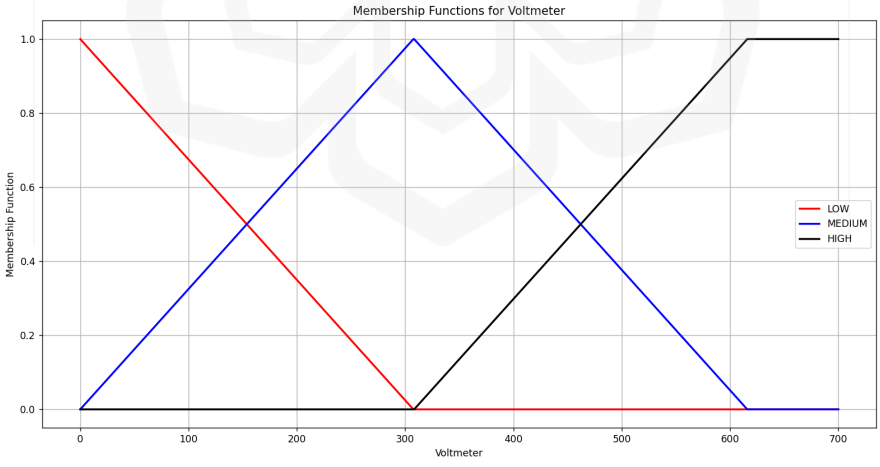

Figure 3.9: The Triangle Membership Function of Defuzzification of Voltmeter (Forward Calculation) Derived from a Triangle Membership Function Formula.

Defuzzification is an essential process in fuzzy logic systems that transforms fuzzy outputs into a crisp, precise value. This step is particularly crucial when dealing with systems that have uncertain or imprecise inputs, as is the case with voltage readings from a voltmeter in the context of ammonia detection. The fuzzy outputs from a system, such as the "Low," "Moderate," and "High" concentrations, are based on certain degrees of membership that describe how much each value belongs to a particular fuzzy category. For example, a voltage of 154 mV might belong to the "Low" category, 308 mV to the "Moderate" category, and 462 mV to the "High" category, each with varying degrees of membership.

To transition from fuzzy values to a crisp value, defuzzification utilizes various methods, with the centroid method being the most common. The centroid method, also known as the center of gravity, computes the weighted average of all fuzzy values, where the weights are determined by the degree of membership for each fuzzy set. This means that a higher degree of membership for a specific value will contribute more to the final defuzzified result. In the case of voltage values, if the system detects a voltage of 154 mV, 308 mV, and 462 mV, each of these values will have an associated degree of membership, indicating how strongly they belong to the "Low," "Moderate," and "High" categories, respectively.

The defuzzification formula calculates the crisp output by multiplying each fuzzy value by its corresponding degree of membership and then dividing by the sum of all membership values. This weighted average approach ensures that the final output reflects the combined influence of all input values. For instance, if the membership for "Low" is 0.8 at 154 mV, for "Moderate" at 308 mV is 0.6, and for "High" at 462 mV is 0.2, the defuzzified value is calculated by averaging these weighted values. This resulting crisp value represents a specific voltage reading that can be used to determine the ammonia concentration, providing a clear and actionable result.

In ammonia detection, this defuzzified value is crucial because it bridges the gap between the imprecise, fuzzy measurements of voltage and a precise, numerical concentration of ammonia. Instead of simply knowing whether the concentration is "Low," "Moderate," or "High," the system provides a specific voltage reading that correlates to the actual ammonia concentration in the sample. This crisp value is then used to make further decisions or control processes, such as triggering alarms, activating filters, or adjusting chemical treatment processes. Through defuzzification, the fuzzy logic system is able to provide reliable, actionable data that helps in real-world applications.

In the case of ammonia detection, this value might directly correlate to the ammonia concentration in the sample, providing the system with a specific reading that can be used for further analysis or action.

Thus, defuzzification helps convert the fuzzy logic-based system's uncertain and imprecise outputs into precise, actionable data that is crucial for the correct operation of systems such as ammonia detection using TiO_2-based sensors with voltage outputs.

3.5 SUMMARY

In summary, this project consists of three main components, the TiO_2 photosensor and its circuitry, varying concentrations of ammonia, and voltage measurement. The necessary components are procured, the circuit is assembled, and data is systematically recorded.

CHAPTER FOUR

RESULT AND DISCUSSION

4.1 OVERVIEW

This chapter will show the result, discussion and conclusion of the experiment. As mentioned earlier, this research uses fuzzy logic in the calculation to predict the concentration of the ammonia concentration. The prediction error should be minimized for the calculation to be considered acceptable.

The result of the 2 experiments will be tabulated and execute fuzzification. Then, fuzzy interference will be performed from the obtained results. Lastly, the output can be deduced from defuzzification. This is the 3 calculations need to be done in fuzzy logic. At the end, the error percentage will be calculated to know the percentage of error.

4.2 RESULT EXPERIMENT

4.2.1 Error Percentages Between Result of Arduino and Digital Multimeter

Table 4.1: Table of Output Result of Voltage Output in Arduino and Digital Multimeter with The Error Percentages Between Them When Using the Same Distance of UV Light and TiO_2 Sensor and Different Ammonia Concentration.

No	Distance (cm)	Ammonia Concentration (g/ml)	Voltage Output in Arduino (millivolt)	Voltage Output in Digital Multimeter (millivolt)	Error Percentage (%)
1	3	0.30	397.91	398.30	0.10
2	3	0.40	473.64	474.03	0.08
3	7	0.40	399.43	399.89	0.12
4	7	0.54	482.44	482.85	0.08
5	7	1.00	616.64	616.98	0.06
6	9	0.20	290.23	290.60	0.13
7	9	0.30	369.81	369.20	0.17
8	9	0.54	458.18	458.59	0.0
9	9	0.64	559.98	560.45	0.08
10	11	0.20	252.02	251.97	0.02
11	11	0.64	489.05	489.02	0.01
12	13	0.54	258.54	258.42	0.05

13	15	0.54	178.78	178.70	0.04
14	15	0.64	193.72	193.62	0.05
15	17	0.04	7.83	7.72	1.42
16	17	0.14	19.83	19.79	0.20
17	17	0.54	25.07	25.05	0.08
18	17	1.00	85.12	85.01	0.13
19	19	0.10	7.54	7.33	2.86
20	19	0.14	6.83	6.63	3.02
21	19	0.20	4.87	4.87	0.00
22	19	0.24	35.55	35.51	0.11
23	19	0.94	28.07	27.95	0.43
24	19	1.00	30.11	30.03	0.27

From Table 4.1, the error percentage of difference between digital multimeter and Arduino is very low. The result is acceptable with very low percentage of error with the lowest is 0% and the highest is 3.02%. The percentage of error for the voltage output in Arduino and digital multimeter is very low and can be neglected. The objectives 1 and 2 are done successfully.

Table 4.1 presents data for a fixed UV lamp distance with varying ammonia concentrations. For instance, a comparison voltage generated between 0.3 g/ml and 0.4 g/ml at a constant TiO_2 distance of 3 cm (as seen in rows 1 and 2) highlights the impact of concentration changes. Meanwhile, Table 4.2 reorganizes the data by keeping the ammonia concentration constant while varying the UV lamp distance from the TiO_2, providing an alternative perspective on the relationship between these variables.

Table 4.2: Table of Output Result of Voltage Output in Arduino and Digital Multimeter with The Error Percentages Between Them When Using the Same Ammonia Concentration Sensor and Different Distance of UV Light and TiO_2.

No	Distance (cm)	Ammonia Concentration (g/ml)	Voltage Output in Arduino (millivolt)	Voltage Output in Digital Multimeter (millivolt)	Error Percentage (%)
1	17	0.04	7.83	7.72	1.42
2	19	0.10	7.54	7.33	2.86
3	17	0.14	19.83	19.79	0.20
4	19	0.14	6.83	6.63	3.02
5	9	0.20	290.23	290.60	0.13
6	11	0.20	252.02	251.97	0.02
7	19	0.20	4.87	4.87	0.00
8	19	0.24	35.55	35.51	0.11
9	3	0.30	397.91	398.30	0.10
10	9	0.30	369.81	369.20	0.17
11	3	0.40	473.64	474.03	0.08
12	7	0.40	399.43	399.89	0.12
13	7	0.54	482.44	482.85	0.08
14	9	0.54	458.18	458.59	0.09
15	13	0.54	258.54	258.42	0.05
16	15	0.54	178.78	178.70	0.04
17	17	0.54	25.07	25.05	0.08
18	9	0.64	559.98	560.45	0.08
19	11	0.64	489.05	489.02	0.01
20	15	0.64	193.72	193.62	0.05

21	19	0.94	28.07	27.95	0.43
22	7	1.00	616.64	616.98	0.06
23	17	1.00	85.12	85.01	0.13
24	19	1.00	30.11	30.03	0.27

The voltage generated varies when the distance between the UV lamp and TiO_2 is set at 9 cm, 11 cm, and 20 cm while maintaining a constant ammonia concentration of 0.2 g/ml, as observed in rows 5, 6, and 7. By analyzing both tables, it can be concluded that a higher ammonia concentration results in a higher voltage output. Conversely, increasing the distance between the UV lamp and TiO_2 leads to a decrease in the voltage produced.

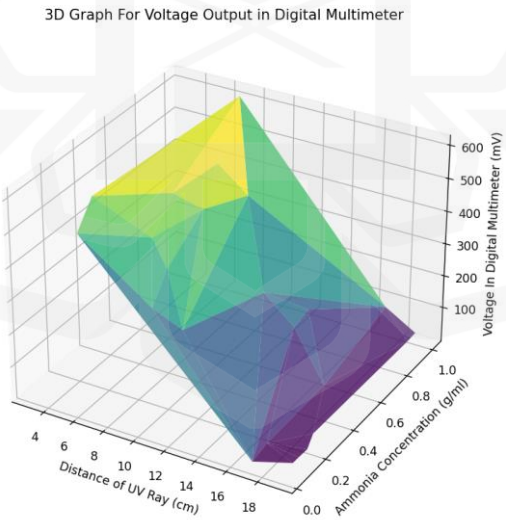

Figure 4.1: 3D Graph for Voltage Output in Digital Multimeter Build from The Result Table of Output.

From Table 4.1 and Table 4.2, a 3D graph was generated to provide a clearer visualization and better understanding of the results. Figure 4.1 presents the 3D graph of the output voltage measured using a digital multimeter (DMM), while Figure 4.2 displays the output voltage obtained from Arduino. As observed, both graphs exhibit similar patterns, indicating that the difference between the two measurements is minimal and can be considered negligible.

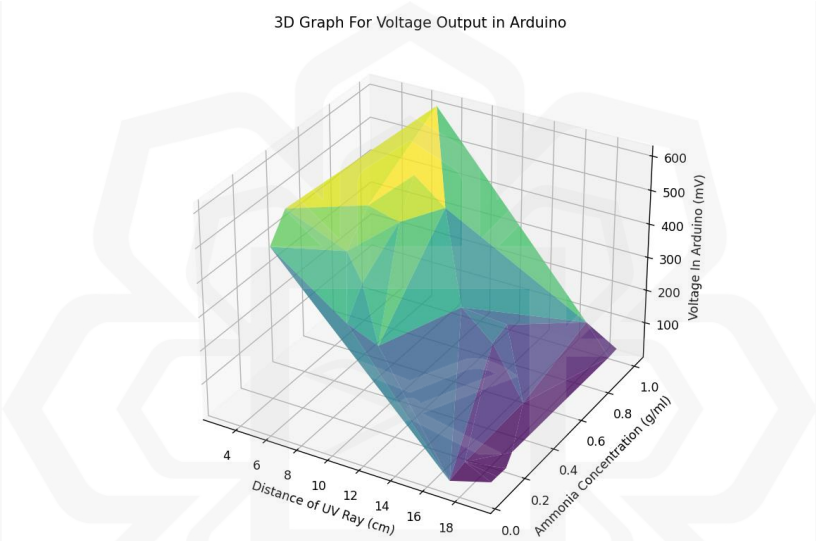

Figure 4.2: 3D Graph for Voltage Output in Arduino Build from The Result Table of Output.

Figure 4.3 illustrates the 3D graph of the error in output voltage between the DMM and Arduino. As observed, the error remains minimal, ranging from 0% to a maximum of only 3.02%. This indicates that Arduino can serve as a reliable alternative to the DMM. One of the key advantages of Arduino is its versatility, as it can be integrated with multiple computers and various electronic devices, making it a more flexible option compared to the DMM.

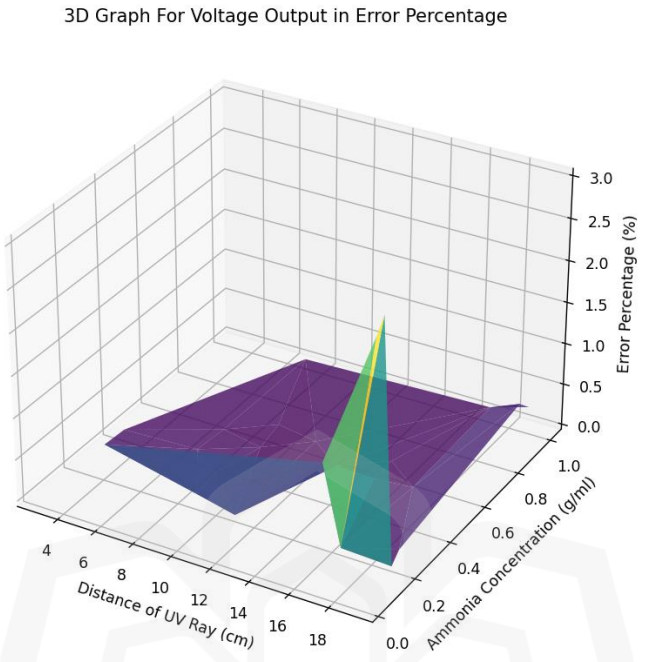

Figure 4.3: 3D Graph for Voltage Output in Error Percentage Between Arduino and Digital Multimeter.

4.2.2 Error Percentages Between Result of Fuzzy Logic and Experiment

4.2.2.1 Centroid Method

Table 4.3: Defuzzification Results Using the Centroid Method for Voltage Estimation

No	Distance (cm)	Ammonia Concentration (g/ml)	Voltage in Fuzzy Logic (mV)	Voltage In Experiment (mV)	Error Percentage (%)
1	3	0.30	308.00	397.91	22.60
2	3	0.40	308.00	473.64	34.97
3	7	0.40	308.00	399.43	22.89
4	7	0.54	347.83	482.44	27.90
5	7	1.00	354.20	616.64	42.56
6	9	0.20	308.00	290.23	6.12
7	9	0.30	308.00	368.81	16.49
8	9	0.54	321.28	458.18	29.88
9	9	0.64	320.83	559.98	42.71
10	11	0.20	294.00	252.02	16.66
11	11	0.64	308.00	489.05	37.02
12	13	0.54	308.00	258.54	19.13
13	15	0.54	308.00	178.78	72.28
14	15	0.64	308.00	193.72	58.99
15	17	0.04	204.74	7.83	2514.82

16	17	0.14	231.24	19.83	1066.11
17	17	0.54	308.00	25.07	1128.56
18	17	1.00	308.00	85.12	261.84
19	19	0.10	184.80	7.54	2350.93
20	19	0.14	197.12	6.83	2786.09
21	19	0.20	215.60	4.87	4327.11
22	19	0.24	227.92	35.55	541.13
23	19	0.94	308.00	28.07	997.26
24	19	1.00	308.00	30.11	922.92

Table 4.3 presents the defuzzification results using the centroid method for voltage estimation. It compares the voltage values obtained through fuzzy logic with experimental results and calculates the error percentage. For lower ammonia concentrations and shorter distances between the UV lamp and TiO_2, the estimated fuzzy logic voltage closely matches the experimental values, resulting in relatively small error percentages. For example, at 9 cm with 0.2 g/ml ammonia, the error is only 6.12%.

However, as the ammonia concentration increases and the distance becomes greater, discrepancies between the estimated and experimental values become more pronounced. In some cases, such as at 19 cm with 0.20 g/ml ammonia concentration, the error reaches exceptionally high values, indicating that the fuzzy model's accuracy decreases significantly under certain conditions.

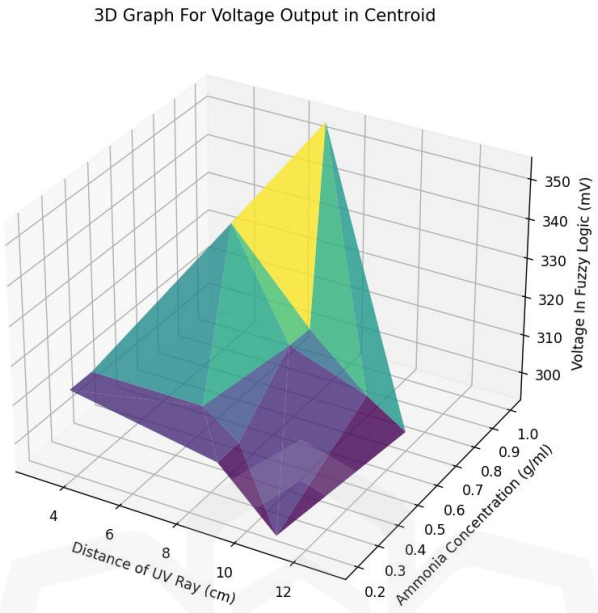

Figure 4.4: 3D Voltage Results from Centroid Method Defuzzification for Voltage Estimation

Figure 4.4 visualizes the 3D voltage results from centroid method defuzzification, illustrating how the estimated voltages vary with changes in distance and ammonia concentration. Meanwhile, Figure 4.5 presents the 3D error percentage results, highlighting the areas where the fuzzy model exhibits higher deviations from experimental values. These visual representations further emphasize that while the fuzzy logic model provides reasonable estimations in some scenarios, its accuracy diminishes under extreme conditions, suggesting the need for further refinement of fuzzy logic parameters.

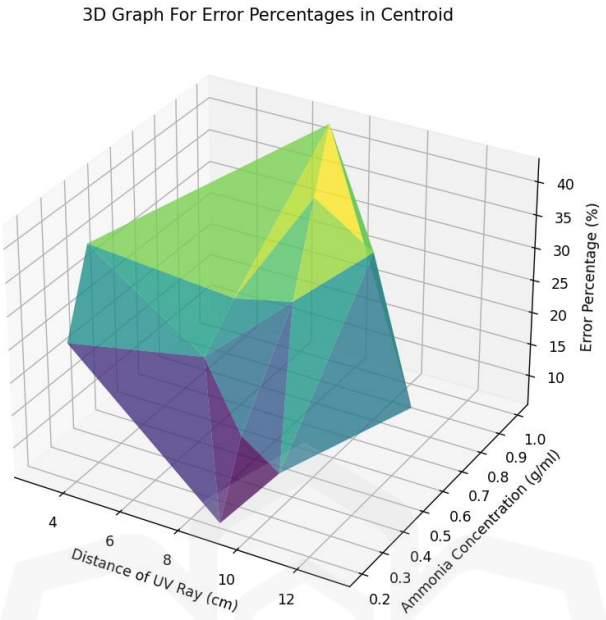

Figure 4.5: 3D Error Percentage Result from Centroid Method Defuzzification for Voltage Estimation.

4.2.2.2 Weight Average Method (WAM)

Table 4.4: Defuzzification Results Using the WAM Method for Voltage Estimation.

No	Distance (cm)	Ammonia Concentration (g/ml)	Voltage in Fuzzy Logic (mV)	Voltage In Experiment (mV)	Error Percentage (%)
1	3	0.30	308.00	397.91	22.60
2	3	0.40	308.00	473.64	34.97
3	7	0.40	308.00	399.43	22.89
4	7	0.54	326.67	482.44	32.29
5	7	1.00	354.20	616.64	42.56
6	9	0.20	308.00	290.23	6.12
7	9	0.30	308.00	368.81	16.49
8	9	0.54	320.83	458.18	29.98
9	9	0.64	320.83	559.98	42.71
10	11	0.20	290.89	252.02	15.42
11	11	0.64	308.00	489.05	37.02
12	13	0.54	308.00	258.54	19.13
13	15	0.54	308.00	178.78	72.28
14	15	0.64	308.00	193.72	58.99
15	17	0.04	188.22	7.83	2303.83
16	17	0.14	188.22	19.83	849.17
17	17	0.54	308.00	25.07	1128.56
18	17	1.00	308.00	85.12	261.84

19	19	0.10	154.00	7.54	1942.44
20	19	0.14	154.00	6.83	2154.76
21	19	0.20	154.00	4.87	3062.22
22	19	0.24	154.00	35.55	333.19
23	19	0.94	308.00	28.07	997.26
24	19	1.00	308.00	30.11	922.92

Table 4.4 presents the defuzzification results using the Weighted Average Method (WAM) for voltage estimation. The table compares the voltage values obtained through fuzzy logic with experimental results and calculates the corresponding error percentages. The results indicate that for shorter distances and lower ammonia concentrations, the WAM method provides reasonably accurate voltage estimations. For instance, at a distance of 9 cm with an ammonia concentration of 0.2 g/ml, the error percentage is only 6.12%, which suggests that the method can effectively estimate voltage under these conditions.

However, as the ammonia concentration increases and the distance becomes larger, the discrepancies between the fuzzy logic estimations and the experimental values become more significant. This trend is particularly noticeable at distances of 17 cm and 19 cm, where the error percentages exceed 1000%. For example, at 19 cm with an ammonia concentration of 0.20 g/ml, the error reaches 3062.22%, indicating a substantial deviation from the actual measured voltage.

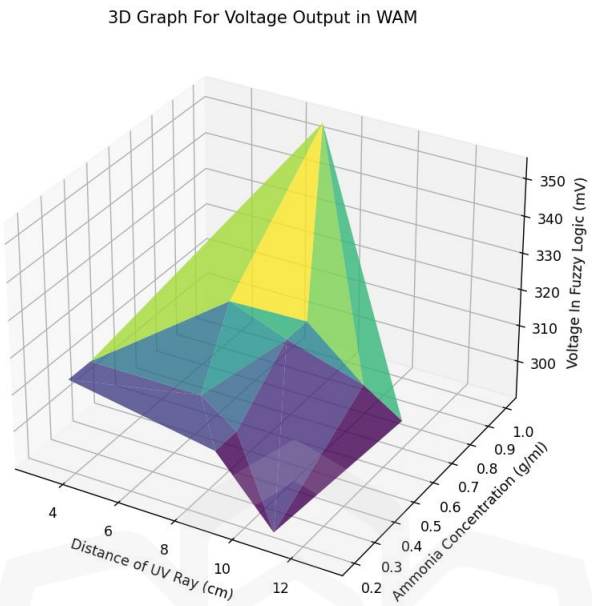

Figure 4.6: 3D Voltage Results from WAM Method Defuzzification for Voltage Estimation.

Figures 4.6 and 4.7 provide a visual representation of these results. Figure 4.6 illustrates the 3D voltage distribution based on the WAM defuzzification method, showing how voltage levels change with varying ammonia concentrations and distances. Meanwhile, Figure 4.7 highlights the error percentages, clearly demonstrating the increased inaccuracies at higher distances and extreme ammonia concentrations.

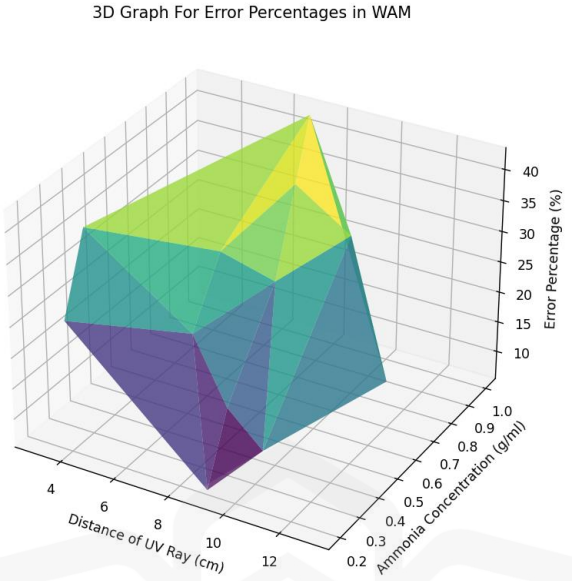

Figure 4.7: 3D Error Percentage Results from WAM Method Defuzzification for Voltage Estimation.

4.2.2.3 Mean Of Center Method (MOC)

Table 4.5: Defuzzification Results Using the MOC Method for Voltage Estimation.

No	Distance (cm)	Ammonia Concentration (g/ml)	Voltage in Fuzzy Logic (mV)	Voltage In Experiment (mV)	Error Percentage (%)
1	3	0.30	308.00	397.91	22.60
2	3	0.40	308.00	473.64	34.97

3	7	0.40	308.00	399.43	22.89
4	7	0.54	347.83	482.44	27.90
5	7	1.00	354.20	616.64	42.56
6	9	0.20	308.00	290.23	6.12
7	9	0.30	308.00	368.81	16.49
8	9	0.54	321.28	458.18	29.88
9	9	0.64	320.83	559.98	42.71
10	11	0.20	294.00	252.02	16.66
11	11	0.64	308.00	489.05	37.02
12	13	0.54	308.00	258.54	19.13
13	15	0.54	308.00	178.78	72.28
14	15	0.64	308.00	193.72	58.99
15	17	0.04	204.74	7.83	2514.82
16	17	0.14	231.24	19.83	1066.11
17	17	0.54	308.00	25.07	1128.56
18	17	1.00	308.00	85.12	261.84
19	19	0.10	184.80	7.54	2350.93
20	19	0.14	197.12	6.83	2786.09
21	19	0.20	215.60	4.87	4327.11
22	19	0.24	227.92	35.55	541.13
23	19	0.94	308.00	28.07	997.26
24	19	1.00	308.00	30.11	922.92

Table 4.5 presents the voltage estimation results using the Mean of Maximum (MOC) defuzzification method. The table compares the estimated fuzzy logic voltages with the experimental values and provides the corresponding error percentages.

Similar to the Centroid and WAM methods, the MOC method demonstrates reasonable accuracy for shorter distances and lower ammonia concentrations. For example, at a distance of 9 cm with an ammonia concentration of 0.2 g/ml, the error is relatively low at 6.12%. However, as the distance increases beyond 15 cm, the error percentages become significantly larger, reaching over 4000% in some cases.

The trend suggests that the MOC method struggles to maintain accuracy at greater distances, particularly when the ammonia concentration is low. For instance, at 19 cm with 0.20 g/ml ammonia, the error percentage is 4327.11%, indicating a substantial deviation from the experimental results.

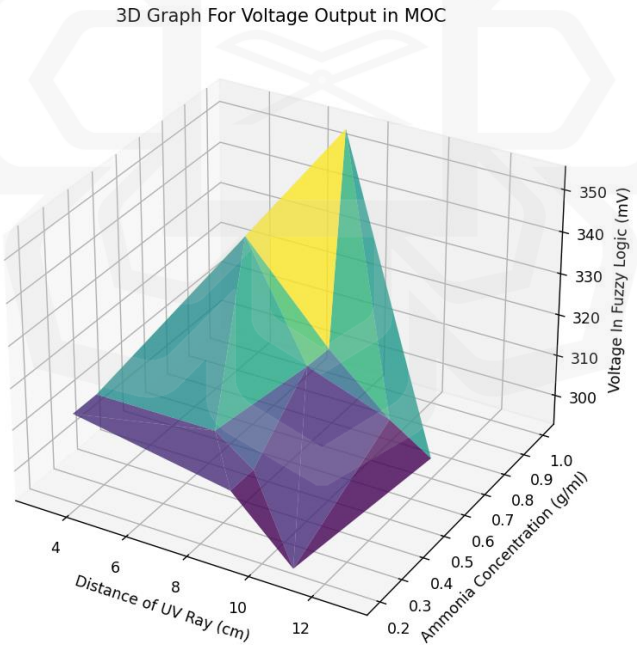

Figure 4.8: 3D Voltage Results from MOC Method Defuzzification for Voltage Estimation.

Figures 4.8 and 4.9 illustrate these trends through 3D visualizations. Figure 4.8 shows the estimated voltage distribution, while Figure 4.9 highlights the error percentages, reinforcing the observation that errors increase significantly at larger distances and lower ammonia concentrations.

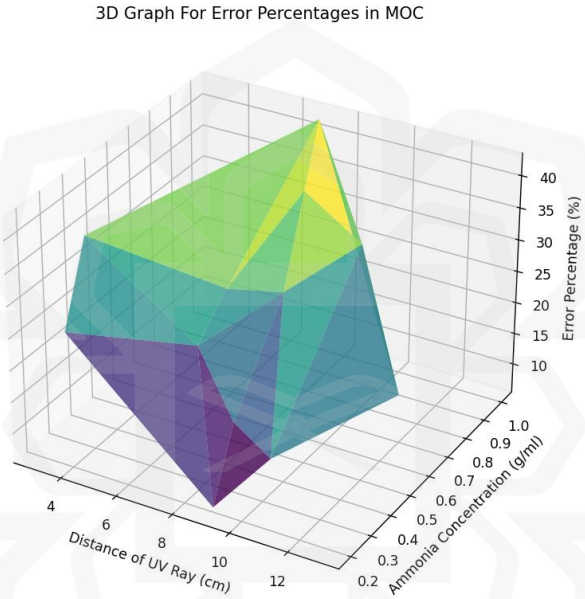

Figure 4.9: 3D Error Percentage from MOC Method Defuzzification for Voltage Estimation.

4.2.2.4 Modified Weighted Average Method (MWA)

Table 4.6: Defuzzification Results Using the MWA Method for Voltage Estimation.

No	Distance (cm)	Ammonia Concentration (g/ml)	Voltage in Fuzzy Logic (mV)	Voltage In Experiment (mV)	Error Percentage (%)
1	3	0.30	308.00	397.91	22.60
2	3	0.40	308.00	473.64	34.97
3	7	0.40	308.00	399.43	22.89
4	7	0.54	347.83	482.44	27.90
5	7	1.00	354.20	616.64	42.56
6	9	0.20	308.00	290.23	6.12
7	9	0.30	308.00	368.81	16.49
8	9	0.54	321.28	458.18	29.88
9	9	0.64	320.83	559.98	42.71
10	11	0.20	294.00	252.02	16.66
11	11	0.64	308.00	489.05	37.02
12	13	0.54	308.00	258.54	19.13
13	15	0.54	308.00	178.78	72.28
14	15	0.64	308.00	193.72	58.99
15	17	0.04	204.74	7.83	2514.82
16	17	0.14	231.24	19.83	1066.11
17	17	0.54	308.00	25.07	1128.56
18	17	1.00	308.00	85.12	261.84

19	19	0.10	184.80	7.54	2350.93
20	19	0.14	197.12	6.83	2786.09
21	19	0.20	215.60	4.87	4327.11
22	19	0.24	227.92	35.55	541.13
23	19	0.94	308.00	28.07	997.26
24	19	1.00	308.00	30.11	922.92

Table 4.6 presents the defuzzification results using the Mean of Weighted Averages (MWA) method for voltage estimation. The table compares fuzzy logic voltage estimations with experimental values and their respective error percentages.

The MWA method exhibits patterns similar to those observed in the previous defuzzification techniques. At shorter distances (3 cm to 9 cm) and moderate ammonia concentrations, the method maintains reasonable accuracy. For instance, at 9 cm with an ammonia concentration of 0.2 g/ml, the estimated voltage is 308.00 mV, while the experimental value is 290.23 mV, resulting in a relatively low error of 6.12%.

However, as the distance increases, particularly beyond 15 cm, the error percentages rise significantly. For example, at 17 cm with an ammonia concentration of 0.04 g/ml, the error reaches 2514.82%, indicating a major discrepancy between the estimated and actual voltages. The highest errors are observed at 19 cm with low ammonia concentrations (0.20 g/ml), where the error percentage exceeds 4000%.

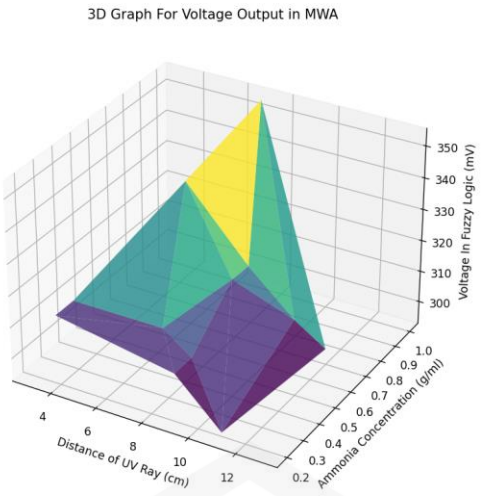

Figure 4.10: 3D Voltage Results from MWA Method Defuzzification for Voltage Estimation.

Figures 4.10 and 4.11 illustrate these trends in 3D visualizations. Figure 4.10 shows the estimated voltage distribution, while Figure 4.11 highlights the error percentages, confirming that the accuracy of the MWA method declines at extreme values of distance and ammonia concentration.

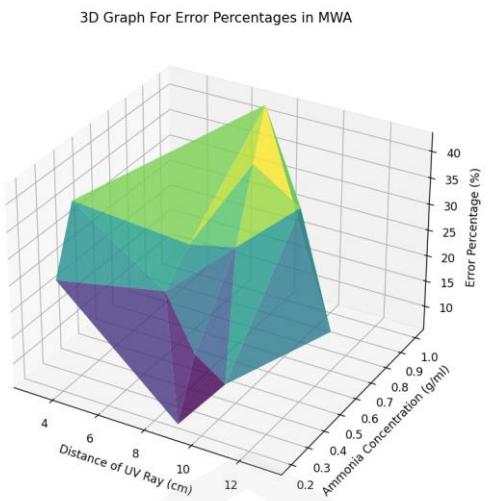

Figure 4.11: 3D Error Percentage from MWA Method Defuzzification for Voltage Estimation.

4.2.2.5 Center of Maximum Method (COM)

Table 4.7: Defuzzification Results Using the COM Method for Voltage Estimation.

No	Distance (cm)	Ammonia Concentration (g/ml)	Voltage in Fuzzy Logic (mV)	Voltage In Experiment (mV)	Error Percentage (%)
1	3	0.30	308.00	397.91	22.60
2	3	0.40	308.00	473.64	34.97
3	7	0.40	308.00	399.43	22.89
4	7	0.54	347.83	482.44	27.90
5	7	1.00	354.20	616.64	42.56

6	9	0.20	308.00	290.23	6.12
7	9	0.30	308.00	368.81	16.49
8	9	0.54	321.28	458.18	29.88
9	9	0.64	320.83	559.98	42.71
10	11	0.20	294.00	252.02	16.66
11	11	0.64	308.00	489.05	37.02
12	13	0.54	308.00	258.54	19.13
13	15	0.54	308.00	178.78	72.28
14	15	0.64	308.00	193.72	58.99
15	17	0.04	204.74	7.83	2514.82
16	17	0.14	231.24	19.83	1066.11
17	17	0.54	308.00	25.07	1128.56
18	17	1.00	308.00	85.12	261.84
19	19	0.10	184.80	7.54	2350.93
20	19	0.14	197.12	6.83	2786.09
21	19	0.20	215.60	4.87	4327.11
22	19	0.24	227.92	35.55	541.13
23	19	0.94	308.00	28.07	997.26
24	19	1.00	308.00	30.11	922.92

Table 4.7 presents the defuzzification results using the Center of Maximum (COM) method for voltage estimation. The estimated fuzzy logic voltage values are compared with experimental results, and the corresponding error percentages are calculated.

The COM method follows similar trends observed in previous defuzzification methods, where errors remain moderate at shorter distances and increase significantly at longer distances.

At short distances (3 cm to 9 cm), the estimated voltage values align relatively well with experimental results. For instance, at 9 cm with 0.20 g/ml ammonia concentration, the estimated voltage is 308.00 mV, while the experimental value is 290.23 mV, leading to an error of only 6.12%.

However, at longer distances (15 cm and beyond), errors start to increase drastically. For example, at 17 cm with 0.04 g/ml ammonia concentration, the estimated voltage is 204.74 mV, whereas the experimental result is 7.83 mV, leading to an extreme error of 2514.82%. The highest error recorded is at 19 cm with 0.20 g/ml ammonia concentration, where the error reaches 4327.11%.

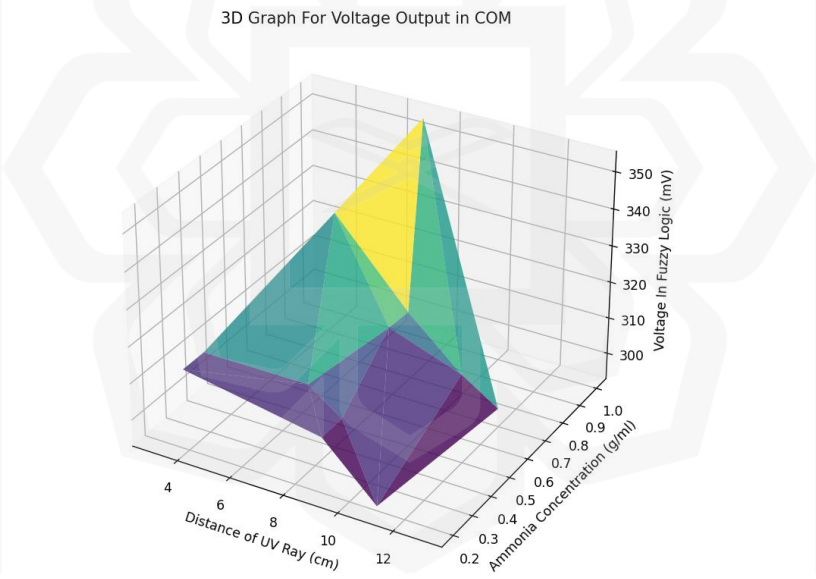

Figure 4.12: 3D Voltage Results from COM Method Defuzzification for Voltage Estimation.

Figures 4.12 and 4.13 illustrate these trends. Figure 4.12 presents the estimated voltage values in a 3D plot, while Figure 4.13 highlights the error distribution. The figures confirm that the COM method struggles with extreme conditions, particularly at low ammonia concentrations and long distances.

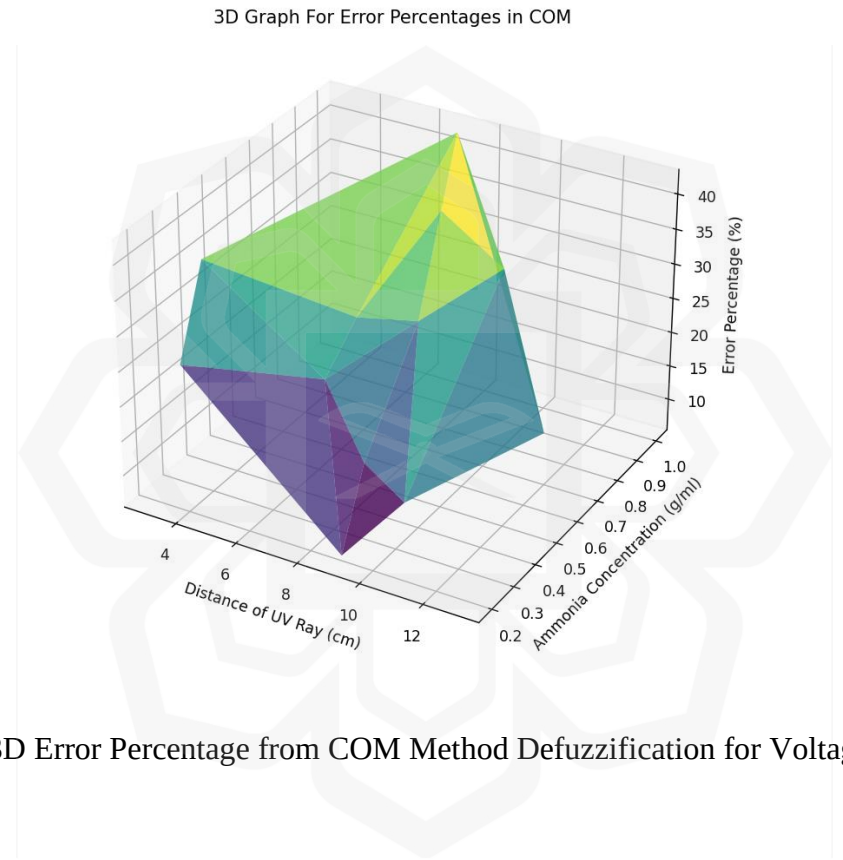

Figure 4.13: 3D Error Percentage from COM Method Defuzzification for Voltage Estimation.

4.2.2.6 Center of Sums Method (CoS)

Table 4.8: Defuzzification Results Using the COS Method for Voltage Estimation.

No	Distance (cm)	Ammonia Concentration (g/ml)	Voltage in Fuzzy Logic (mV)	Voltage In Experiment (mV)	Error Percentage (%)
1	3	0.30	308.00	397.91	22.60
2	3	0.40	308.00	473.64	34.97
3	7	0.40	308.00	399.43	22.89
4	7	0.54	347.83	482.44	27.90
5	7	1.00	354.20	616.64	42.56
6	9	0.20	308.00	290.23	6.12
7	9	0.30	308.00	368.81	16.49
8	9	0.54	321.28	458.18	29.88
9	9	0.64	320.83	559.98	42.71
10	11	0.20	294.00	252.02	16.66
11	11	0.64	308.00	489.05	37.02
12	13	0.54	308.00	258.54	19.13
13	15	0.54	308.00	178.78	72.28
14	15	0.64	308.00	193.72	58.99
15	17	0.04	204.74	7.83	2514.82
16	17	0.14	231.24	19.83	1066.11
17	17	0.54	308.00	25.07	1128.56
18	17	1.00	308.00	85.12	261.84

19	19	0.10	184.80	7.54	2350.93
20	19	0.14	197.12	6.83	2786.09
21	19	0.20	215.60	4.87	4327.11
22	19	0.24	227.92	35.55	541.13
23	19	0.94	308.00	28.07	997.26
24	19	1.00	308.00	30.11	922.92

Table 4.8 presents the defuzzification results using the Center of Sums (COS) method for voltage estimation, where the fuzzy logic voltage values are compared with the experimental results. The error percentages are also calculated to gauge the accuracy of the voltage estimation. The COS method shows a similar pattern to other defuzzification techniques, with moderate accuracy at short distances but increasing error percentages at longer distances and lower ammonia concentrations.

Short Distances (3 cm to 9 cm): The voltage estimates are reasonably close to the experimental results. For instance, at 9 cm with 0.20 g/ml ammonia concentration, the fuzzy logic estimate is 308.00 mV, while the experimental result is 290.23 mV, yielding an error of 6.12%. Moderate to Long Distances (11 cm to 17 cm): As the distance increases, errors grow. At 17 cm with 0.04 g/ml ammonia concentration, the estimated voltage is 204.74 mV, while the experimental value is 7.83 mV, producing an extremely high error percentage of 2514.82%. High Error at 19 cm: The error percentage becomes notably high at 19 cm. For instance, at 0.20 g/ml ammonia concentration, the error percentage reaches 4327.11%, with an estimated voltage of 215.60 mV versus an experimental value of 4.87 mV.

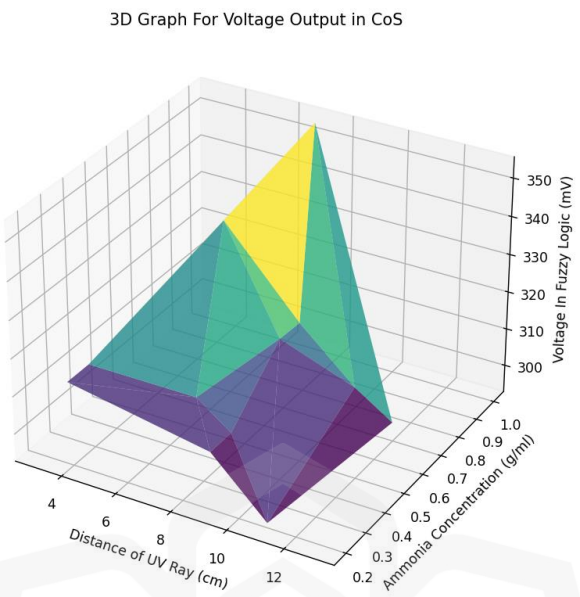

Figure 4.14: 3D Voltage Results from COS Method Defuzzification for Voltage Estimation.

Similar to previous methods like Centroid, MOC, and COM, the COS method performs relatively well at moderate distances and concentrations but has increasing errors at extreme conditions. This method is not immune to the limitations faced by other methods, particularly when ammonia concentrations are very low, or the distance is large. The COS method performs similarly to the other methods, with fairly accurate voltage estimates. At Longer Distances: As with the COM method, the COS method's errors become substantial at longer distances, particularly when the ammonia concentration is low.

Figure 4.14 presents a 3D plot of the voltage results from the COS method, visually showing how the estimated values compare with the experimental data. Figure 4.15 displays the error percentages in a 3D plot, highlighting the growing discrepancy as distance and concentration vary.

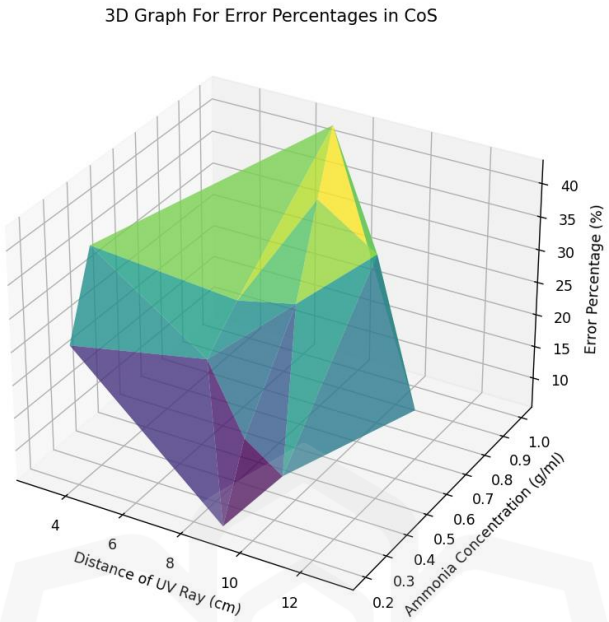

Figure 4.15: 3D Error Percentage from COS Method Defuzzification for Voltage Estimation.

4.2.2.7 Modified Height Method

Table 4.9: Defuzzification Results Using the Modified Height Method for Voltage Estimation.

No	Distance (cm)	Ammonia Concentration (g/ml)	Voltage in Fuzzy Logic (mV)	Voltage In Experiment (mV)	Error Percentage (%)
1	3	0.30	308.00	397.91	22.60
2	3	0.40	308.00	473.64	34.97

3	7	0.40	308.00	399.43	22.89
4	7	0.54	347.83	482.44	27.90
5	7	1.00	354.20	616.64	42.56
6	9	0.20	308.00	290.23	6.12
7	9	0.30	308.00	368.81	16.49
8	9	0.54	321.28	458.18	29.88
9	9	0.64	320.83	559.98	42.71
10	11	0.20	294.00	252.02	16.66
11	11	0.64	308.00	489.05	37.02
12	13	0.54	308.00	258.54	19.13
13	15	0.54	308.00	178.78	72.28
14	15	0.64	308.00	193.72	58.99
15	17	0.04	204.74	7.83	2514.82
16	17	0.14	231.24	19.83	1066.11
17	17	0.54	308.00	25.07	1128.56
18	17	1.00	308.00	85.12	261.84
19	19	0.10	184.80	7.54	2350.93
20	19	0.14	197.12	6.83	2786.09
21	19	0.20	215.60	4.87	4327.11
22	19	0.24	227.92	35.55	541.13
23	19	0.94	308.00	28.07	997.26
24	19	1.00	308.00	30.11	922.92

Table 4.9 presents the defuzzification results using the Modified Height Method (MHM) for voltage estimation. As with other methods, the fuzzy logic voltage estimates are compared with experimental results, and the error percentages are calculated. The Modified Height Method shows a similar pattern to previous defuzzification techniques, with lower error percentages at

short distances and higher discrepancies as the distance increases or ammonia concentration decreases.

The voltage estimates are relatively accurate. For example, at 9 cm with 0.20 g/ml ammonia concentration, the estimated voltage is 308.00 mV, while the experimental voltage is 290.23 mV, resulting in an error of 6.12%. Other values at short distances also show reasonable accuracy with error percentages generally below 30%. The error percentage increases notably as the distance increases. At 17 cm with 0.04 g/ml ammonia concentration, the error becomes significant, reaching 2514.82%, with an estimated voltage of 204.74 mV and an experimental value of 7.83 mV. At 19 cm, particularly with low ammonia concentrations, the error percentages become extremely high. For example, at 0.20 g/ml ammonia concentration, the error percentage reaches 4327.11%, with a voltage estimate of 215.60 mV versus an experimental value of 4.87 mV.

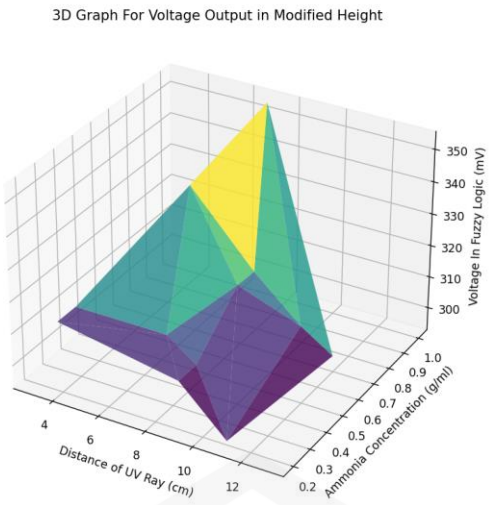

Figure 4.16: 3D Voltage Results from Modified Height Method Defuzzification for Voltage Estimation.

Figure 4.16 provides a 3D plot of the voltage estimates using the Modified Height Method, showcasing how the fuzzy logic estimates align with the experimental data. Figure 4.17 presents a 3D error percentage plot for the same method, highlighting where the method experiences substantial errors, particularly at larger distances and lower ammonia concentrations.

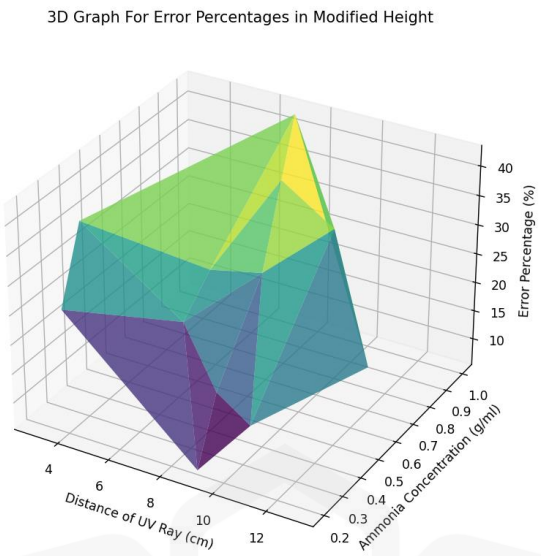

Figure 4.17: 3D Error Percentage from Modified Height Method Defuzzification for Voltage Estimation.

The Modified Height Method shows that, while it works well under moderate experimental conditions, it struggles with extreme cases (large distances and low ammonia concentrations). The error percentages increase drastically in these cases, similar to the behavior of other defuzzification methods like Centroid and COS.

As with other methods, there is potential for improving the accuracy of voltage estimation by combining or adapting these techniques to account for extreme values. Future improvements could involve using adaptive models or hybrid approaches to better handle the limitations observed in the current results.

4.2.2.8 Collection of Error Percentages in Different Defuzzification

Table 4.10: Comparison of Defuzzification Methods of Error Percentage for Voltage Estimation.

No	Centroid	WAM	MOC	MWA	COM	COS	Modified Height
1	22.60	22.60	22.60	22.60	22.60	22.60	22.60
2	34.97	34.97	34.97	34.97	34.97	34.97	34.97
3	22.89	22.89	22.89	22.89	22.89	22.89	22.89
4	27.90	32.29	27.90	27.90	27.90	27.90	27.90
5	42.56	42.56	42.56	42.56	42.56	42.56	42.56
6	6.12	6.12	6.12	6.12	6.12	6.12	6.12
7	16.49	16.49	16.49	16.49	16.49	16.49	16.49
8	29.88	29.98	29.88	29.88	29.88	29.88	29.88
9	42.71	42.71	42.71	42.71	42.71	42.71	42.71
10	16.66	15.42	16.66	16.66	16.66	16.66	16.66
11	37.02	37.02	37.02	37.02	37.02	37.02	37.02
12	19.13	19.13	19.13	19.13	19.13	19.13	19.13
13	72.28	72.28	72.28	72.28	72.28	72.28	72.28
14	58.99	58.99	58.99	58.99	58.99	58.99	58.99

15	2514.82	2303.83	2514.82	2514.82	2514.82	2514.82	2514.82
16	1066.11	849.17	1066.11	1066.11	1066.11	1066.11	1066.11
17	1128.56	1128.56	1128.56	1128.56	1128.56	1128.56	1128.56
18	261.84	261.84	261.84	261.84	261.84	261.84	261.84
19	2350.93	1942.44	2350.93	2350.93	2350.93	2350.93	2350.93
20	2786.09	2154.76	2786.09	2786.09	2786.09	2786.09	2786.09
21	4327.11	3062.22	4327.11	4327.11	4327.11	4327.11	4327.11
22	541.13	333.19	541.13	541.13	541.13	541.13	541.13
23	997.26	997.26	997.26	997.26	997.26	997.26	997.26
24	922.92	922.92	922.92	922.92	922.92	922.92	922.92

The comparison of defuzzification methods for voltage estimation error percentage, presented in Table 4.10, reveals that all the defuzzification methods—Centroid, WAM, MOC, MWA, COM, COS, and the Modified Height method—yield nearly identical results across all test cases. This consistency suggests that the different methods, although varied in their approach to defuzzification, perform similarly in terms of error percentage when applied to this specific voltage estimation task.

When analyzing the data, it is evident that for most test cases, particularly those involving lower distances and moderate ammonia concentrations, the error percentages are relatively low and consistent across all methods. For example, in test cases with distances ranging from 3 cm to 9 cm and ammonia concentrations from 0.04 g/ml to 0.64 g/ml, the error percentages are generally in the range of 6% to 42%. These low error values indicate that the defuzzification methods are effective at estimating voltage when the conditions are within a typical range.

However, as the distance increases and ammonia concentration decreases, the error percentages start to rise significantly. Test cases with larger distances, such as 17 cm and 19 cm, exhibit error percentages as high as 2514.82% and 4327.11%, respectively. This sharp increase in error percentages across all defuzzification methods suggests that the methods struggle when estimating voltage under these extreme conditions. It is noteworthy that these high error values are consistent for all methods, implying that the issue may be related to the nature of the data or the limitations of the defuzzification process rather than the specific method chosen.

In intermediate cases, where the distance is moderate (e.g., 13 cm) and the ammonia concentration falls within a middle range, the error percentages range from 261.84% to 1128.56%. Again, the methods show no significant difference in performance. This indicates that while the methods are able to handle moderate conditions relatively well, they still face challenges when the conditions become more complex.

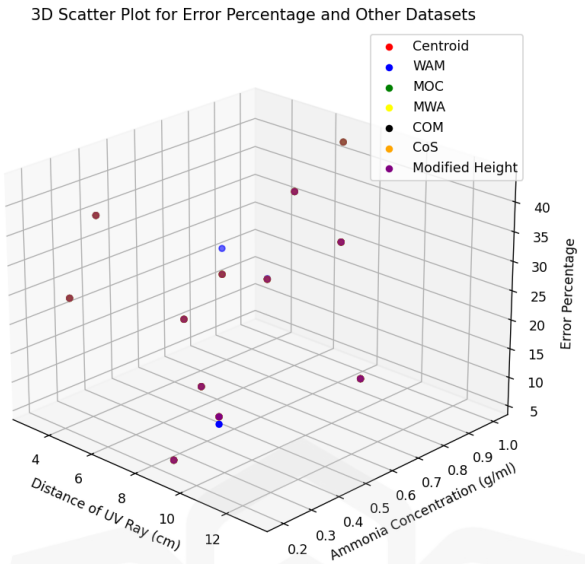

Figure 4.18: Graph of Comparison of Defuzzification Methods of Error Percentage for Voltage Estimation.

The graphical representation in Figure 4.18 reinforces these findings, illustrating that the error percentages across the defuzzification methods are indeed very similar. The graph also highlights the significant spikes in error percentage at higher distances, confirming that the defuzzification methods do not perform well under extreme conditions.

In conclusion, the comparison suggests that while all the defuzzification methods work similarly under typical conditions, they all share common limitations when dealing with extreme cases of large distances and low ammonia concentrations. The consistency of the error percentages across different methods implies that further adjustments or improvements to the voltage estimation process may be necessary, especially in situations where the conditions deviate significantly from the norm. This could involve refining the defuzzification methods or exploring alternative approaches to improve accuracy in such extreme scenarios.

4.2.3 Ammonia Concentration Output in Fuzzy Logic (Reverse Calculation)

Table 4.11: Defuzzification Results Using the Centroid Method for Ammonia Concentration Estimation.

No	Distance (cm)	Voltage (millivolt)	Concentration in Fuzzy Logic (g/ml)	Concentration In Experiment (g/ml)	Error Percentage (%)
1	3	397.91	0.61	0.30	103.33
2	3	473.64	0.57	0.40	42.50
3	7	399.43	0.55	0.40	37.50
4	7	482.44	0.55	0.54	1.85
5	7	616.64	0.58	1.00	42.00
6	9	290.23	0.50	0.20	150.00
7	9	368.81	0.52	0.30	73.33
8	9	458.18	0.52	0.54	3.70
9	9	559.98	0.52	0.64	18.75
10	11	252.02	0.48	0.20	140.00
11	11	489.05	0.50	0.64	21.88
12	13	258.54	0.47	0.54	12.96
13	15	178.78	0.44	0.54	18.52
14	15	193.72	0.45	0.64	29.69
15	17	7.83	0.31	0.04	675.00
16	17	19.83	0.33	0.14	135.71
17	17	25.07	0.33	0.54	38.89
18	17	85.12	0.37	1.00	63.00

19	19	7.54	0.26	0.10	160.00
20	19	6.83	0.26	0.14	85.71
21	19	4.87	0.25	0.20	25.00
22	19	35.55	0.29	0.24	20.83
23	19	28.07	0.27	0.94	71.28
24	19	30.11	0.27	1.00	73.00

The data presented in Table 4.11 showcases the defuzzification results using the Centroid method for ammonia concentration estimation, emphasizing the comparison between the concentration values obtained through fuzzy logic and experimental measurements, as well as the associated error percentages.

For the majority of test cases, the error percentages for ammonia concentration estimation vary significantly, ranging from a few percent to as high as 675%. In general, the error percentages are high when the estimated concentrations deviate substantially from the experimental values. For instance, in the case of test number 15 (where the distance is 17 cm, and the estimated concentration is 0.31 g/ml while the actual concentration is 0.04 g/ml), the error percentage reaches a notably high 675%. This indicates that the Centroid method struggles with significant deviations between the fuzzy logic results and the actual concentrations.

However, there are also instances where the error percentage is relatively low. For example, in test number 4 (at 7 cm distance), the fuzzy logic concentration estimate of 0.55 g/ml closely matches the experimental concentration of 0.54 g/ml, resulting in a minimal error of 1.85%. This demonstrates that the Centroid method is more accurate under conditions where the estimated and actual concentrations are relatively close.

Other instances, such as tests at distances of 3 cm, 9 cm, and 11 cm, show varying degrees of accuracy. For instance, the error percentage for test number 2 (distance 3 cm) is 42.50%, which is a moderate error, whereas test number 8 (distance 9 cm) results in a 3.70% error, suggesting a much better match between the fuzzy logic estimate and the experimental data.

Overall, the error percentage fluctuates significantly across different tests, indicating that the Centroid method's performance is highly sensitive to the specific test conditions. High distances, such as 17 cm and 19 cm, seem to correlate with higher error percentages, suggesting that the method may have difficulties with extreme values or certain outlier conditions. Conversely, the method tends to perform better when the input conditions are within a more typical range, resulting in lower error percentages.

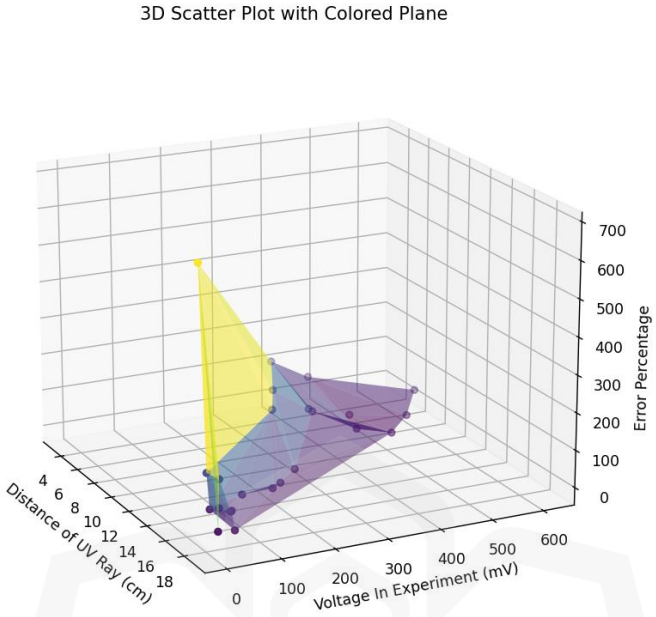

Table 4.19: 3D Error Percentage from Centroid Method Defuzzification for Ammonia Concentration Estimation

In Table 4.19, the 3D error percentage data from the Centroid method for ammonia concentration estimation is visualized, further illustrating the variations in error across different test cases. The 3D visualization likely provides a clearer understanding of how the error percentages fluctuate with both distance and estimated concentration, offering valuable insights into the behavior of the Centroid method in estimating ammonia concentrations under various conditions.

In conclusion, while the Centroid method demonstrates potential for ammonia concentration estimation, its performance is inconsistent, with noticeable challenges in accurately estimating concentrations when there are significant discrepancies between fuzzy logic estimates

and experimental values. The method appears to perform best under more typical conditions but faces considerable challenges when handling extreme or outlier cases, as evidenced by the high error percentages observed in certain test cases. Further refinements or alternative methods may be needed to improve accuracy in such scenarios.

4.3 DISCUSSION OF THE RESULT

From Table 4.1, the error percentage between the digital multimeter and Arduino is very low, ranging from 0% to 3.02%. This minimal discrepancy makes the voltage output difference negligible. Therefore, the results are reliable, successfully achieving the first and second objectives.

Reaction in Ammonia

Anode Reaction: $NH_3 + 3OH^- \rightarrow 1/2N_2 + 3H_2O + 3e^-$

Cathode Reaction: $3H_2O + 3e^- \rightarrow 3/2H_2 + 3OH^-$

Based on the equation above, the ammonia will donate 3 electrons. When the concentration of ammonia increases, the voltage generated also increases. The hypothesis aligns with the findings of our study. Based on Table 4.1, we can conclude that the increase of ammonia concentration will increase the output voltage. This is because increasing ammonia concentration will increase the amount electron donate in reaction and as a result it will produce a higher electricity. While Table 4.2, we can conclude that the increasing of UV distance will decrease the output voltage. This is because increasing the distance of UV rays from TiO_2 sensor will decrease

the intensity of UV ray that reaction with ammonia and as the result it will decrease a lower electricity

From the experiment, the TiO_2 produced different values of output voltage in different distance of UV ray and different concentration of ammonia. This is proof that the different concentration of ammonia and different distance of UV ray will affect the TiO_2 reaction when UV ray penetrate through it. However, the highest distance that is suitable to use is only up to 15 cm because other distances that more than 13 cm cannot give a good voltage output. The TiO_2 cannot detect accurately if the distance is more than 13 cm.

For the fuzzy logic part in both voltage output and ammonia concentration, we can separate it into two parts for the discussion that is forward calculation and reverse calculation. Forward calculation is just a basic calculation in fuzzy logic. Although we get huge percentage of errors, it is because the TiO_2 sensor that we use does not have a high detection capability. The distance of UV ray that is 13 cm and below will give error of percentage below than 45%. It is a very promising study considering that the TiO_2 that we used does not have a high detection capability.

From Figure 4.11, we use 7 types of defuzzification method and most of them give the same result. That is why there are not many points scattered in the 3d graph because most them are point at the same coordinate. This is evidence that change of defuzzification will not change the result output in fuzzy logic calculation.

However, for the reverse calculation in fuzzy logic, we get different results. Although for the distance below than 13 cm, provided us results that are not consistent. Based on the output,

the percentage of error is really big and not consistent. It cannot be neglected. This is because the fuzzy logic system cannot be calculated in reverse like Algebra or Matrices.

For a clearer and more detailed understanding, kindly refer to the two tables provided below. These tables will offer a comprehensive overview and further clarify the key points discussed.

Table 4.12: Normal Fuzzy Logic: Relationship Between Ammonia Concentration, UV Light Distance, and Generated Electricity.

Input 1 (Ammonia concentration)	Input 2 (Distance of UV light from TiO_2 Sensor)	Output (Electric Generated)
Low	Low	Low
Low	Moderate	Moderate
Low	High	Moderate
Moderate	Low	Moderate
Moderate	Moderate	Moderate
Moderate	High	Moderate
High	Low	Moderate
High	Moderate	Moderate
High	High	High

Table 4.13: Reverse Fuzzy Logic: Estimating Ammonia Concentration from Generated Electricity and UV Light Distance.

Input 1 (Electric Generated)	Input 2 (Distance of UV light from TiO_2 Sensor)	Output (Ammonia concentration)
Low	Low	Low
Moderate	Moderate	Low
Moderate	High	Low
Moderate	Low	Moderate
Moderate	Moderate	Moderate
Moderate	High	Moderate
Moderate	Low	High
Moderate	Moderate	High
High	High	High

When we reverse the fuzzy logic, it cannot be the same as the original. Unlike Function and Matrices in mathematics, we can reverse the calculation and it will give the same with the original number.

Mathematic formula can be divided into 2 categories that are reversible and non-reversible. Reversible is an equation that can reverse calculation. It can be calculated in forward and backward. Unlike non-reversible, it can just calculate in forward and cannot be calculated backward. Here are some examples and explanations of reversible and non-reversible calculation.

4.4 REVERSIBLE

4.4.1 Function

Function is an interrelation between a set of inputs (domain) and a set of possible outputs (codomain). Function is a bridge that connects the domain and codomain. The normal method to express a function is y=f(x) and the inverse is $f^{-1}(x)=y$.

f(x) = x + 3

Table 4.14: Forward Function: Mapping Inputs to Outputs.

x	f(x)
1	4
2	5
3	6
4	7
5	8
6	9
7	10
8	11
9	12

$f^{-1}(x) = x-3$

Table 4.15: Inverse Function: Mapping Inputs to Outputs.

$f^{-1}(x)$	**x**
4	1
5	2
6	3
7	4
8	5
9	6
10	7
11	8
12	9

4.4.2 Matrices

A matrix is a rectangular array of numbers arranged in rows and columns. It is an essential concept in linear algebra and is always used to represent and manipulate linear transformations. The size of a matrix is described by its number of rows and columns, often written as m×n. The example below is showed that how inverse matrices is calculated.

$$\begin{Bmatrix} 5 & 1 \\ 3 & -4 \end{Bmatrix} \begin{Bmatrix} x \\ y \end{Bmatrix} = \begin{Bmatrix} 8 \\ 14 \end{Bmatrix}$$

Inverse Matrices

$$\begin{Bmatrix} x \\ y \end{Bmatrix} = -\frac{1}{23} \begin{Bmatrix} -4 & -1 \\ -3 & 5 \end{Bmatrix} \begin{Bmatrix} 8 \\ 14 \end{Bmatrix}$$

$$\begin{Bmatrix} x \\ y \end{Bmatrix} = \begin{Bmatrix} 2 \\ -2 \end{Bmatrix}$$

4.4.3 Bitwise NOT

The Bitwise NOT operation is reversible because it performs a simple inversion of each bit in the binary representation of a number. When you apply NOT twice to a value, you essentially invert each bit twice, bringing it back to its original state. If we denote the NOT operation as NOT(x)=y, then

Table 4.16: Truth Table for Bitwise NOT Operation For Forward and Inverse Calculation.

Operand (Binary)	NOT Result	Reversed Result (Binary)
1100	0011	1100
0101	1010	0101
0011	1100	0011

1110	0001	1110
1000	0111	1000
0010	1101	0010
1101	0010	1101
0110	1001	0110
1111	0000	1111
0000	1111	0000

4.4.4 Logarithm and exponentiation

For the exponentiation, if $a^b=c$, then taking the logarithm base a of c will give b. The equation is $\log_a(c)=b$. While for the logarithm, if $\log_a(c)=b$, then raising a to the power of b will give c. The equation is $a^b=c$.

For example, we can calculate $2^3 = 8$ in exponentiation. We can reverse the calculation by using logarithm with $\log_2 8 = 3$. Table below show more example:

Table 4.17: Function Table for Exponent and Logarithm Operation for Forward and Inverse Calculation.

Base (a)	Exponent (b)	Exponentiation Result (c)	Logarithm Result (b)
2	8	3	3
10	2	100	2
3	4	81	4
5	2	25	2
2	5	32	5
4	3	64	3
10	0	1	0
e	1	e	1
2	-1	0.5	-1
3	0.5	1.732	0.5
6	2	36	2

4.4.5 Radicals and Inverse Radicals

In mathematics, a root is the inverse operation of raising a number to a power. Specifically, the square root is the most common example, where finding the square root of a number $y=\sqrt{x}$ gives a value y such as $y^2=x$. The inverse operation would be squaring the root, resulting in the original value.

Table 4.18: Function Table for Radicals and Inverse Radicals Operation for Forward and Inverse Calculation.

Number	Power	Answer	Inverse Answer
27	1/3	3	27
3	3	27	3
1024	1/5	4	1024
4	5	1024	4
2	7	128	2
128	1/7	2	128
10	9	1 953 125	10
1 953 125	1/9	10	1 953 125
2	-3	1/8	2
1/8	-1/3	2	1/8
4	-1	1/4	4
1/4	-1	4	1/4

4.4.6 Derivative and Integration

The derivative of a mathematical function calculates the rate at which the function's output converts concerning its input. It gives information about the slope or rate of change of the function at any given position and point. The reverse of the derivative is called integration, it involves discovering the primary function given its derivative.

f(x) is a differentiable function, the derivative f′(x) represents the rate of change of f(x) with respect to x. The formula is here:

$$f'(x) = \lim_{h \to 0} \frac{f(x+h) - f(\lambda)}{h}$$

For integration, if F(x) is an antiderivative of f(x), then F′(x)=f(x). Its mathematical formula as below:

$\int f(x)dx=F(x)+C$, where C is the constant of integration.

Table 4.19: Function Table for Derivative and Integration Operation for Forward and Inverse Calculation.

Original	Derivative	Integration
$3x^2$	6x	$3x^2+c$
$2x^2 + 3x + 5$	4x + 3	$2x^2 + 3x + 5 + c$
$5x^3 + 2x^2 – 4x + 2$	$15x^2 + 4x -4$	$5x^3 + 2x^2 – 4x + c$
$3x^{-2}$	-6x	$3x^{-2} + c$
$(x+2)^3$	$3(x+2)^2$	$(x+2)^3 + c$
$(-2x+5)^5$	$-10(-2x+5)^4$	$(-2x+5)^5 + c$
$3(3x-1)^4$	$36(3x-1)^3$	$3(3x-1)^4 + c$
$1/ (x+3)^2$	$1/ 2(x+3)^3$	$1/ (x+3)^2 + c$
$1 / 4(2x-5)^3$	$1 / 24(2x-5)^4$	$1 / 4(2x-5)^3 + c$

In each case, the derivative process operation gives the rate of change, and the antiderivative operation process (indefinite integral) reverse the effect of the derivative, retrieve the original function up to a constant of integration *C*. This demonstrates the reversibility of derivative and antiderivative operations.

4.4.7 Algebraic Formulae

Algebraic operations refer to calculations and manipulations involving algebraic equations and expressions. While individual algebraic operations like addition, subtraction, multiplication, and division are reversible in nature, the wider context of algebraic formulas may include more complex and difficult relationships.

(i) If $a + b = c$, then $c - b = a$.

(ii) If $a \times b = c$, then $c/b = a$.

Below are some examples of the algebraic formula with its inverse with more complex examples.

Table 4.20: Function Table for Algebraic Formulae Operation for Forward and Inverse Calculation.

Original	Inverse
$x + 3 = y$	$x = y - 3$
$3x + 4 = y$	$x = (y – 4) / 3$
$(x – 3)/ 2 = y$	$x = 2y + 3$
$5x/3 = y$	$x = 3y/5$
$x/2 + 4 = y$	$x = 2(y-4)$
$2(x + 3) = y$	$x = y/2 - 3$
$3(4x+3) = y$	$x = (y/3 -3) / 4$
$x^2 = y$	$x = \sqrt{y}$
$x/3 = y$	$x = 3y$
$-3x = y$	$x = -y/3$

4.5 NON-REVERSIBLE

4.5.1 Round Off

Rounding off is a process of approximating a number to a specified number of digits or to a certain place value. While rounding is a common way to simplify numbers for practical use, it introduces a level of ambiguity and information loss, making it non-reversible.

Table 4.21: Function Table for Round Off Table Operation for Forward Calculation.

Original	Rounded to the nearest ten
30	30
31	30
32	30
33	30
34	30
35	40
36	40
37	40
38	40
39	40
40	40

Figure 4.20: Round Off Examples Operation for Forward Calculation.

Figure 4.21: Round Off Examples Operation for Reverse Calculation.

From the table and figures above, round off is using many-to-one function. we can see that when we round off the number from original, there are many inputs number (original number) will become just one number in output (after round off).

We can achieve accurate results when performing forward calculations because the process follows a well-defined mathematical path. However, reversing the calculation is impossible in certain cases, particularly when dealing with rounding operations. This is because a single input value, once rounded, can correspond to multiple possible original values, making it impossible to uniquely determine the exact initial input. Thus, rounding is non-reversible due to lost precision.

4.5.2 Hash Function

For example, we will set 10 numbers for the calculation in the example. The numbers are 23, 37, 45, 51, 62, 78, 84, 96, 103, and 117. We will hash each of these numbers using a simple hash

function. The hash function processes each input number using a specific mathematical operation. In this example, we will use a basic hash function that takes the remainder when dividing each number by 10. The result of output of the hash function is a fixed-size numeric value. We will use the remainder of the division by 10 as the hash value. So, the output result will be a number between 0 and 9.

Table 4.22: Function Table for Hash Function Table Operation for Forward Calculation.

Original Number	Hash Calculation	Hash Value
23	23 % 10 = 3	3
37	37 % 10 = 7	7
45	45 % 10 = 5	5
51	51 % 10 = 1	1
62	62 % 10 = 2	2
78	78 % 10 = 8	8
84	84 % 10 = 4	4
96	96 % 10 = 6	6
103	103 % 10 = 3	3
117	117 % 10 = 7	7

It is impossible to reserve the calculation from hash value to become original number. When we calibrate the remainder of a number when divided by 10, we are effectively reducing the information to a single digit. As an example, even if anyone know the hash value is 3, it could

correspond to multiple original numbers like 43, 33, 23, and 13. So, the person still cannot determine which one was the original number.

Then, hash functions, especially simple ones like remainder calculations, may result in collisions. That means different original numbers can generate the same number in hash value. For example, both 37 and 117 result in a hash value of 7. Therefore, any person cannot uniquely determine the original number from the hash value alone.

After that, the calculation of taking a remainder or applying a hash function is inherently irreversible. There is no general mathematical formula and method to retrieve the exact original number from its hash value.

4.5.3 Truncation

Truncation is the process of disposing of the decimal part of a number by rounding it towards zero to obtain the integer part. It is non-reversible because various different numbers can generate the same truncated result. After the decimal part is removed, it cannot be uniquely recovered.

Table 4.23: Function Table for Truncation Table Operation for Forward Calculation.

Original Number	Truncated Result
7.92	7
7.25	7
1.84159	1
1.11	1
4.75	4
4.999	4
-8.999	-8
0.5	0
0	0
-3.33	-3

In each number, when the decimal part is removed, it will produce an integer number. Notice how different original numbers can result to the same truncated result. For example, both 7.92 and 7.25 truncate to 7, demonstrating the non-reversible calculation of the truncation operation.

4.5.4 Fractional Part Extraction

Unlike truncation, the fractional part extraction calculation process involves isolating the decimal portion of a real number and leaving only the fractional component after the decimal point. This

process is non-reversible because once the calculation extracted the fractional part, it discarded the integer part, and multiple different numbers may have the same output result.

Table 4.24: Function Table for Fractional Part Extraction Table Operation for Forward Calculation.

Original Number	Result
7.92	0.92
6.92	0.92
3.14	0.14
21.14	0.14
4.35	0.35
800.35	0.35
2.25	0.75
0.75	0.75
90.112	0.112

When the different original numbers can generate the same result of output. It is the evidence that it cannot calculate in reverse. For example, both 7.92 and 6.92 produce the output result of 0.92.

4.5.5 Bitwise XOR

Bitwise XOR (Exclusive OR) is a binary operation calculation that takes 2 binary digits (bits) of same length and generate a new binary digit according to the following rules:

1. If the corresponding bits are different (one is 0, and the other is 1), the result is 1.
2. If the corresponding bits are the same (both 0 and both 1), the result is 0.

The XOR operation cannot be calculated in reverse calculation because different pairs of operands can produce the same XOR result. Here is some of the examples:

Table 4.25: Truth Table for Bitwise XOR Table Operation for Forward and Inverse Calculation.

Operand A	Operand B	XOR Result
1100	0111	1011
0101	1010	1011
0011	1010	1001
1110	0011	1001
1000	1111	0111
0010	0101	0111
1101	1010	0111
0011	0100	0111
0110	1011	1101

In every row, the operation is using bitwise XOR between the corresponding bits of Operand A and Operand B and generate the output result in the given XOR Result. Different pairs of operands can produce the same XOR result is the proof the non-reversibility of the XOR operation.

4.5.6 Bitwise AND

The bitwise AND operation is a binary operation that calculate on each bit of two binary numbers, generating a new binary number by combining the corresponding bits using the AND logic. The bitwise NAND operation results in 1 only if both corresponding bits are 1, otherwise, it results in 0.

(iii) If the corresponding bits are not 1 (both are not 1), the result is 0.

(iv) If the corresponding bits are the 1 (both 1), the result is 1.

As an example, if the two binary numbers a and b, the bitwise AND operation (&) produces a new binary number c as follows:

c= a & b

The bitwise AND operation is non-reversible because, given the result *c*, it cannot uniquely determine the original values of *a* and *b* since multiple pairs of *a* and *b* can produce the same *c*.

Table 4.26: Truth Table for Bitwise AND Table Operation for Forward and Inverse Calculation.

Operand A	Operand B	Result
1100	1011	1000
1101	1010	1000
1000	1111	1000
0011	1010	0010
1110	0011	0010
0101	1000	0000
0010	0101	0000
0011	0100	0000
101010	110011	100010
11110000	10101010	10100000

The bitwise AND operation loses information about the original pairs of bits and as the result, it can generate the same output number although with different inputs number. There are multiple possible pairs of operands that could have generate the same output result, it is evidence that the loss of information happens in the process. It cannot uniquely determine which specific pair of operands was used. Multiple combinations of Operand A and Operand B can lead to the same result, making it impossible to reverse the calculation and evaluate the original operands.

4.5.7 Bitwise OR

Bitwise OR is a binary operation that operates on each pair of corresponding bits of two binary numbers, setting the result bit to 1 if at least one of the corresponding bits in the operands is 1. While the operation is straightforward, it is non-reversible because different pairs of input numbers can produce the same result. When you perform a bitwise OR operation, each bit in the result can be set to 1 if at least one of the corresponding bits in the operands is 1. This means that different combinations of bits in the operands can lead to the same result, making it challenging to uniquely determine the original operands from the result.

Table 4.27: Truth Table for Bitwise OR Table Operation for Forward and Inverse Calculation.

Operand A	Operand B	Result
0010	1101	1111
1001	0110	1111
0111	1000	1111
0100	1011	1111
0010	1101	1111
0000	1111	1111
1110	0001	1111
1011	0100	1111
1111	0000	1111
1100	0011	1111

4.5.8 Bitwise NAND

Bitwise NAND (NOT-AND) is a binary operation that negates the result of the AND operation. The NAND operation returns 0 (false) only when both of its inputs are 1 (true); otherwise, it produces a 1 (true). Like other bitwise operations, NAND is non-reversible because different combinations of input values can lead to the same output.

The NAND operation is non-reversible because it outputs 0 only when both inputs are 1. When you observe a NAND output of 0, you cannot uniquely determine whether both inputs were 1 or if one or both of them were 0. Therefore, there are multiple input combinations that result in the same NAND output, making it non-reversible.

Table 4.28: Truth Table for Bitwise NAND Operation for Forward and Inverse Calculation.

Operand A	Operand B	Result
0	0	1
0	1	1
1	0	1
1	1	0

4.5.9 Fuzzy Logic

Fuzzy logic is a form of logic that deals with approximate reasoning and allows for degrees of truth. Unlike classical (crisp) logic, which is binary and assumes a statement is either true or false, fuzzy logic allows for intermediate values between true and false, expressed as degrees of membership in a set.

Table 4.29: Function Table for Fuzzy Logic Table Operation for Forward Calculation.

Input 1	Input 2	Output
Low	Low	Low
Low	Moderate	Moderate
Low	High	Moderate
Moderate	Low	Moderate
Moderate	Moderate	Moderate
Moderate	High	Moderate
High	Low	Moderate
High	Moderate	Moderate
High	High	High

At the moderate output, it uses the many-to-one function. As mentioned above at round off method, there are impossible to reverse the calculation because one input cannot produce many outputs.

4.6 CONCLUSION

From Table 4.1, it can be observed that the error percentage between the digital multimeter and the Arduino measurements is remarkably low. The results demonstrate excellent accuracy, with the error percentage ranging from a minimum of 0% to a maximum of only 3.02%. Given the minimal error margin, the voltage output discrepancy between the Arduino and the digital multimeter is negligible. Therefore, it can be concluded that the results are highly reliable, fulfilling the first and second objectives of the study successfully.

TiO_2 can be used as a sensor to evaluate the concentration of ammonia. TiO_2 will generate electricity when the UV ray penetrates through it. Different concentration of ammonia and different range of UV rays from TiO_2 will generate different values of electricity. This is evidence that TiO_2 can be sensor because it can give different output when the inputs are changing.

The Arduino and digital multimeter will be used to evaluate the amount of electricity generated. From the experiment, the output value that showed in Arduino and digital multimeter is almost same with the highest error of different is 3.02%. With this low of error of different, it shows that the Arduino can be used with TiO_2 to detect the ammonia concentration.

However, when we use the fuzzy logic to calculate the output of the electricity generated by TiO_2, it gives unstable values. From distance 1 cm to 13 cm of UV ray from TiO_2, the range of errors of different is below 50%. It is still can be tolerable because the sensor that we use does not have a high sensing ability and we use different types of defuzzification to calculate it and still get the almost the same value.

However, when the UV ray is 15 cm to 19 cm, the error of different is high until over 1000%. It shows that 13 cm is the maximum distance of UV rays that can be used from TiO_2. Maybe the radiation of UV rays is too low and the sensor cannot detect it properly. Hence, the maximum length that can be used is only up to 13 cm.

The fuzzy logic can be calculated only in forward calculation. It cannot calculate in backward because the fuzzy logic uses many-to-one functions. Fuzzy logic can be considered as non-reversible function.

CHAPTER FIVE

CONCLUSION

5.1 CONCLUSION

The TiO_2 can be used to detect concentration of ammonia in water. It is successful in detecting and giving different values of voltage when we change the ammonia concentration and place the UV ray at different distance but the maximum distance is only 13 cm because higher than that it will give inaccurate voltage output values. The first hypothesis is that the higher concentration of ammonia will generate higher voltage output. The second hypothesis is the higher the distance of UV ray from TiO_2 will generate lower voltage output. This research findings align with our initial hypothesis. The objectives 1 and 2 have been achieved successfully.

Other than that, fuzzy logic has successfully in predicting voltage output in forward calculation. The prediction of output voltage is below 50% and it is acceptable because the TiO_2 that has been used do not have a high sensing capability. However, we fail in predicting ammonia concentration in reserve calculation. This is because fuzzy logic cannot be calculated in reserve like in inverse function and inverse matrices. Our theory is already has been discussed in chapter 4.

The first objective of this project is to design a PEC-based UV-assisted water monitoring sensor using TiO_2, which has been successfully achieved. The TiO_2 sensor demonstrates its ability to detect variations in ammonia concentration as well as changes in the distance between the UV light source and the TiO_2 surface. This proves that TiO_2 is effective in capturing UV rays

as they penetrate through the material, highlighting its potential for accurate and efficient environmental monitoring applications.

Then, to develop a portable water monitoring system for ammonia detection using the designed sensor. This is done successfully. TiO_2 is small, lightweight and just needs a small circuit and a battery to function. It does not need plug for power supply.

The last is to evaluate the performance of the developed portable water monitoring system using fuzzy logic. Unfortunately, this part did not meet expectations. We success in forward calculation only that is to predict the output voltage and fail in predicting the ammonia concentration that need to be calculated in reverse calculation in fuzzy logic. This is because the fuzzy logic cannot be calculated in reverse.

5.2 FUTURE RESEARCH DEVELOPMENT

Overall, TiO_2 is a good sensor to be used with UV rays. It can detect well and it is very responsive. It can expand to become more useful in the future if we can improve it. One of the improvements is, run experiments using TiO_2 by different harmful chemical solution other than ammonia. There are many hazardous chemicals present in the waterways, seas, and rivers over there such as petroleum, heavy metal and pesticide. TiO_2 can be used to detect all of them by generating voltage when put different concentration on it. Because TiO_2 is small and portable, it can be done easily. Other than that, TiO_2 can be dopped with light-harvesting materials such as zinc oxide or cadmium sulfide to increase the efficiency light absorption. During photocatalysis, light absorption plays a vital role to capture the UV ray and improve the output result. Without excellent substance, the best output cannot be produced.

REFERENCES

A.M. Selman, Z. Hassan, Highly sensitive fast-response UV photodiode fabricated from rutile TiO2 nanorod array on silicon subst rate, Sensors and Actuators A: Physical, 221 (2015) 15-21.

Aggarwal, N., Krishna, S., Sharma, A., Goswami, L., Kumar, D., Husale, S., & Gupta, G. (2017). A highly responsive self-driven UV photodetector using GaN nanoflowers. Advanced Electronic Materials, 3(5), 1700036.

Alhazmi, A. I., Mohsin, B., & Khamis, S. S. (2020). Portable Hemodialysis Machine for Chronic Hemodialysis in Hospital—Advantages and Future Uses. Open Journal of Nephrology, 10(2), 158-169.

Askim, J.R., Mahmoudi, M., Suslick, K.S. Chem.Soc.Rev.42,8649–8682, 2013.

Atique, U., & An, K. G. (2018). Stream health evaluation using a combined approach of multi-metric chemical pollution and biological integrity models. Water, 10(5), 661.

B. Liu, X. Wu, K. W. L. Kam, W.-F. Cheung, and B. Zheng, "Cuprous Oxide Based Chemiresistive Electronic Nose for Discrimin ation of Volatile Organic Compounds," ACS Sensors, vol. 4, no. 11, pp. 3051-3055, 2019/11/22, 2019.

B. Liu, Y. Huang, K. W. L. Kam, W.-F. Cheung, N. Zhao, and B. Zheng, "Functionalized graphene-based chemiresistive electroni c nose for discrimination of disease-related volatile organic compounds," Biosensors and Bioelectronics: X, vol. 1, p. 100016, 2019/0 6/01/ 2019.

Bae, J. W., Kwon, H. J., Kim, S. H., Ma, L., Im, H., Kim, E., ... & Kwon, W. S. (2020). Inhalation of ammonium sulfate and ammonium nitrate adversely affect sperm function. Reproductive Toxicology, 96, 424-431.

Bakar, N. A., Rosbi, S., & Bakar, A. A. (2020). Robust estimation of student performance in massive open online course using fuzzy logic approach. Int. J. Eng. Technol, 143-152.

Bakar, N. A., Rosbi, S., & Bakar, A. A. (2020). Robust estimation of student performance in massive open online course using fuzzy logic approach. *Int. J. Eng. Technol*, 143-152.

Bharat Sharma, Jung-Suk Sung, Avinash A. Kadam, Jae-ha Myung, Adjustable n-p-n gas sensor response of Fe3O4-HNTs doped Pd nanocomposites for hydrogen sensors, Applied Surface Science, Volume 530, 2020.

C. O'Rourke and D. R. Bowler, "Intrinsic Oxygen Vacancy and Extrinsic Aluminum Dopant Interplay: A Route to the Restoration of Defective TiO2," The Journal of Physical Chemistry C, vol. 118, pp. 7261-7271, 2014.

Canu, I. G., Fraize-Frontier, S., Michel, C., & Charles, S. (2020). Weight of epidemiological evidence for titanium dioxide risk assessment: current state and further needs. Journal of exposure science & environmental epidemiology, 30(3), 430-435.

Chen, P. F., Zhang, R. J., Huang, S. B., Shao, J. H., Cui, B., Du, Z. L., ... & Lin, C. (2020). UV dose effects on the revival characteristics of microorganisms in darkness after UV disinfection: evidence from a pilot study. Science of the Total Environment, 713, 136582.

Chen, Y., Li, T., Yang, Q., Zhang, Y., Zou, J., Bian, Z., & Wen, X. (2019). UVA radiation is beneficial for yield and quality of indoor cultivated lettuce. Frontiers in plant science, 10, 1563.

Courbat, J., Briand, D., Damon-Lacoste, J., Wöllenstein, J., & De Rooij, N. F. (2009). Evaluation of pH indicator-based colorimetric films for ammonia detection using optical waveguides. Sensors and Actuators B: Chemical, 143(1), 62-70.

Dallavecchia, D. L., Ricardo, E., Aguiar, V. M., da Silva, A. S., & Rodrigues, A. G. (2019). Efficacy of UV-C ray sterilization of calliphora vicina (diptera: Calliphoridae) eggs for use in maggot debridement therapy. Journal of medical entomology, 56(1), 40-44.

Dasarathy, S., Mookerjee, R. P., Rackayova, V., Thrane, V. R., Vairappan, B., Ott, P., & Rose, C. F. (2017). Ammonia toxicity: from head to toe?. Metabolic brain disease, 32(2), 529-538.

Dernoncourt, F. (2013). Introduction to fuzzy logic. Massachusetts Institute of Technology, 21, 50-56.

Dos Santos, T., & de Castro, L. F. (2021). Evaluation of a portable Ultraviolet C (UV-C) device for hospital surface decontamination. Photodiagnosis and Photodynamic Therapy, 33, 102161.

Ezzahra Chakik, F., Kaddami, M., & Mikou, M. (2017). Effect of operating parameters on hydrogen production by electrolysis of water. international journal of hydrogen energy, 42(40), 25550-25557.

Figueiró, C. S. M., De Oliveira, D. B., Russo, M. R., Caires, A. R. L., & Rojas, S. S. (2018). Fish farming water quality monitored by optical analysis: The potential application of UV–Vis absorption and fluorescence spectroscopy. Aquaculture, 490, 91-97.

Gao, J., Song, J., Ye, J., Duan, X., Dionysiou, D. D., Yadav, J. S., ... & Luo, S. (2021). Comparative toxicity reduction potential of UV/sodium percarbonate and UV/hydrogen peroxide treatments for bisphenol A in water: An integrated analysis using chemical, computational, biological, and metabolomic approaches. Water Research, 190, 116755.

Giddey, S., Badwal, S. P. S., Munnings, C., & Dolan, M. (2017). Ammonia as a renewable energy transportation media. ACS Sustainable Chemistry & Engineering, 5(11), 10231-10239.

H. Choi, H. Ryu, W.-J. Lee, Study of the morphological, optical, structural and photoelectrochemical properties of TiO2 nanorods grown with various precursor concentrations, Electronic Materials Letters, 13 (2017) 497-504.

Haider, A. J., Jameel, Z. N., & Al-Hussaini, I. H. (2019). Review on: titanium dioxide applications. Energy Procedia, 157, 17-29.

Haider, I., Ali, A., Arifeen, T., & Hassan, A. S. (2020). Far UV-C lights and fiber optics induced and selective far UV-C treatment against COVID-19 for fatality-survival tradeoff.

Hanada, N., Kohase, Y., Hori, K., Sugime, H., & Noda, S. (2020). Electrolysis of ammonia in aqueous solution by platinum nanoparticles supported on carbon nanotube film electrode. Electrochimica Acta, 341, 136027.

Hellmann, M. (2001). Fuzzy logic introduction. Université de Rennes, 1(1).

Hönigsmann, H. (2020). UVB therapy (broadband and narrowband).

Hosseinpour, S., & Martynenko, A. (2022). Application of fuzzy logic in drying: A review. Drying Technology, 40(5), 797-826.

Huang, Y., Kong, M., Coffin, S., Cochran, K. H., Westerman, D. C., Schlenk, D., ... & Dionysiou, D. D. (2020). Degradation of contaminants of emerging concern by UV/H2O2 for water reuse: Kinetics, mechanisms, and cytotoxicity analysis. Water research, 174, 115587.

Huangfu, G., Xiao, H., Guan, L., Zhong, H., Hu, C., Shi, Z., & Guo, Y. (2020). Visible or Near-Infrared Light Self-Powered Photodetectors Based on Transparent Ferroelectric Ceramics. ACS Applied Materials & Interfaces, 12(30), 33950-33959.

K. Das, S. N. Sharma, M. Kumar, "Morphology Dependent Luminescence Properties of Co Doped TiO2," The Journal of Physica l Chemistry C, vol. 113, pp.14783-14792, 2009.

K. Liang et al., "An Electronic Nose Based on Copper Oxide Heterojunctions for Rapid Assessment of Liquor," Chinese Journal of Analytical Chemistry, vol. 47, no. 7, pp. e19073-e19080, 2019/07/01/ 2019.

Kaptan, M. (2021). Risk assessment for transporting ammonium nitrate-based fertilizers with bulk carriers. Journal of ETA Maritime Science, 9(2), 130-137.

Karri, R. R., Sahu, J. N., & Chimmiri, V. (2018). Critical review of abatement of ammonia from wastewater. Journal of Molecular Liquids, 261, 21-31.

Kasani, S., Curtin, K., & Wu, N. (2019). A review of 2D and 3D plasmonic nanostructure array patterns: fabrication, light management and sensing applications. Nanophotonics, 8(12), 2065-2089.

Khan, A. Q., Travers, J. B., & Kemp, M. G. (2018). Roles of UVA radiation and DNA damage responses in melanoma pathogenesis. Environmental and molecular mutagenesis, 59(5), 438-460.

Kwak, D., Lei, Y., & Maric, R. (2019). Ammonia gas sensors: A comprehensive review. Talanta, 204, 713-730.

Labille, J., Slomberg, D., Catalano, R., Robert, S., Apers-Tremelo, M. L., Boudenne, J. L., ... & Radakovitch, O. (2020). Assessing UV filter inputs into beach waters during recreational activity: A field study of three French Mediterranean beaches from consumer survey to water analysis. Science of the Total Environment, 706, 136010.

Lan, C. C. E., Hung, Y. T., Fang, A. H., & Ching-Shuang, W. (2019). Effects of irradiance on UVA-induced skin aging. Journal of dermatological science, 94(1), 220-228.

Li, D., & Liu, S. (2018). Water quality monitoring and management: Basis, technology and case studies. Academic Press.

Li, D., Xu, X., Li, Z., Wang, T., & Wang, C. (2020). Detection methods of ammonia nitrogen in water: A review. TrAC Trends in Analytical Chemistry, 127, 115890.

Li, J. K., Ge, C., Jin, K. J., Du, J. Y., Yang, J. T., Lu, H. B., & Yang, G. Z. (2017). Self-driven visible-blind photodetector based on ferroelectric perovskite oxides. Applied Physics Letters, 110(14), 142901.

Liao, C., Li, Y., & Tjong, S. C. (2020). Visible-light active titanium dioxide nanomaterials with bactericidal properties. Nanomaterials, 10(1), 124.

M. Iraj, F.D. Nayeri, E. Asl-Soleimani, K. Narimani, Controlled growth of vertically aligned TiO2 nanorod arrays using the improved hydrothermal method and their application to dye-sensitized solar cells, Journal of Alloys and Compounds, 659 (2016) 44-50.

M. Okuya, K. Shiozaki, N. Horikawa, T. Kosugi, G. R. A. Kumara, J. Madarász, et al., "Porous TiO2 thin films prepared by spra y pyrolysis deposition (SPD) technique and their application to UV sensors," Solid State Ionics, vol. 172, pp. 527-531, 2004.

M.I. Kim, J. Shim, T. Li, J. Lee, H.G. Park, Fabrication of nanoporous nanocomposites entrapping Fe3O4 magnetic nanoparticle s and oxidases for colorimetric biosensing, Chem. Eur. J. 17 (2011) 10700-10707.

Magalhães, P., Andrade, L., Nunes, O. C., & Mendes, A. (2017). Titanium dioxide photocatalysis: Fundamentals and application on photoinactivation. Reviews on Advanced Materials Science, 51(2).

Mahala, P., Patel, M., Ban, D. K., Nguyen, T. T., Yi, J., & Kim, J. (2020). High-performing self-driven ultraviolet photodetector by TiO2/Co3O4 photovoltaics. Journal of Alloys and Compounds, 827, 154376.

Marrani, E., Foeldvari, I., Lopez, J. A., Cimaz, R., & Simonini, G. (2018, December). Comparing ultraviolet light A photo (chemo) therapy with Methotrexate protocol in childhood localized scleroderma: Evidence from systematic review and meta-analysis approach. In Seminars in arthritis and rheumatism (Vol. 48, No. 3, pp. 495-503). WB Saunders.

Mendel, J. M. (1995). Fuzzy logic systems for engineering: a tutorial. Proceedings of the IEEE, 83(3), 345-377.

Min Deng, Xiaodong Wu, Aimei Zhu, Qiugen Zhang, Qinglin Liu, Well-dispersed TiO2 nanoparticles anchored on Fe3O4 magneti c nanosheets for efficient arsenic removal, Journal of Environmental Management, Volume 237, 2019.

Mitsuishi, T. (2022). Definition of Centroid Method as Defuzzification. *Formalized Mathematics*, *30*(2), 125-134.

Mittal, K., Jain, A., Vaisla, K. S., Castillo, O., & Kacprzyk, J. (2020). A comprehensive review on type 2 fuzzy logic applications: Past, present and future. Engineering Applications of Artificial Intelligence, 95, 103916.

Moukayed, M., & Grant, W. B. (2017). The roles of UVB and vitamin D in reducing risk of cancer incidence and mortality: A review of the epidemiology, clinical trials, and mechanisms. Reviews in Endocrine and Metabolic Disorders, 18(2), 167-182.

Nisha Rani, Brijnandan S. Dehiya, Influence of anionic and non-ionic surfactants on the synthesis of core-shell Fe3O4@TiO2 nan ocomposite synthesized by hydrothermal method, Ceramics International, Volume 46, Issue 15, 2020.

Oregon Department of Human Services, "HEALTH EFFECTS INFORMATION", ENVIRONMENTAL TOXICOLOGY SECTION, Office of Environmental Public Health, (January 2000), Retrieve from https://www.oregon.gov/oha/PH/HealthyEnvironments/DrinkingWater/Monitoring/Documents/health/ammonia.pdf

Pandey, B. K., Dias, S., Nanda, K. K., & Krupanidhi, S. B. (2017). Deep UV-Vis photodetector based on ferroelectric/semiconductor heterojunction. Journal of Applied Physics, 122(23), 234502.

Patrizi, A., Raone, B., & Ravaioli, G. M. (2017). Safety and Efficacy of Phototherapy in the Management of Eczema. Ultraviolet Light in Human Health, Diseases and Environment, 319-331.

Phuong, N. H., & Kreinovich, V. (2001). Fuzzy logic and its applications in medicine. International journal of medical informatics, 62(2-3), 165-173.

Ploydaeng, M., Rajatanavin, N., & Rattanakaemakorn, P. (2021). UV-C light: A powerful technique for inactivating microorganisms and the related side effects to the skin. Photodermatology, Photoimmunology & Photomedicine, 37(1), 12-19.

Randhawa, S., Sandha, S. S., & Srivastava, B. (2016, August). A multi-sensor process for in-situ monitoring of water pollution in rivers or lakes for high-resolution quantitative and qualitative water quality data. In 2016 IEEE Intl Conference on Computational Science and Engineering (CSE) and IEEE Intl Conference on Embedded and Ubiquitous Computing (EUC) and 15th Intl Symposium on Distributed Computing and Applications for Business Engineering (DCABES) (pp. 122-129). IEEE.

Ruhua Zha, Tuo Shi, Liu He, Xueying Sun, Yufei Jia, Min Zhang, Engineering the surface active sites of actiniae-like hierarchical Fe3O4/Co3O4 nanoheterojunction for efficient oxygen reduction reaction, Dyes and Pigments, Volume 180, 2020.

Sabir, F. K., Genç, F., & Çavdarci, M. (2018). Effects of postharvest UV-C treatments on storage duration and quality of strawberry. Yüzüncü Yil Üniversitesi Journal of Agricultural Sciences, 28(4), 458-465.

Shi, G., He, Y., Luo, Q., Li, B., & Zhang, C. (2018). Portable device for acetone detection based on cataluminescence sensor utilizing wireless communication technique. Sensors and Actuators B: Chemical, 257, 451-459.

Shi, Z., Chow, C. W., Fabris, R., Liu, J., & Jin, B. (2020). Alternative particle compensation techniques for online water quality monitoring using UV–Vis spectrophotometer. Chemometrics and Intelligent Laboratory Systems, 204, 104074.

Subhapriya, S., & Gomathipriya, P. (2018). Green synthesis of titanium dioxide (TiO2) nanoparticles by Trigonella foenum-graecum extract and its antimicrobial properties. Microbial pathogenesis, 116, 215-220.

Surjadinata, B. B., Jacobo-Velázquez, D. A., & Cisneros-Zevallos, L. (2017). UVA, UVB and UVC light enhances the biosynthesis of phenolic antioxidants in fresh-cut carrot through a synergistic effect with wounding. Molecules, 22(4), 668.

Van Damme, M., Clarisse, L., Whitburn, S., Hadji-Lazaro, J., Hurtmans, D., Clerbaux, C., & Coheur, P. F. (2018). Industrial and agricultural ammonia point sources exposed. Nature, 564(7734), 99-103.

Wang, X., Li, J., Chen, J., Cui, L., Li, W., Gao, X., & Liu, Z. (2020). Water quality criteria of total ammonia nitrogen (TAN) and un-ionized ammonia (NH3-N) and their ecological risk in the Liao River, China. Chemosphere, 243, 125328.

Wolfrum, E.J., Meglen,R.M., Peterson, D., Sluiter, J, Sens.ActuatorsB115, 322–329, 2006.

X. Zu, H. Wang, G. Yi, Z. Zhang, X. Jiang, J. Gong, H. Luo, Self-powered UV photodetector based on heterostructured TiO2 nano wire arrays and polyaniline nanoflower arrays, Synthetic Metals, 200 (2015)

Y. Cao, Z. Li, Y. Wang, T. Zhang, Y. Li, X. Liu, F. Li, Influence of TiO2 Nanorod Arrays on the Bilayered Photoanode for Dye-Se nsitized Solar Cells, Journal of Electronic Materials, 45 (2016) 4989-4998.

Y. Xie, L. Wei, G. Wei, Q. Li, D. Wang, et al., "A self-powered UV photodetector based on TiO2 nanorod arrays," Nanoscale Res earch Letters, vol. 8, p. 188, 2013.

Yan, Z., Zheng, X., Fan, J., Zhang, Y., Wang, S., Zhang, T., ... & Huang, Y. (2020). China national water quality criteria for the protection of freshwater life: Ammonia. Chemosphere, 251, 126379.

Ye, J., Huang, H., Luo, G., Yin, L., Li, B., Chen, S., ... & Yang, X. (2020). NB-UVB irradiation attenuates inflammatory response in psoriasis. Dermatologic Therapy, 33(4), e13626.

Yen, J. (1999). Fuzzy logic-a modern perspective. IEEE transactions on knowledge and data engineering, 11(1), 153-165.

Yooyen, S., Iamopas, J., Changnoi, V., Kammee, W., Khanthawiti, T., & Sompornpailin, K. (2021). Efficacy of Ultraviolet Radiation on Microbial Eliminations from Conditioning Airflow. In Presented at the 2nd Innovation Aviation & Aerospace Industry-International Conference (Vol. 28, p. 30).

Yusoff, M. M., Mamat, M. H., & Mahmood, M. R. (2017). Synthesis of Titanium Dioxide Nanorod Arrays Using a Facile Aqueous Sol-Gel Route for Ultraviolet Photosensor Applications. Recent Applications in Sol-Gel Synthesis.

Yusoff, M. M., Mamat, M. H., Abdullah, M. A. R., Ismail, A. S., Malek, M. F., Zoolfakar, A. S., … Rusop, M. (2019). Coupling Heterostructure of Thickness-Controlled Nickel Oxide Nanosheets Layer and Titanium Dioxide Nanorod Arrays via Immersion Route for Self-Powered Solid-State Ultraviolet Photosensor Applications. Measurement, 106982.

Yusoff, M. M., Mamat, M. H., Ismail, A. S., Malek, M. F., Khusaimi, Z., Suriani, A. B., … Rusop, M. (2018). Enhancing the performance of self-powered ultraviolet photosensor using rapid aqueous chemical-grown aluminum-doped titanium oxide nanorod arrays as electron transport layer. Thin Solid Films, 655, 1–12.

Yusoff, M. M., Mamat, M. H., Ismail, A. S., Malek, M. F., Zoolfakar, A. S., Suriani, A. B., … Rusop, M. (2018). Low-temperature-dependent growth of titanium dioxide nanorod arrays in an improved aqueous chemical growth method for photoelectrochemical ultraviolet sensing. Journal of Materials Science: Materials in Electronics.

Yusoff, M. M., Mamat, M. H., Malek, M. F., Abdullah, M. A. R., Ismail, A. S., Saidi, S. A., … Rusop, M. (2018). Preparation of TNAs/NiO p-n heterojunction and their applications in UV photosensor.

Yusoff, M. M., Mamat, M. H., Malek, M. F., Abdullah, M. A. R., Ismail, A. S., Saidi, S. A., … Rusop, M. (2018). Sn-doped TiO2 nanorod arrays produced by facile one step aqueous chemical route: Structural characterization.

Yusoff, M. M., Mamat, M. H., Malek, M. F., Suriani, A. B., Mohamed, A., Ahmad, M. K., … Rusop, M. (2016). Growth of titanium dioxide nanorod arrays through the aqueous chemical route under a novel and facile low-cost method. Materials Letters, 164, 294–298.

Zadeh, L. A. (1988). Fuzzy logic. Computer, 21(4), 83-93.

Zadeh, L. A. (2008). Is there a need for fuzzy logic?. Information sciences, 178(13), 2751-2779.

Zhang, B., Cao, S., Du, M., Ye, X., Wang, Y., & Ye, J. (2019). Titanium dioxide (TiO2) mesocrystals: Synthesis, growth mechanisms and photocatalytic properties. Catalysts, 9(1), 91.

Zhang, D., Du, S., Su, S., Wang, Y., & Zhang, H. (2019). Rapid detection method and portable device based on the photothermal effect of gold nanoparticles. Biosensors and Bioelectronics, 123, 19-24.

Zhang, K., Ren, J., Ren, J. X., Liu, C., & Sun, L. (2020). Successful treatment of verruca plana with NB-UVB: A case report. Dermatologic therapy, 33(2), e13207.

Zhou, C., Raju, S., Li, B., Chan, M., Chai, Y., & Yang, C. Y. (2018). Self-driven metal–semiconductor–metal WSe2 photodetector with asymmetric contact geometries. Advanced Functional Materials, 28(45), 1802954.

Zoerner, A., Oertel, S., Jank, M. P., Frey, L., Langenstein, B., & Bertsch, T. (2018). Human Sweat Analysis Using a Portable Device Based on a Screen-printed Electrolyte Sensor. Electroanalysis, 30(4), 665-671.

INDEX

Arduino Coding

```
const int analogPin1 = A0;  // Analog input pin 1 for voltage measurement
const int analogPin2 = A5;  // Analog input pin 2 for voltage measurement
const float referenceVoltage = 5.0;  // Reference voltage for the ADC (adjust as needed)
const int measurementDuration = 10000;  // Measurement duration in milliseconds
const int measurementInterval = 1000;  // Interval between voltage measurements in milliseconds
const int initialDelay = 3000;  // Delay before starting voltage measurement in milliseconds

void setup() {
  Serial.begin(9600);  // Initialize serial communication at 9600 baud rate
}

void loop() {
  delay(initialDelay);  // Delay before starting voltage measurement

  unsigned long startTime = millis();  // Start time of the measurement
  unsigned long endTime = startTime + measurementDuration;  // End time of the measurement
  int numMeasurements = 0;  // Number of measurements taken
  float totalVoltage1 = 0.0;  // Accumulated total voltage for A0
  float totalVoltage2 = 0.0;  // Accumulated total voltage for A5

while (millis() < endTime) {
    int sensorValue1 = analogRead(analogPin1);  // Read the analog input voltage for A0
    float voltage1 = (sensorValue1 * referenceVoltage) / 1023.0;  // Convert sensor value to
voltage for A0
    totalVoltage1 += voltage1;  // Accumulate the voltage for A0
```

```
  int sensorValue2 = analogRead(analogPin2);  // Read the analog input voltage for A5
  float voltage2 = (sensorValue2 * referenceVoltage) / 1023.0;  // Convert sensor value to voltage for A5
  totalVoltage2 += voltage2;  // Accumulate the voltage for A5

  numMeasurements++;  // Increment the number of measurements

  if (millis() % measurementInterval == 0) {
    float averageVoltage1 = totalVoltage1 / numMeasurements;  // Calculate the average voltage for A0
    Serial.print("Voltage A0: ");
    Serial.print(averageVoltage1 * 1000, 2);  // Print average voltage in millivolts with 2 decimal places for A0
    Serial.println(" mV");

    float averageVoltage2 = totalVoltage2 / numMeasurements;  // Calculate the average voltage for A5
    Serial.print("Voltage A5: ");
```

Centroid Fuzzy Logic Coding

```
print('LOGIK FUZZY')

x_con = float(input('Enter Ammonia Concentration Value (mV): '))
y_distance = float(input('Enter Distance Value (cm): '))

con = float(x_con)
distance = int(y_distance)

# FUZZYFICATION VOLT
if con >= 0 and con < 0.5:
    con_low = (0.5 - con) / (0.5 - 0)
    con_moderate = (con - 0) / (0.5 - 0)
    con_high = 0

if con == 0.5:
    con_low = 0
    con_moderate = 1
    con_high = 0

if con > 0.5 and con <= 1.0:
    con_low = 0
    con_moderate = (con - 0.5) / (1 - 0.5)
    con_high = (1.0 - con) / (1 - 0.5)

if con >= 1:
    con_low = 0
    con_moderate = 0
    con_high = 1
```

```
print('Degree of Ammonia concentration is :')
print('Ammonia Concentration low: ', con_low)
print('Ammonia Concentration moderate: ', con_moderate)
print('Ammonia Concentration high: ', con_high)

# FUZZYFICATION DISTANCE
if distance >= 0 and distance < 10:
    distance_high = (10 - distance) / (10 - 0)
    distance_moderate = (distance - 0) / (10 - 0)
    distance_low = 0

if distance == 10:
    distance_high = 0
    distance_moderate = 1
    distance_low = 0

if distance > 10 and distance <= 19:
    distance_high = 0
    distance_moderate = (19 - distance) / (19 - 10)
    distance_low = (distance - 10) / (19 - 10)

print('Degree of Distance is :')
print('Distance Low: ', distance_low)
print('Distance Moderate: ', distance_moderate)
print('Distance High: ', distance_high)

ammonia = []
```

```
def fungsi_low(variable_volt, variable_distance):
    if variable_volt != 0:
        if variable_distance != 0:
            hasil_output = min(variable_volt, variable_distance)
            ammonia.append([hasil_output, 154])

def fungsi_moderate(variable_volt, variable_distance):
    if variable_volt != 0:
        if variable_distance != 0:
            hasil_output = min(variable_volt, variable_distance)
            ammonia.append([hasil_output, 308])

def fungsi_high(variable_volt, variable_distance):
    if variable_volt != 0:
        if variable_distance != 0:
            hasil_output = min(variable_volt, variable_distance)
            ammonia.append([hasil_output, 462])

fungsi_low(con_low, distance_low)
fungsi_moderate(con_low, distance_moderate)
fungsi_moderate(con_low, distance_high)
fungsi_moderate(con_moderate, distance_low)
fungsi_moderate(con_moderate, distance_moderate)
fungsi_moderate(con_moderate, distance_high)
fungsi_moderate(con_high, distance_low)
fungsi_moderate(con_high, distance_moderate)
fungsi_high(con_high, distance_high)

print('Concentration Voltage is', ammonia)
```

```
# Calculate the centroid for defuzzification
numerator = sum([item[0] * item[1] for item in ammonia])
denominator = sum([item[0] for item in ammonia])

z = numerator / denominator

print('Voltage is', z, 'v')
```

Weight Average Method Fuzzy Logic Coding

```
print('LOGIK FUZZY')

x_con = float(input('Enter Ammonia Concentration Value (mV): '))
y_distance = float(input('Enter Distance Value (cm): '))

con = float(x_con)
distance = int(y_distance)

#FUZZYFICATION VOLT
if con>=0 and con<0.5 :
    con_low= (0.5 - con)/(0.5-0)
    con_moderate=(con-0)/(0.5-0)
    con_high=0



if con ==0.5:
    con_low=0
    con_moderate=1
    con_high=0

if con>0.5 and con<=1.0:
    con_low = 0
    con_moderate = (con - 0.5)/(1-0.5)
    con_high = (1.0 - con)/(1-0.5)

if con>=1:
    con_low = 0
    con_moderate = 0
```

```
    con_high = 1



print('Degree of Ammonia concentration is :')
print('Ammonia Concentration low: ', con_low)
print('Ammonia Concentration moderate: ', con_moderate)
print('Ammonia Concentration high: ', con_high)


#FUZZYFICATION DISTANCE

if distance >=0 and distance<10 :
    distance_high= (10- distance)/(10-0)
    distance_moderate=(distance-0)/(10-0)
    distance_low=0



if distance ==10:
    distance_high=0
    distance_moderate=1
    distance_low=0

if distance>10 and distance<=19:
    distance_high = 0
    distance_moderate = (19 - distance)/(19-10)
    distance_low = (distance-10)/(19-10)

print('Degree of Distance is :')
print('Distance Low: ', distance_low)
```

```
print('Distance Moderate: ', distance_moderate)
print('Distance High: ', distance_high)

ammonia=[]

def fungsi_low(variable_volt, variable_distance):
    if variable_volt != 0:
        if variable_distance != 0:
            hasil_output = min(variable_volt, variable_distance)
            ammonia.append([hasil_output,154])

def fungsi_moderate(variable_volt, variable_distance):
    if variable_volt != 0:
        if variable_distance != 0:
            hasil_output = min(variable_volt, variable_distance)
            ammonia.append([hasil_output,308])


def fungsi_high(variable_volt, variable_distance):
    if variable_volt != 0:
        if variable_distance != 0:
            hasil_output = min(variable_volt, variable_distance)
            ammonia.append([hasil_output,462])

fungsi_low(con_low, distance_low)
fungsi_moderate(con_low, distance_moderate)
fungsi_moderate(con_low, distance_high)
fungsi_moderate(con_moderate, distance_low)
fungsi_moderate(con_moderate, distance_moderate)
```

```
fungsi_moderate(con_moderate, distance_high)
fungsi_moderate(con_high, distance_low)
fungsi_moderate(con_high, distance_moderate)
fungsi_high(con_high, distance_high)

print('Concentration Voltage is ',ammonia)

perkalian_new=0
pembahagian_new=0

for j in range(0,len(ammonia)):
    perkalian=ammonia[j][0]*ammonia[j][1]
    pembahagian=ammonia[j][0]
    perkalian_new = perkalian_new + perkalian
    pembahagian_new = pembahagian_new +pembahagian

z= perkalian_new/pembahagian_new


print('Voltage is ', z ,'v')
```

Mean of Centre Fuzzy Logic Coding

```
print('LOGIK FUZZY')

x_con = float(input('Enter Ammonia Concentration Value (mV): '))
y_distance = float(input('Enter Distance Value (cm): '))

con = float(x_con)
distance = int(y_distance)

# FUZZYFICATION VOLT
if con >= 0 and con < 0.5:
    con_low = (0.5 - con) / (0.5 - 0)
    con_moderate = (con - 0) / (0.5 - 0)
    con_high = 0

if con == 0.5:
    con_low = 0
    con_moderate = 1
    con_high = 0

if con > 0.5 and con <= 1.0:
    con_low = 0
    con_moderate = (con - 0.5) / (1 - 0.5)
    con_high = (1.0 - con) / (1 - 0.5)

if con >= 1:
    con_low = 0
    con_moderate = 0
    con_high = 1
```

```
print('Degree of Ammonia concentration is :')
print('Ammonia Concentration low: ', con_low)
print('Ammonia Concentration moderate: ', con_moderate)
print('Ammonia Concentration high: ', con_high)

# FUZZYFICATION DISTANCE
if distance >= 0 and distance < 10:
    distance_high = (10 - distance) / (10 - 0)
    distance_moderate = (distance - 0) / (10 - 0)
    distance_low = 0

if distance == 10:
    distance_high = 0
    distance_moderate = 1
    distance_low = 0

if distance > 10 and distance <= 19:
    distance_high = 0
    distance_moderate = (19 - distance) / (19 - 10)
    distance_low = (distance - 10) / (19 - 10)

print('Degree of Distance is :')
print('Distance Low: ', distance_low)
print('Distance Moderate: ', distance_moderate)
print('Distance High: ', distance_high)

ammonia = []
```

```
def fungsi_low(variable_volt, variable_distance):
    if variable_volt != 0:
        if variable_distance != 0:
            hasil_output = min(variable_volt, variable_distance)
            ammonia.append([hasil_output, 154])

def fungsi_moderate(variable_volt, variable_distance):
    if variable_volt != 0:
        if variable_distance != 0:
            hasil_output = min(variable_volt, variable_distance)
            ammonia.append([hasil_output, 308])

def fungsi_high(variable_volt, variable_distance):
    if variable_volt != 0:
        if variable_distance != 0:
            hasil_output = min(variable_volt, variable_distance)
            ammonia.append([hasil_output, 462])

fungsi_low(con_low, distance_low)
fungsi_moderate(con_low, distance_moderate)
fungsi_moderate(con_low, distance_high)
fungsi_moderate(con_moderate, distance_low)
fungsi_moderate(con_moderate, distance_moderate)
fungsi_moderate(con_moderate, distance_high)
fungsi_moderate(con_high, distance_low)
fungsi_moderate(con_high, distance_moderate)
fungsi_high(con_high, distance_high)

print('Concentration Voltage is', ammonia)
```

```
# Calculate the Mean of Centers for defuzzification
numerator = 0
denominator = 0

for j in range(0, len(ammonia)):
    center = ammonia[j][1]
    numerator += center * ammonia[j][0]
    denominator += ammonia[j][0]

z = numerator / denominator

print('Voltage is', z, 'v')
```

Modified Weighted Average Method Fuzzy Logic Coding

```
print('LOGIK FUZZY')

x_con = float(input('Enter Ammonia Concentration Value (mV): '))
y_distance = float(input('Enter Distance Value (cm): '))

con = float(x_con)
distance = int(y_distance)

# FUZZYFICATION VOLT
if con >= 0 and con < 0.5:
    con_low = (0.5 - con) / (0.5 - 0)
    con_moderate = (con - 0) / (0.5 - 0)
    con_high = 0

if con == 0.5:
    con_low = 0
    con_moderate = 1
    con_high = 0

if con > 0.5 and con <= 1.0:
    con_low = 0
    con_moderate = (con - 0.5) / (1 - 0.5)
    con_high = (1.0 - con) / (1 - 0.5)

if con >= 1:
    con_low = 0
    con_moderate = 0
    con_high = 1
```

```
print('Degree of Ammonia concentration is :')
print('Ammonia Concentration low: ', con_low)
print('Ammonia Concentration moderate: ', con_moderate)
print('Ammonia Concentration high: ', con_high)

# FUZZYFICATION DISTANCE

if distance >= 0 and distance < 10:
    distance_high = (10 - distance) / (10 - 0)
    distance_moderate = (distance - 0) / (10 - 0)
    distance_low = 0

if distance == 10:
    distance_high = 0
    distance_moderate = 1
    distance_low = 0

if distance > 10 and distance <= 19:
    distance_high = 0
    distance_moderate = (19 - distance) / (19 - 10)
    distance_low = (distance - 10) / (19 - 10)

print('Degree of Distance is :')
print('Distance Low: ', distance_low)
print('Distance Moderate: ', distance_moderate)
print('Distance High: ', distance_high)

ammonia = []
```

```
def fungsi_low(variable_volt, variable_distance):
    if variable_volt != 0:
        if variable_distance != 0:
            hasil_output = min(variable_volt, variable_distance)
            ammonia.append([hasil_output, 154])

def fungsi_moderate(variable_volt, variable_distance):
    if variable_volt != 0:
        if variable_distance != 0:
            hasil_output = min(variable_volt, variable_distance)
            ammonia.append([hasil_output, 308])

def fungsi_high(variable_volt, variable_distance):
    if variable_volt != 0:
        if variable_distance != 0:
            hasil_output = min(variable_volt, variable_distance)
            ammonia.append([hasil_output, 462])

fungsi_low(con_low, distance_low)
fungsi_moderate(con_low, distance_moderate)
fungsi_moderate(con_low, distance_high)
fungsi_moderate(con_moderate, distance_low)
fungsi_moderate(con_moderate, distance_moderate)
fungsi_moderate(con_moderate, distance_high)
fungsi_moderate(con_high, distance_low)
fungsi_moderate(con_high, distance_moderate)
fungsi_high(con_high, distance_high)
```

```
print('Concentration Voltage is ', ammonia)

weighted_sum = 0
total_membership = 0

for j in range(0, len(ammonia)):
    weighted_sum += ammonia[j][0] * ammonia[j][1]
    total_membership += ammonia[j][0]

z = weighted_sum / total_membership

print('Voltage is ', z, 'v')
```

Center of Maximum Fuzzy Logic Coding

```
print('LOGIK FUZZY')

x_con = float(input('Enter Ammonia Concentration Value (mV): '))
y_distance = float(input('Enter Distance Value (cm): '))

con = float(x_con)
distance = int(y_distance)

# FUZZYFICATION VOLT
if con >= 0 and con < 0.5:
    con_low = (0.5 - con) / (0.5 - 0)
    con_moderate = (con - 0) / (0.5 - 0)
    con_high = 0

if con == 0.5:
    con_low = 0
    con_moderate = 1
    con_high = 0

if con > 0.5 and con <= 1.0:
    con_low = 0
    con_moderate = (con - 0.5) / (1 - 0.5)
    con_high = (1.0 - con) / (1 - 0.5)

if con >= 1:
    con_low = 0
    con_moderate = 0
    con_high = 1
```

```
print('Degree of Ammonia concentration is:')
print('Ammonia Concentration low: ', con_low)
print('Ammonia Concentration moderate: ', con_moderate)
print('Ammonia Concentration high: ', con_high)

# FUZZYFICATION DISTANCE

if distance >= 0 and distance < 10:
    distance_high = (10 - distance) / (10 - 0)
    distance_moderate = (distance - 0) / (10 - 0)
    distance_low = 0

if distance == 10:
    distance_high = 0
    distance_moderate = 1
    distance_low = 0

if distance > 10 and distance <= 19:
    distance_high = 0
    distance_moderate = (19 - distance) / (19 - 10)
    distance_low = (distance - 10) / (19 - 10)

print('Degree of Distance is:')
print('Distance Low: ', distance_low)
print('Distance Moderate: ', distance_moderate)
print('Distance High: ', distance_high)

ammonia = []
```

```
def fungsi_low(variable_volt, variable_distance):
    if variable_volt != 0:
        if variable_distance != 0:
            hasil_output = min(variable_volt, variable_distance)
            ammonia.append([hasil_output, 154])

def fungsi_moderate(variable_volt, variable_distance):
    if variable_volt != 0:
        if variable_distance != 0:
            hasil_output = min(variable_volt, variable_distance)
            ammonia.append([hasil_output, 308])

def fungsi_high(variable_volt, variable_distance):
    if variable_volt != 0:
        if variable_distance != 0:
            hasil_output = min(variable_volt, variable_distance)
            ammonia.append([hasil_output, 462])

fungsi_low(con_low, distance_low)
fungsi_moderate(con_low, distance_moderate)
fungsi_moderate(con_low, distance_high)
fungsi_moderate(con_moderate, distance_low)
fungsi_moderate(con_moderate, distance_moderate)
fungsi_moderate(con_moderate, distance_high)
fungsi_moderate(con_high, distance_low)
fungsi_moderate(con_high, distance_moderate)
fungsi_high(con_high, distance_high)
```

```
print('Concentration Voltage is ', ammonia)


# Calculate Center of Maximum (CoM)
total_ammonia = sum(item[0] for item in ammonia)
z = sum((item[0] * item[1]) / total_ammonia for item in ammonia)


print('Voltage is ', z, 'v')
```

Center of Sums Fuzzy Logic Coding

```
print('LOGIK FUZZY')

x_con = float(input('Enter Ammonia Concentration Value (mV): '))
y_distance = float(input('Enter Distance Value (cm): '))

con = float(x_con)
distance = int(y_distance)

# FUZZYFICATION VOLT
if con >= 0 and con < 0.5:
    con_low = (0.5 - con) / (0.5 - 0)
    con_moderate = (con - 0) / (0.5 - 0)
    con_high = 0

if con == 0.5:
    con_low = 0
    con_moderate = 1
    con_high = 0

if con > 0.5 and con <= 1.0:
    con_low = 0
    con_moderate = (con - 0.5) / (1 - 0.5)
    con_high = (1.0 - con) / (1 - 0.5)

if con >= 1:
    con_low = 0
    con_moderate = 0
    con_high = 1
```

```
print('Degree of Ammonia concentration is :')
print('Ammonia Concentration low: ', con_low)
print('Ammonia Concentration moderate: ', con_moderate)
print('Ammonia Concentration high: ', con_high)

# FUZZYFICATION DISTANCE
if distance >= 0 and distance < 10:
    distance_high = (10 - distance) / (10 - 0)
    distance_moderate = (distance - 0) / (10 - 0)
    distance_low = 0

if distance == 10:
    distance_high = 0
    distance_moderate = 1
    distance_low = 0

if distance > 10 and distance <= 19:
    distance_high = 0
    distance_moderate = (19 - distance) / (19 - 10)
    distance_low = (distance - 10) / (19 - 10)

print('Degree of Distance is :')
print('Distance Low: ', distance_low)
print('Distance Moderate: ', distance_moderate)
print('Distance High: ', distance_high)

ammonia = []
```

```
def fungsi_low(variable_volt, variable_distance):
    if variable_volt != 0:
        if variable_distance != 0:
            hasil_output = min(variable_volt, variable_distance)
            ammonia.append([hasil_output, 154])

def fungsi_moderate(variable_volt, variable_distance):
    if variable_volt != 0:
        if variable_distance != 0:
            hasil_output = min(variable_volt, variable_distance)
            ammonia.append([hasil_output, 308])

def fungsi_high(variable_volt, variable_distance):
    if variable_volt != 0:
        if variable_distance != 0:
            hasil_output = min(variable_volt, variable_distance)
            ammonia.append([hasil_output, 462])

fungsi_low(con_low, distance_low)
fungsi_moderate(con_low, distance_moderate)
fungsi_moderate(con_low, distance_high)
fungsi_moderate(con_moderate, distance_low)
fungsi_moderate(con_moderate, distance_moderate)
fungsi_moderate(con_moderate, distance_high)
fungsi_moderate(con_high, distance_low)
fungsi_moderate(con_high, distance_moderate)
fungsi_high(con_high, distance_high)

print('Concentration Voltage is ', ammonia)
```

```
# Defuzzification using the Center of Sums (CoS) Method
defuzzified_value = sum(x[0] * x[1] for x in ammonia) / sum(x[0] for x in ammonia)

print('Voltage is ', defuzzified_value, 'v')
```

Modified Height Fuzzy Logic Coding

```
print('LOGIK FUZZY')

x_con = float(input('Enter Ammonia Concentration Value (mV): '))
y_distance = float(input('Enter Distance Value (cm): '))

con = float(x_con)
distance = int(y_distance)

# FUZZYFICATION VOLT
if con >= 0 and con < 0.5:
    con_low = (0.5 - con) / (0.5 - 0)
    con_moderate = (con - 0) / (0.5 - 0)
    con_high = 0

if con == 0.5:
    con_low = 0
    con_moderate = 1
    con_high = 0

if con > 0.5 and con <= 1.0:
    con_low = 0
    con_moderate = (con - 0.5) / (1 - 0.5)
    con_high = (1.0 - con) / (1 - 0.5)

if con >= 1:
    con_low = 0
    con_moderate = 0
    con_high = 1
```

```
print('Degree of Ammonia concentration is :')
print('Ammonia Concentration low: ', con_low)
print('Ammonia Concentration moderate: ', con_moderate)
print('Ammonia Concentration high: ', con_high)

# FUZZYFICATION DISTANCE
if distance >= 0 and distance < 10:
    distance_high = (10 - distance) / (10 - 0)
    distance_moderate = (distance - 0) / (10 - 0)
    distance_low = 0

if distance == 10:
    distance_high = 0
    distance_moderate = 1
    distance_low = 0

if distance > 10 and distance <= 19:
    distance_high = 0
    distance_moderate = (19 - distance) / (19 - 10)
    distance_low = (distance - 10) / (19 - 10)

print('Degree of Distance is :')
print('Distance Low: ', distance_low)
print('Distance Moderate: ', distance_moderate)
print('Distance High: ', distance_high)

ammonia = []
```

```
def fungsi_low(variable_volt, variable_distance):
    if variable_volt != 0:
        if variable_distance != 0:
            hasil_output = min(variable_volt, variable_distance)
            ammonia.append([hasil_output, 154])

def fungsi_moderate(variable_volt, variable_distance):
    if variable_volt != 0:
        if variable_distance != 0:
            hasil_output = min(variable_volt, variable_distance)
            ammonia.append([hasil_output, 308])

def fungsi_high(variable_volt, variable_distance):
    if variable_volt != 0:
        if variable_distance != 0:
            hasil_output = min(variable_volt, variable_distance)
            ammonia.append([hasil_output, 462])

fungsi_low(con_low, distance_low)
fungsi_moderate(con_low, distance_moderate)
fungsi_moderate(con_low, distance_high)
fungsi_moderate(con_moderate, distance_low)
fungsi_moderate(con_moderate, distance_moderate)
fungsi_moderate(con_moderate, distance_high)
fungsi_moderate(con_high, distance_low)
fungsi_moderate(con_high, distance_moderate)
fungsi_high(con_high, distance_high)

print('Concentration Voltage is ', ammonia)
```

```
# Modify the Height Method to consider the weighted sum
weighted_sum = 0
total_membership = 0

for j in range(0, len(ammonia)):
    weighted_sum += ammonia[j][0] * ammonia[j][1]
    total_membership += ammonia[j][0]

if total_membership != 0:
    z = weighted_sum / total_membership
else:
    z = 0

print('Voltage is:', z, 'v')
```

Inverse Fuzzy Logic (Centroid Method)

```
print('LOGIK FUZZY')

x_con = float(input('Enter Ammonia Concentration Value (mV): '))
y_distance = float(input('Enter Distance Value (cm): '))

volt = float(x_con)
distance = int(y_distance)

# FUZZYFICATION VOLT
if volt >= 0 and volt < 308:
    volt_low = (308 - volt) / (308 - 0)
    volt_moderate = (volt - 0) / (308 - 0)
    volt_high = 0

if volt == 308:
    volt_low = 0
    volt_moderate = 1
    volt_high = 0

if volt > 308 and volt <= 616:
    volt_low = 0
    volt_moderate = (volt - 308) / (616 - 308)
    volt_high = (616 - volt) / (616 - 308)

if volt >= 616:
    volt_low = 0
    volt_moderate = 0
    volt_high = 1
```

```
print('Degree of Voltage is :')
print('Volatge low: ', volt_low)
print('Voltage moderate: ', volt_moderate)
print('Voltage high: ', volt_high)

# FUZZYFICATION DISTANCE
if distance >= 0 and distance < 10:
    distance_high = (10 - distance) / (10 - 0)
    distance_moderate = (distance - 0) / (10 - 0)
    distance_low = 0

if distance == 10:
    distance_high = 0
    distance_moderate = 1
    distance_low = 0

if distance > 10 and distance <= 19:
    distance_high = 0
    distance_moderate = (19 - distance) / (19 - 10)
    distance_low = (distance - 10) / (19 - 10)

print('Degree of Distance is :')
print('Distance Low: ', distance_low)
print('Distance Moderate: ', distance_moderate)
print('Distance High: ', distance_high)

ammonia = []
```

```
def fungsi_low(variable_volt, variable_distance):
    if variable_volt != 0:
        if variable_distance != 0:
            hasil_output = min(variable_volt, variable_distance)
            ammonia.append([hasil_output, 0.25])

def fungsi_moderate(variable_volt, variable_distance):
    if variable_volt != 0:
        if variable_distance != 0:
            hasil_output = min(variable_volt, variable_distance)
            ammonia.append([hasil_output, 0.5])

def fungsi_high(variable_volt, variable_distance):
    if variable_volt != 0:
        if variable_distance != 0:
            hasil_output = min(variable_volt, variable_distance)
            ammonia.append([hasil_output, 0.75])

fungsi_low(volt_low, distance_low)
fungsi_moderate(volt_low, distance_moderate)
fungsi_moderate(volt_low, distance_high)
fungsi_moderate(volt_moderate, distance_low)
fungsi_moderate(volt_moderate, distance_moderate)
fungsi_moderate(volt_moderate, distance_high)
fungsi_moderate(volt_high, distance_low)
fungsi_moderate(volt_high, distance_moderate)
fungsi_high(volt_high, distance_high)

print('Concentration Voltage is', ammonia)
```

```
# Calculate the centroid for defuzzification
numerator = sum([item[0] * item[1] for item in ammonia])
denominator = sum([item[0] for item in ammonia])

z = numerator / denominator

print('Ammonia is', z, 'g/l')
```